SANDIA REPORT

SAND95–1606 • UC–814
Unlimited Release
Printed September 1996

Yucca Mountain Site Characterization Project

Near-Surface Velocity Modeling at Yucca Mountain using Borehole and Surface Records from Underground Nuclear Explosions

Bashir A. Durrani, Marianne C. Walck

Prepared by
Sandia National Laboratories
Albuquerque, New Mexico 87185 and Livermore, California 94550
for the United States Department of Energy
under Contract DE-AC04-94AL85000

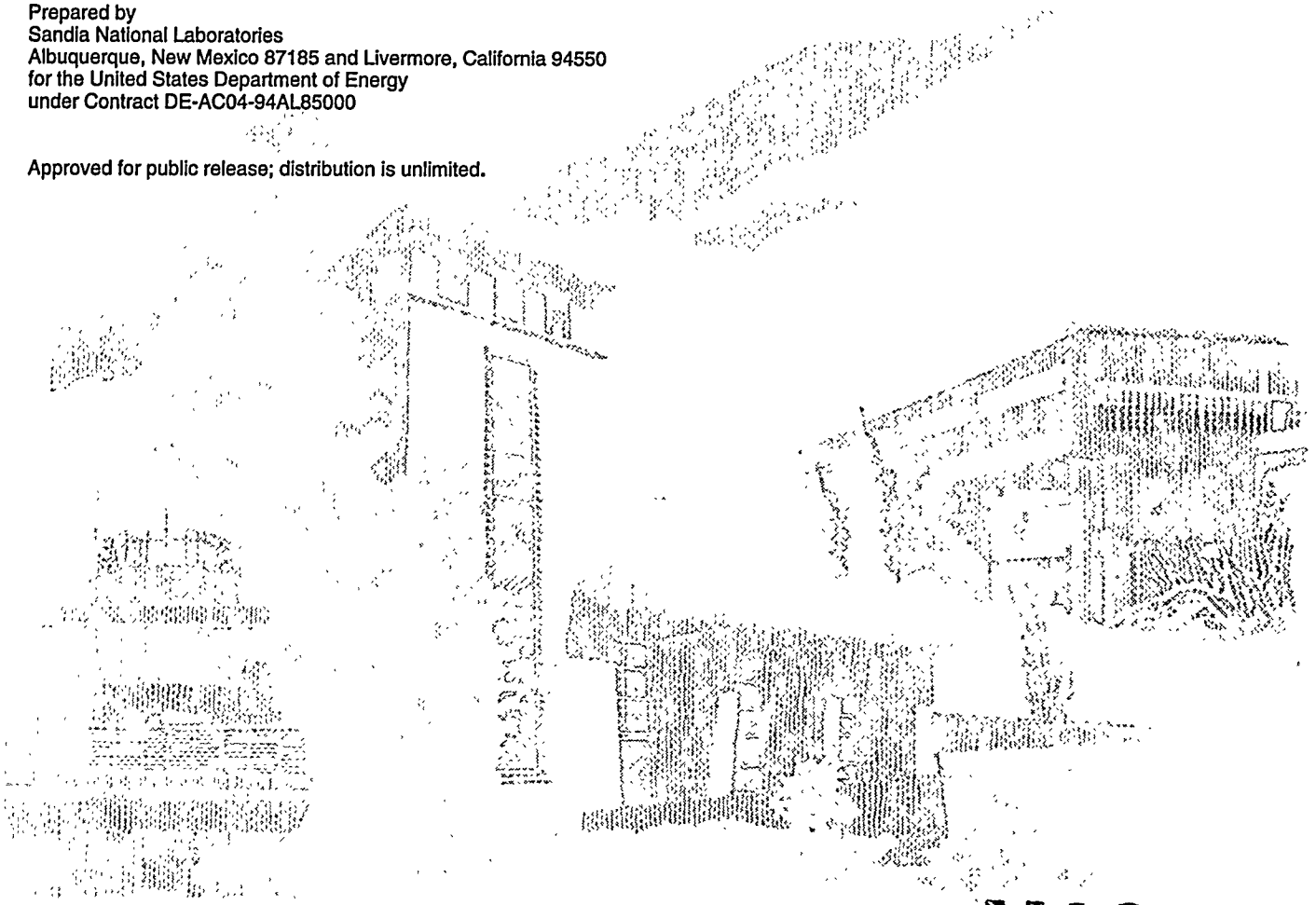

"Prepared by Yucca Mountain Site Characterization Project (YMSCP) participants as part of the Civilian Radioactive Waste Management Program (CRWM). The YMSCP is managed by the Yucca Mountain Project Office of the U.S. Department of Energy, DOE Field Office, Nevada (DOE/NV). YMSCP work is sponsored by the Office of Geologic Repositories (OGR) of the DOE Office of Civilian Radioactive Waste Management (OCRWM)."

Issued by Sandia National Laboratories, operated for the United States Department of Energy by Sandia Corporation.

Available to DOE and DOE contractors from
Office of Scientific and Technical Information
PO Box 62
Oak Ridge, TN 37831

Prices available from (615) 576-8401, FTS 626-8401

Available to the public from
National Technical Information Service
US Department of Commerce
5285 Port Royal Rd
Springfield, VA 22161

NTIS price codes
Printed copy: A05
Microfiche copy: A01

SAND95-1606
Unlimited Release
Printed September 1996

Distribution
Category UC-814

Near-Surface Velocity Modeling at Yucca Mountain using Borehole and Surface Records from Underground Nuclear Explosions

Bashir A. Durrani
Department of Geological Sciences
University of Texas at El Paso
El Paso, TX 79968

Marianne C. Walck
Geophysics Department
Sandia National Laboratories
Albuquerque, NM 87185

ABSTRACT

Borehole and surface recordings of Nevada Test Site nuclear explosions provide the only data available for characterization of ground motions at the potential repository depth at Yucca Mountain. Triaxial accelerometer pairs were located from 1980 to 1990 at four boreholes in the Yucca Mountain area; three of these boreholes are aligned in a north-south profile traversing the potential repository (with downhole instrumentation at 350-375 m depth) while the fourth was located near the suggested site for the associated surface facilities (instrumentation at 82m depth). Thirty-seven nuclear tests recorded at these locations have yielded 86 surface/downhole data pairs useful for modeling near-surface seismic structure.

We have used the propagator matrix method of calculating the full plane wave response for body waves incident on a layered structure to develop synthetic one-dimensional transfer functions for each of the four borehole stations. The velocity models used for calculating the transfer functions are based on available geologic, seismologic, and well-log information for Yucca Mountain, and were developed using forward modeling. The transfer function is the ratio of the spectral response at the depth of the downhole instrument to that at the surface instrument. Convolution of the transfer function with the actual surface seismogram yields a synthetic downhole record that is compared to the data. The modeling process results in one-dimensional velocity models for the four borehole locations. We used the models for the three stations in the north-south profile to construct a two-dimensional velocity model for the uppermost 350m of Yucca Mountain. While none of the boreholes intersect the potential repository, the two-dimensional model provides a means to predict motions at the actual repository location and depth for a specified surface seismogram.

DISCLAIMER

This work was supported by the United States Department of Energy under Contract DE-AC04-94AL85000 and was prepared under the Yucca Mountain Site Characterization Project WBS number 1.2.3.2.8.3.3. The planning document that guided this work activity was Work Agreement #0119, revision 01. The analysis documented in this report was performed under a fully qualified QA program, except for ground motion data from underground nuclear explosions conducted prior to 1989. Events with non-qualified data include Darwin, Goldstone, Serena, Salut, Towanda, Cottage, Tierra, Egmont, Kappeli, Caprock, Mundo, Tortugas, Gorbea, Romano, Techado, Chancellor, Baseball, Atrisco, Cabra, Nebbiolo, Jefferson, Labquark, Belmont, and Bodie (no TDIF numbers). These are non-qualified existing data. These nuclear events occurred prior to the existence of a fully qualified QA program.

Non-qualified data submitted with TDIF numbers (the event names in parentheses) are: 200226 DTN:SNF08000000001.000 (Contact), 200227 DTN:SNF08000000002.000 (Amarillo), 200228 DTN:SNF08000000003.000 (Alamo), 200229 DTN:SNF08000000004.000 (Dalhart), 200230 DTN:SNF080000000005.000 (Kearsarg), 200233 DTN:SNF08000000008.000 (Comstock), 200234 DTN:SNF08000000009.000 (Barnwell), 200236 DTN:SNF08000000010.000 (Delamar), 200237 DTN:SNF08000000011.000 (Kernville), 200238 DTN:SNF08000000012.000 (Lockney), 200239 DTN:SNF08000000013.000 (Hardin) and 200240 DTN:SNF08000000014.000 (Tahoka).

This report supports work defined in the Site Characterization Plan Section 8.3.1.17.3.3.2 and is discussed in Study Plan SP-8.3.1.17.3.3, Revision 0.

Software used in this report was certified for use according to Sandia National Laboratories Quality Assurance Implementing Procedure 19-1 and is named Superplane, version 1.0. (log number 110.180).

Table of Contents

List of Tables

List of Figures

Introduction

The Department of Energy is investigating Yucca Mountain, Nevada as a potential site for commercial radioactive waste disposal in a mined geologic repository. One critical aspect of site suitability is the tectonic stability of the repository site. The levels of risk from both actual fault displacements in the repository block and ground shaking from nearby earthquakes are being examined. In particular, it is necessary to determine the expected level of ground shaking at the repository depth for large seismic sources such as nearby large earthquakes or underground nuclear explosions (UNEs). Earthquakes are expected to cause the largest ground motions at the site, however, only underground nuclear explosion data have been obtained at the repository depth level (about 350m below the ground level) to date. In this study we investigate ground motion from Nevada Test Site underground nuclear explosions recorded at Yucca Mountain to establish a compressional velocity model for the uppermost 350m of the mountain. This model is useful for prediction of repository-level ground motions for potential large nearby earthquakes.

Ground motion data from nuclear explosions were recorded at several surface and borehole sites in the vicinity of Yucca Mountain between 1980 and 1990 (see Figures 1 and 2). Triaxial acceleration data from 37 Nevada Test Site events recorded in four boreholes at Yucca Mountain have been used, coupled with available detailed geologic information, to develop the model velocity structure. Using the well established propagator matrix method (e.g., Shearer and Orcutt, 1987), and a suite of surface/downhole record pairs, we developed a one-dimensional velocity model for each borehole that is most consistent with the available geological information and observed seismograms. From these models, we derived synthetic one-dimensional transfer functions between the surface and downhole recording depths. For a specified surface ground motion, these transfer functions accurately predict the level of motion expected downhole.

Three of the four borehole stations (28, 25, 30; see Figure 2) form a north-south line through the Yucca Mountain block. We use the three independently-derived one-dimensional velocity models for these three stations to construct a north-south two-dimensional model for the uppermost 350m of Yucca Mountain. Because none of the existing borehole stations intersect the potential repository, the two-dimensional model is quite useful for extrapolating the model velocities at the borehole locations to the repository location. Predictions of repository-level ground shaking from UNE-like events can then be made using existing surface recordings at a station that was sited directly over the proposed repository (station 21). The velocity model developed here can also help predict shaking at depth for a nearby earthquake, given a specified shaking level, waveform, or spectrum at the surface.

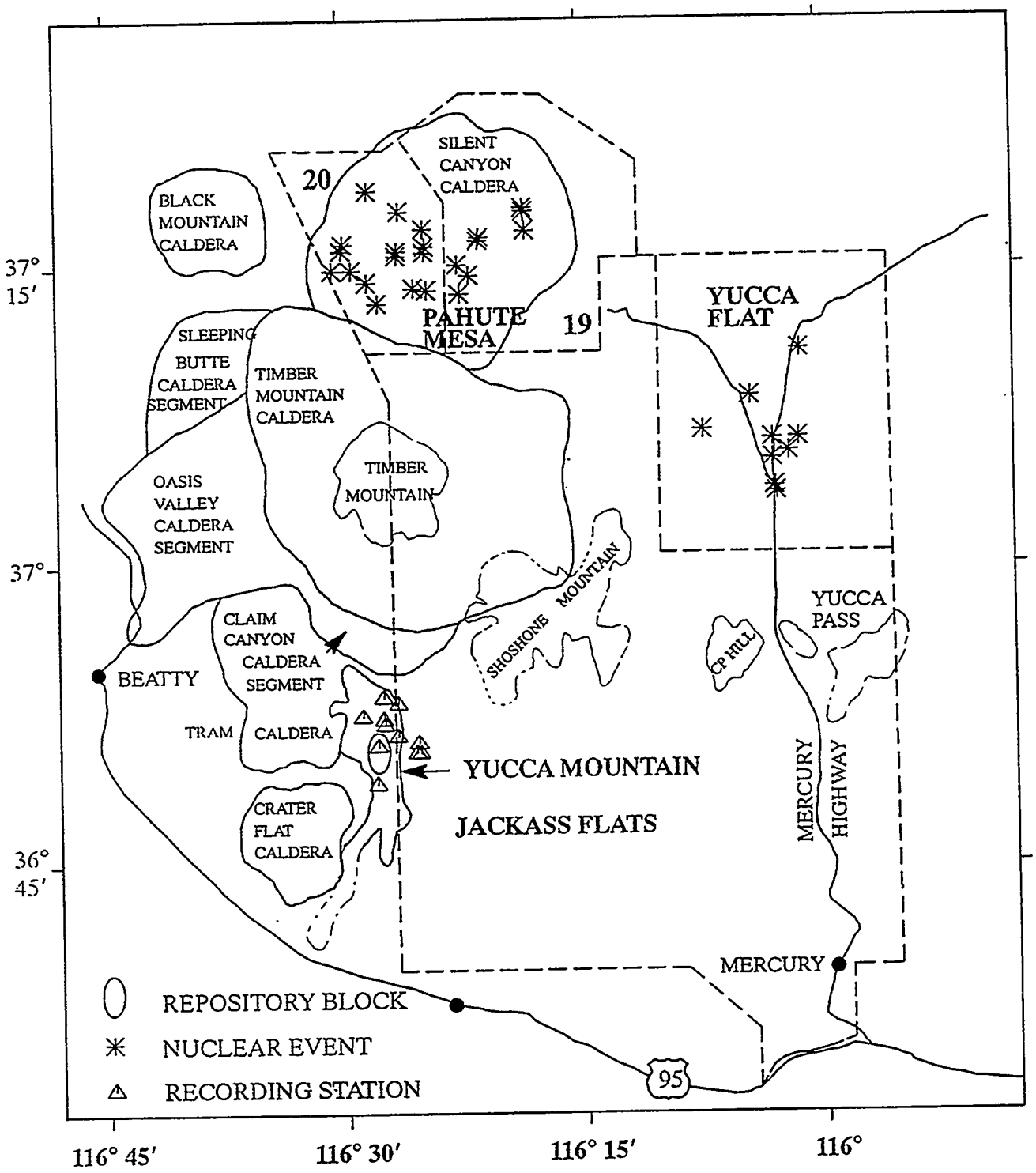

Figure 1: Map of the study area showing various geologic features along with the potential nuclear repository site at Yucca Mountain. Locations of nuclear events (asterisks) and recording stations (triangles) are also shown.

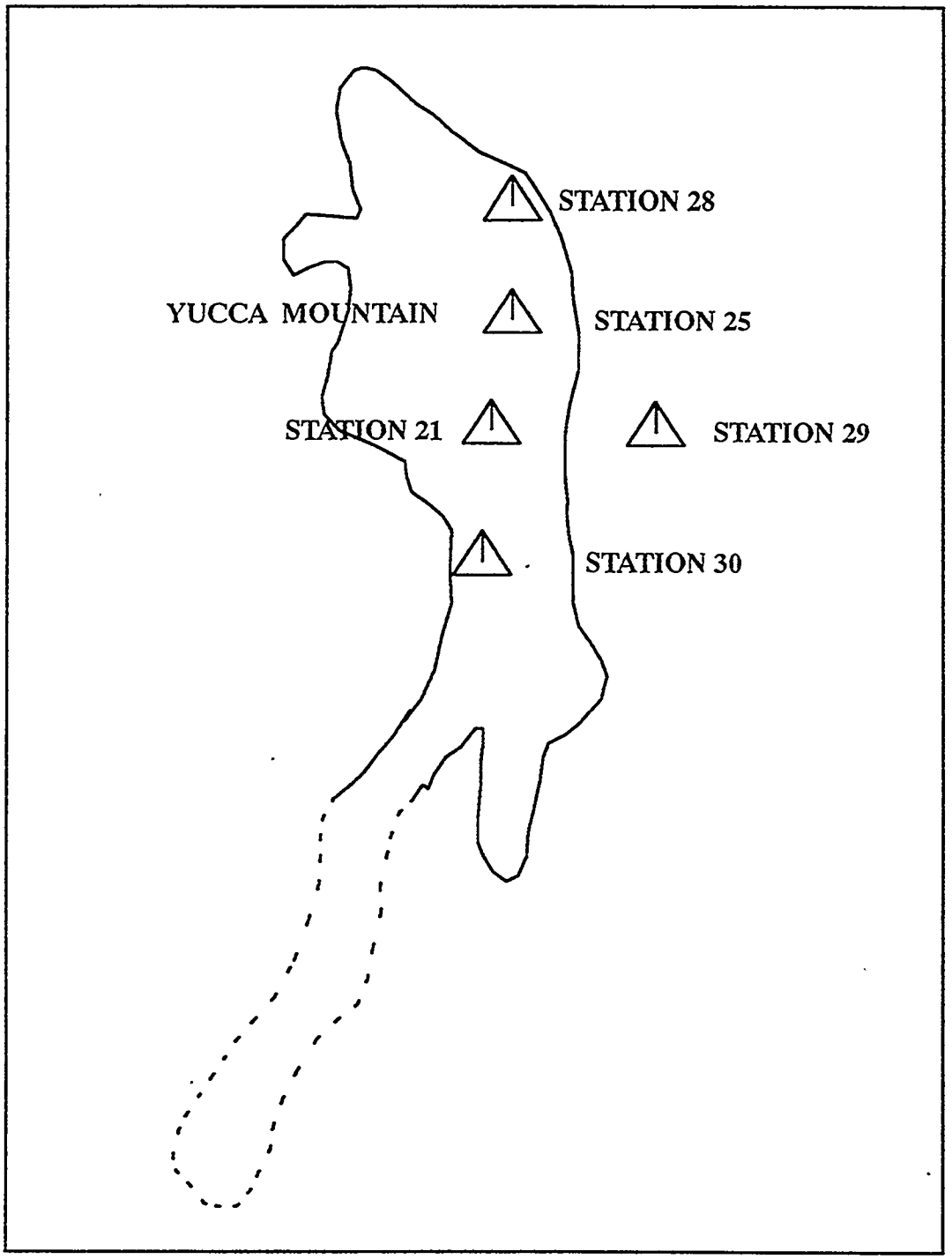

Figure 2: An enlarged view of the Yucca Mountain area, showing the topographic extent of the mountain and the location of recording stations used in the study. Stations 28, 25, and 30 comprise the north-south cross-section used for the 2-D model developed in this report. Station 29 also has borehole instrumentation. Station 21 has surface instrumentation alone and is located directly over the repository site.

Data Summary

To determine a near-surface velocity structure for Yucca Mountain, we used surface and borehole pairs of triaxial accelerations recorded from 37 underground nuclear explosions occurring at the Pahute Mesa and Yucca Flat testing areas at the Nevada Test Site (NTS) between 1980 and 1990. Figure 1 shows an outline of the NTS, some relevant geologic features, the location of underground nuclear testing areas, events used in the study and the locations of the recording stations. The nuclear shots recorded at these stations were conducted in two portions of the NTS, Pahute Mesa and Yucca Flat (Figure 1). Table 1 lists the location of the nuclear events, including latitude and longitude, elevation, depth of burial, and the area where the test was conducted. In the table, Pahute Mesa is subdivided into two areas which correspond to Areas 19 (PM1) and 20 (PM2) in Figure 1. These designations are consistent with those used in the crustal modeling study of Walck and Phillips (1990).

Figure 2 shows a close-up of the Yucca Mountain area: stations 28, 25 and 30 are located at boreholes USW G-2, USW G-1, and USW G-3, respectively, and form a north-south cross-section through the Yucca Mountain ridge. Each of these stations had a surface accelerometer and one at approximately 350m depth. Station 29, located in Midway Valley east of the mountain itself, was sited near the proposed location for repository surface facilities, and had a surface accelerometer and downhole instrumentation at 82m depth. Station 21 indicates the site of a surface-only station that is directly above the potential repository. Table 2 contains the location of the five Yucca Mountain stations at which the nuclear events were recorded that have been used in this study. Four of these stations (25, 28, 29, and 30) had both surface and downhole instrumentation, while station 21 had only surface instrumentation.

The data used in this analysis are 86 uphole/downhole vertical component acceleration pairs and 86 uphole/downhole radial component acceleration pairs from stations 25, 28, 29, and 30, and 12 each uphole vertical and radial component data for station 21. The 37 events yielded only 86 uphole/downhole pairs due to recording site changes and instrumentation failures during the ten year period over which the nuclear explosions were monitored at Yucca Mountain. The data were collected by Sandia National Laboratories as part of the Weapons Test Seismic Investigations project. Digital waveform data sampled at 200 samples/sec were acquired and assembled into a data base designed for easy event retrieval. We picked arrival times for all of the available records. Table 3 displays the event name, station number, event-to-station distance, azimuth, travel time at the surface, and travel-time at depth, respectively for each record pair. The event-to-station distances range from 37-57 km for Pahute Mesa events and from 41-51 km for the Yucca Flat tests. Source to receiver azimuths range from 231° to 241° for the Yucca Flat path and 177° to 197° for the Pahute Mesa path. Travel times recorded for Pahute Mesa shots range between 7.43-10.83

Table 1 : Event Location Data

UNE Name	Latitude	Longitude	Elevation (m)	Test Depth (m)	Area
Barnwell	37.231100	-116.409400	2003	601	PM1
Amarillo	37.275500	-116.353600	2200	640	PM2
Contact	37.282900	-116.412300	2007	544	PM1
Dalhart	37.089000	-116.049300	1259	640	YF
Kearsarg	37.297200	-116.306500	2129	616	PM2
Alamo	37.252400	-116.376700	2012	622	PM2
Comstock	37.260100	-116.441100	1987	620	PM1
Kernville	37.314400	-116.471500	1926	545	PM1
Lockney	37.228000	-116.374700	2072	615	PM2
Tahoka	37.061000	-116.045300	1250	640	YF
Hardin	37.233000	-116.423100	1951	625	PM1
Delamar	37.247900	-116.509100	1902	544	PM1
Bodie	37.263000	-116.411700	2018	635	PM1
Belmont	37.220200	-116.461600	1900	605	PM1
Labquark	37.300100	-116.307400	2100	616	PM2
Jefferson	37.264100	-116.440200	1981	609	PM1
Nebbiolo	37.236220	-116.370170	2065	640	PM2
Cabra	37.300680	-116.460030	1934	543	PM1

Table 1 : Event Location Data (continued)

UNE Name	Latitude	Longitude	Elevation (m)	Test Depth (m)	Area
Darwin	37.264600	-116.499300	1875	549	PM1
Goldstone	37.237800	-116.472800	1914	549	PM1
Serena	37.297200	-116.438100	1969	597	PM1
Salut	37.247900	-116.489100	1900	608	PM1
Towanda	37.243700	-116.36500	2112	665	PM2
Hermosa	37.094800	-116.032300	1278	640	YF
Cottage	37.179600	-116.020300	1389	515	YF
Tierra	37.281400	-116.305400	2145	640	PM2
Egmont	37.270100	-116.497600	1867	546	PM1
Kappeli	37.267800	-116.410600	2010	640	PM1
Caprock	37.065800	-116.047300	1243	600	YF
Mundo	37.106200	-116.024400	1319	320	YF
Tortugas	37.065800	-116.046300	1243	640	YF
Gorbea	37.112700	-116.121700	1371	388	YF
Romano	37.140400	-116.072100	1314	515	YF
Techado	37.105600	-116.049400	1268	533	YF
Chancellor	37.272800	-116.355000	2040	625	PM2
Baseball	37.087060	-116.041710	1259	564	YF
Atrisco	37.084210	-116.006540	1295	640	YF

Table 2: Yucca Mountain Weapons Test Seismic Investigations Stations used in this Study

Station	Latitude degrees	Longitude degrees	Elevation meters
21	36.8488	-116.4654	1482
25	36.8667	-116.4581	1325
28	36.8896	-116.4598	1554
29	36.8435	-116.4204	1109
30	36.8178	-116.4668	1480

Table 3 : Surface/Bottom ground motion travel-time picks for various nuclear explosions (continues)

Event Name	Station	Distance (km)	Azimuth (Degrees)	Travel Time (Top) (Seconds)	Travel Time (Bottom) (Seconds)
BARN-WELL	28	38.164	186.76	7.86	7.69
	25	40.674	186.13	8.27	
	26	42.078	181.60	8.30	
	29	43.026	181.31	8.42	8.38
	30	46.150	186.37	9.15	
AMARILLO	28	43.856	192.46	8.70	8.50
	25	46.311	191.61	9.06	
	26	47.389	187.46	9.02	
	29	48.312	187.08	9.15	9.21
	30	51.785	191.25	9.93	
CONTACT	28	43.853	185.54	8.69	8.53
	25	46.369	185.05	9.10	
	26	47.818	181.10	9.13	
	29	48.770	180.85	9.25	9.21
	30	51.844	185.38	9.95	

Table 3 : Surface/Bottom ground motion travel-time picks for various nuclear explosions (continued)

Event Name	Station	Distance (km)	Azimuth (Degrees)	Travel Time (Top) (Seconds)	Travel Time (Bottom) (Seconds)
DALHART	26	42.381	231.77	7.82	
	28	42.721	238.93	7.94	7.77
	29	42.830	230.61	7.87	7.82
	25	43.972	235.99	8.04	
	30	47.839	231.14	8.64	
KEAR-SARG	28	47.243	196.81	9.21	9.05
	25	49.641	195.80	9.55	9.39
	26	50.465	191.84	9.44	
	29	51.360	191.41	9.58	9.51
	30	55.081	195.05	10.36	
ALAMO	28	40.937	190.42	8.23	8.06
	25	43.413	189.63	8.62	8.46
	26	44.613	185.26	8.60	
	29	45.546	184.91	8.72	8.66
	30	48.495	189.46	9.48	

Table 3 : Surface/Bottom ground motion travel-time picks for various nuclear explosions (continued)

Event Name	Station	Distance (km)	Azimuth (Degrees)	Travel Time (Top) (Seconds)	Travel Time (Bottom) (Seconds)
COM-STOCK	28	41.151	182.32	8.32	8.19
	25	43.685	181.99	8.75	8.62
	26	45.309	177.91	8.81	
	29	46.271	177.71	8.96	8.90
	30	49.139	182.67	9.60	
KERN-VILLE	28	47.155	178.73	9.38	9.21
	25	49.700	178.62	9.81	9.65
	26	51.490	175.14	9.89	
	29	52.458	175.01	10.03	9.97
	30	55.114	179.56	10.64	
LOCKNEY	28	38.310	191.42	7.81	7.63
	25	40.777	190.51	8.20	8.04
	26	41.933	185.85	8.15	
	29	42.865	185.46	8.27	8.24
	30	46.255	190.23	9.01	

Table 3 : Surface/Bottom ground motion travel-time picks for various nuclear explosions (continued)

Event Name	Station	Distance (km)	Azimuth (Degrees)	Travel Time (Top) (Seconds)	Travel Time (Bottom) (Seconds)
TAHOKA	26	40.824	235.51	7.48	
	29	41.216	234.26	7.49	7.44
	28	41.521	242.86	7.65	7.49
	25	42.619	239.73	7.75	7.61
	30	46.242	234.42	8.27	
HARDIN	28	38.250	184.90	7.75	7.58
	25	40.770	184.39	8.20	8.03
	26	42.271	179.94	8.24	
	29	43.228	179.68	8.34	8.30
	30	46.242	184.84	9.03	8.97
DELAMAR	26	44.594	170.04	8.82	
	29	45.569	170.00	9.0	8.92
	30	47.880	175.48	9.55	9.42

Table 3 : Surface/Bottom ground motion travel-time picks for various nuclear explosions (continued)

Event Name	Station	Distance (km)	Azimuth (Degrees)	Travel Time (Top) (Seconds)	Travel Time (Bottom) (Seconds)
BODIE	28	41.660	185.91	8.31	8.16
	26	45.611	181.22	8.75	
	29	46.562	180.95	8.89	8.85
	30	49.649	185.68	9.58	9.46
BELMONT	28	36.691	179.75	7.44	7.28
	25	39.233	179.55	7.89	7.74
	26	40.998	175.13	8.00	
	29	41.966	174.98	8.11	8.07
	30	44.661	180.60	8.72	8.63
LAB-QUARK	28	47.529	196.61	9.32	9.16
	25	49.929	195.61	9.63	9.50
	26	50.764	191.68	9.55	
	29	51.659	191.25	9.68	9.65
	30	55.371	194.88	10.45	10.36

Table 3 : Surface/Bottom ground motion travel-time picks for various nuclear explosions (continued)

Event Name	Station	Distance (km)	Azimuth (Degrees)	Travel Time (Top) (Seconds)	Travel Time (Bottom) (Seconds)
JEFFER-SON	28	41.599	182.41	8.29	8.13
	25	44.131	182.07	8.71	8.57
	26	45.749	178.03	8.76	
	29	46.712	177.83	8.91	8.87
	30	49.586	182.74	9.55	9.48
DARWIN	28	41.765	175.16	8.37	8.21
	25	44.309	175.24	8.81	8.67
	26	46.283	171.50	8.93	
	29	47.258	171.43	9.07	9.03
	30	49.670	176.65	9.68	9.56
GOLD-STONE	28	38.659	178.28	7.95	7.79
	25	41.204	178.18	8.39	8.25
	26	43.036	174.03	8.48	
	29	44.008	173.90	8.61	8.58
	30	46.615	179.34	9.21	9.12

Table 3 : Surface/Bottom ground motion travel-time picks for various nuclear explosions (continued)

Event Name	Station	Distance (km)	Azimuth (Degrees)	Travel Time (Top) (Seconds)	Travel Time (Bottom) (Seconds)
SERENA	28	45.275	182.45	9.06	8.90
	25	47.811	182.14	9.48	9.33
	26	49.416	178.40	9.51	
	29	50.375	178.20	9.53	9.60
	30	53.265	182.76	10.21	10.11
SALUT	28	39.849	176.24	7.88	7.73
	25	42.396	176.26	8.34	8.20
	26	44.322	172.31	8.50	
	29	45.294	172.23	8.60	8.56
	30	47.773	177.61	9.20	9.10
TOWANDA	28	40.191	192.14	8.23	
	25	42.652	191.22	8.55	8.41
	26	43.761	186.74	8.48	
	29	44.686	186.35	8.60	8.57
	30	48.125	190.88	9.40	9.30

Table 3 : Surface/Bottom ground motion travel-time picks for various nuclear explosions (continued)

Event Name	Station	Distance (km)	Azimuth (Degrees)	Travel Time (Top) (Seconds)	Travel Time (Bottom) (Seconds)
HERMOSA	26	43.968	232.34	7.91	
	28	44.348	239.23	8.01	7.87
	29	44.407	231.21	7.95	7.92
	25	45.585	236.40	8.13	8.01
	30	49.420	237.67	8.78	8.65
COTTAGE	28	50.644	230.68	8.39	8.17
	26	51.018	224.69	8.30	
	29	51.567	223.79	8.45	8.39
	25	52.187	228.42	8.55	8.40
	30	56.495	224.84	9.40	9.01
TIERRA	28	45.597	197.57	8.87	8.73
	25	47.984	196.49	9.20	9.05
	26	48.770	192.38	9.17	
EGMONT	25	44.907	175.50	8.90	8.78
	26	46.866	171.80	9.11	
	28	42.361	175.44	0.00	8.31

Table 3 : Surface/Bottom ground motion travel-time picks for various nuclear explosions (concluded)

Event Name	Station	Distance (km)	Azimuth (Degrees)	Travel Time (Top) (Seconds)	Travel Time (Bottom) (Seconds)
KAPPELI	25	44.715	185.44	8.90	8.76
	26	46.146	181.33	8.93	
	27	47.072	181.50	8.87	8.87
	28	42.200	185.96	0.00	8.32
CAPROCK	26	40.981	234.75	7.71	
	25	42.737	238.99	7.95	7.76
MUNDO	26	45.441	231.76	8.31	
	25	47.022	235.71	8.54	8.41
TORTUGAS	25	42.813	239.05	7.83	
GORBEA	25	40.524	227.75	7.48	7.30
ROMANO	25	45.858	228.64	8.63	8.39
TECHADO	25	45.021	234.04	8.43	8.04
CHANCEL-LOR	25	45.992	191.53	8.97	

and between 7.52-8.75 seconds for the Yucca Flat events. In Figure 3, travel times for the three event areas are plotted with respect to distance for the events used in this study. Travel times for Yucca Flat events are significantly shorter than those for Pahute Mesa events at the same distance. This large (0.5 s) travel time difference is likely due to differences in crustal velocity structure between the two paths (see Walck and Phillips, 1990). Relative amplitudes among the Yucca Mountain stations also differ as a function of source amplitude, as seen in Figures 4 and 5. For Pahute Mesa events (e.g., Figure 4), stations located at the north end of Yucca Mountain (28 and 25) typically have the largest first arrival amplitudes, while for Yucca Flat explosions (see Figure 5), stations located to the east of the mountain ridge (26 and 29), have the largest amplitudes. The variations in travel times and relative amplitudes between the two source areas are indicative of significant azimuth-dependent crustal structure, or path effects, as discussed by Walck and Phillips (1990). Simple azimuth-independent site corrections are probably not adequate for predicting absolute ground motions for these stations.

Several examples of vertical acceleration surface/downhole data pairs are shown in Figures 6-11. Obvious differences between the surface and downhole records include the overall amplitude levels and the absolute travel times. As expected, the surface records are larger in overall amplitude, although the level of amplification varies and is not the simple 'factor of two" expected from a half-space velocity structure. Note the differences in surface amplification among the four record pairs shown for the Belmont event in Figures 6 and 7. At stations 28 and 29, the surface records are about twice as large as the downhole records, while the amplification is less than two for station 30 and is a factor of 3-4 for station 25. Travel times between the downhole and uphole instruments also vary by station (see Table 3 for detailed travel time information). Although the relative depths of the three deep borehole stations are quite similar, the average differential travel times up the borehole range from 0.10 s at station 30 to 0.16 s at station 28. These differences indicate differences in the velocity structure among the boreholes, with station 30 having an overall faster velocity structure than stations 25 and 28.

The borehole and surface waveforms are often similar near the beginning of the records, but become much less similar a few cycles into the record, as shown particularly in Figures 6, 8, 9, and 10. Using the method described in the next section, we attempt to explain the differences between the surface and downhole records using geologically reasongable velocity models for each borehole site.

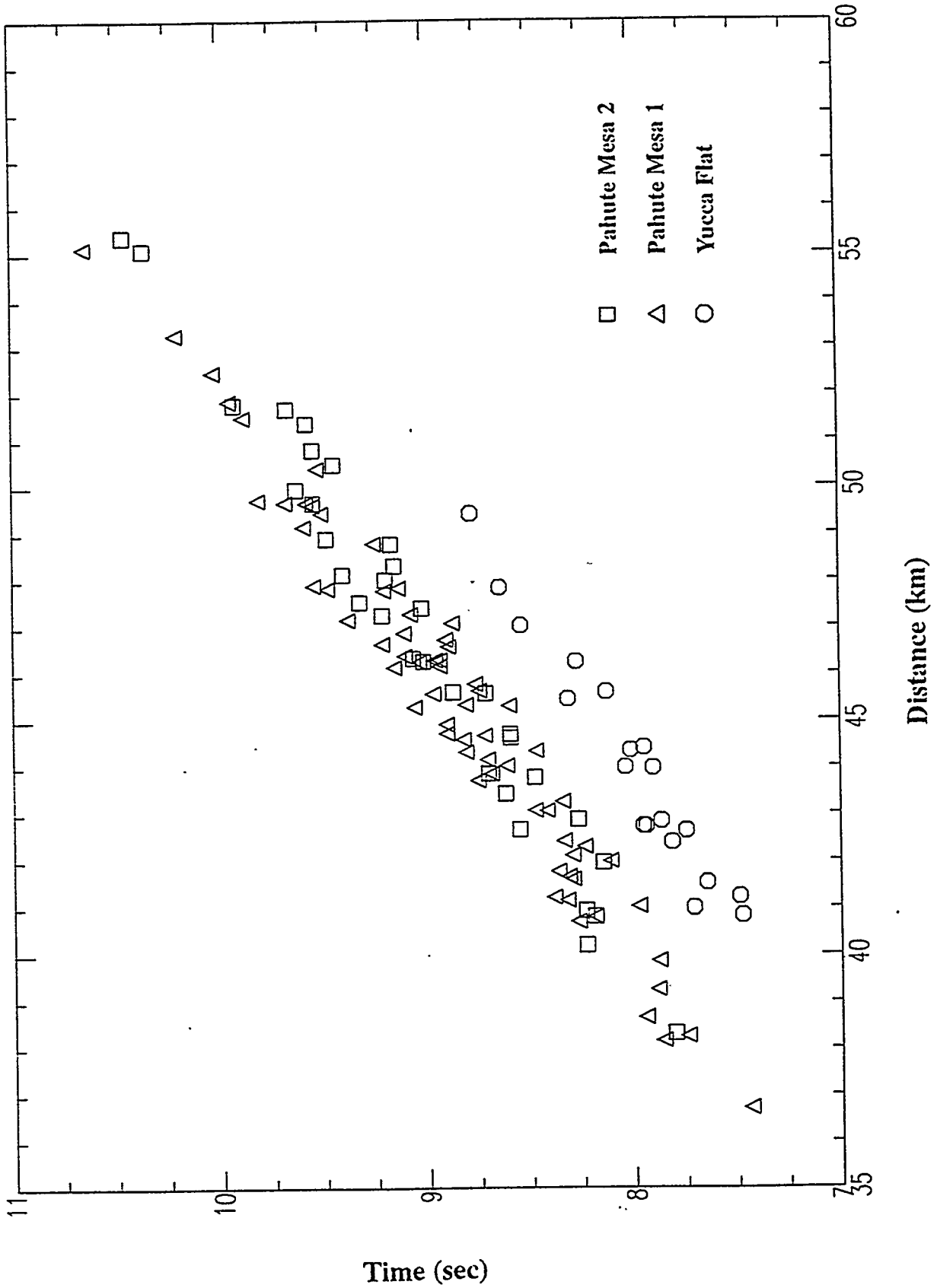

Figure 3: Travel time as a function of distance for nuclear tests recorded at surface accelerometers at Yucca Mountain. Note the significantly faster travel times for Yucca Flat events.

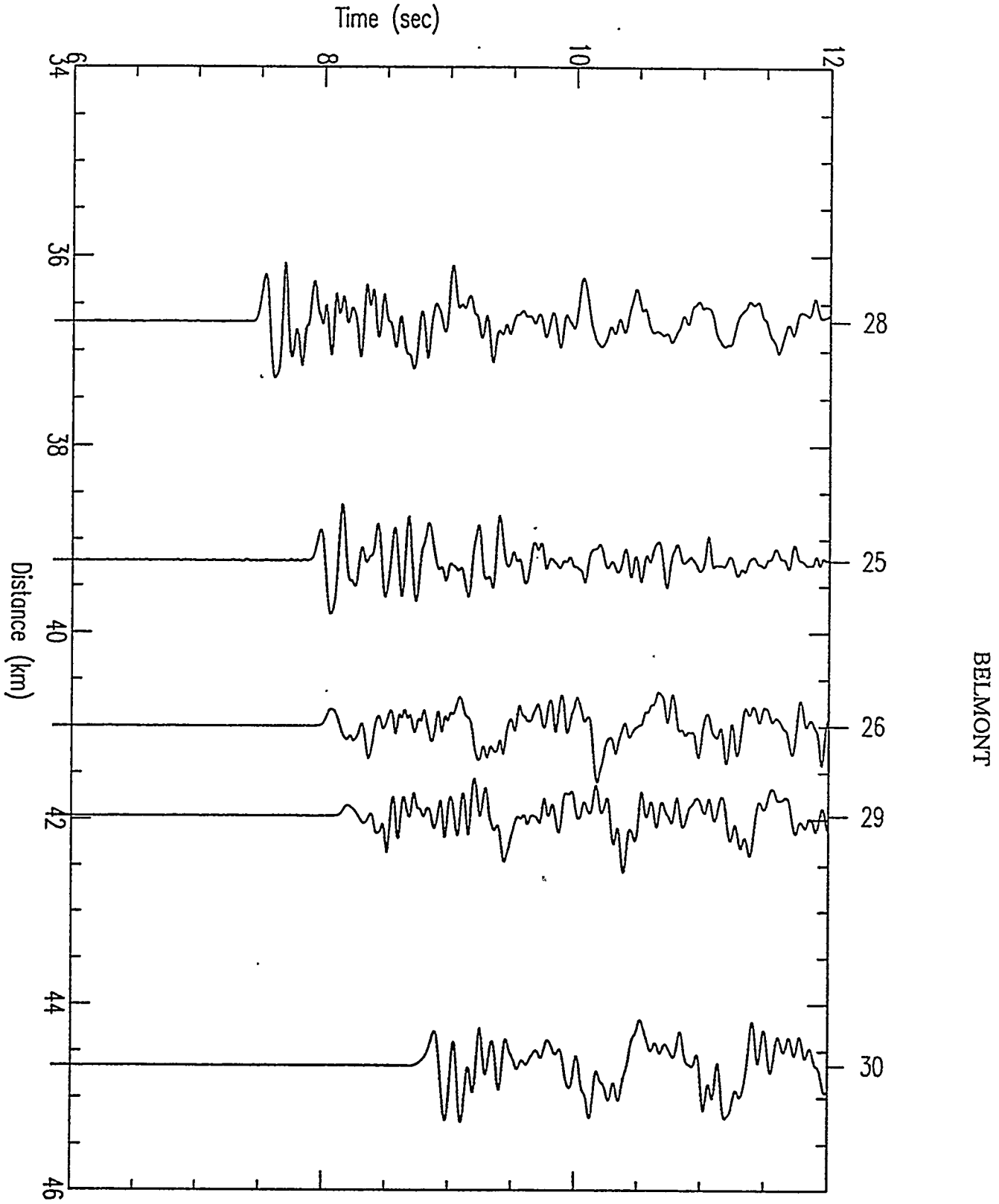

Figure 4: Vertical acceleration waveforms at the surface in record section form for event Belmont (Pahute Mesa). Station numbers are at the right of each trace. First arrival amplitudes are largest at stations 28 and 25.

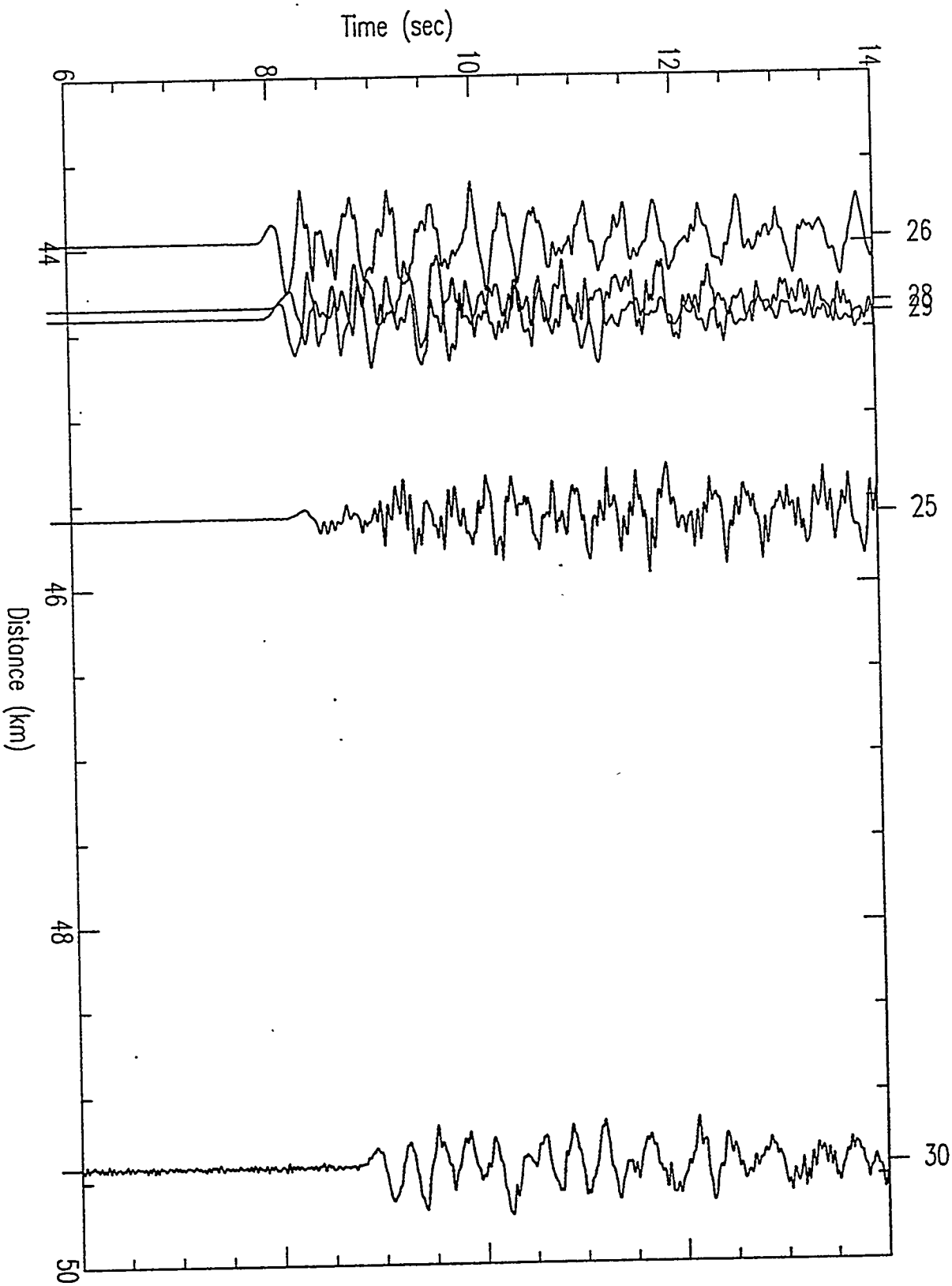

Figure 5: Vertical acceleration waveforms at the surface in record section form for event Hermosa (Yucca Flat). Station numbers are to the right of each trace. First arrival amplitudes are largest at stations 26 and 29.

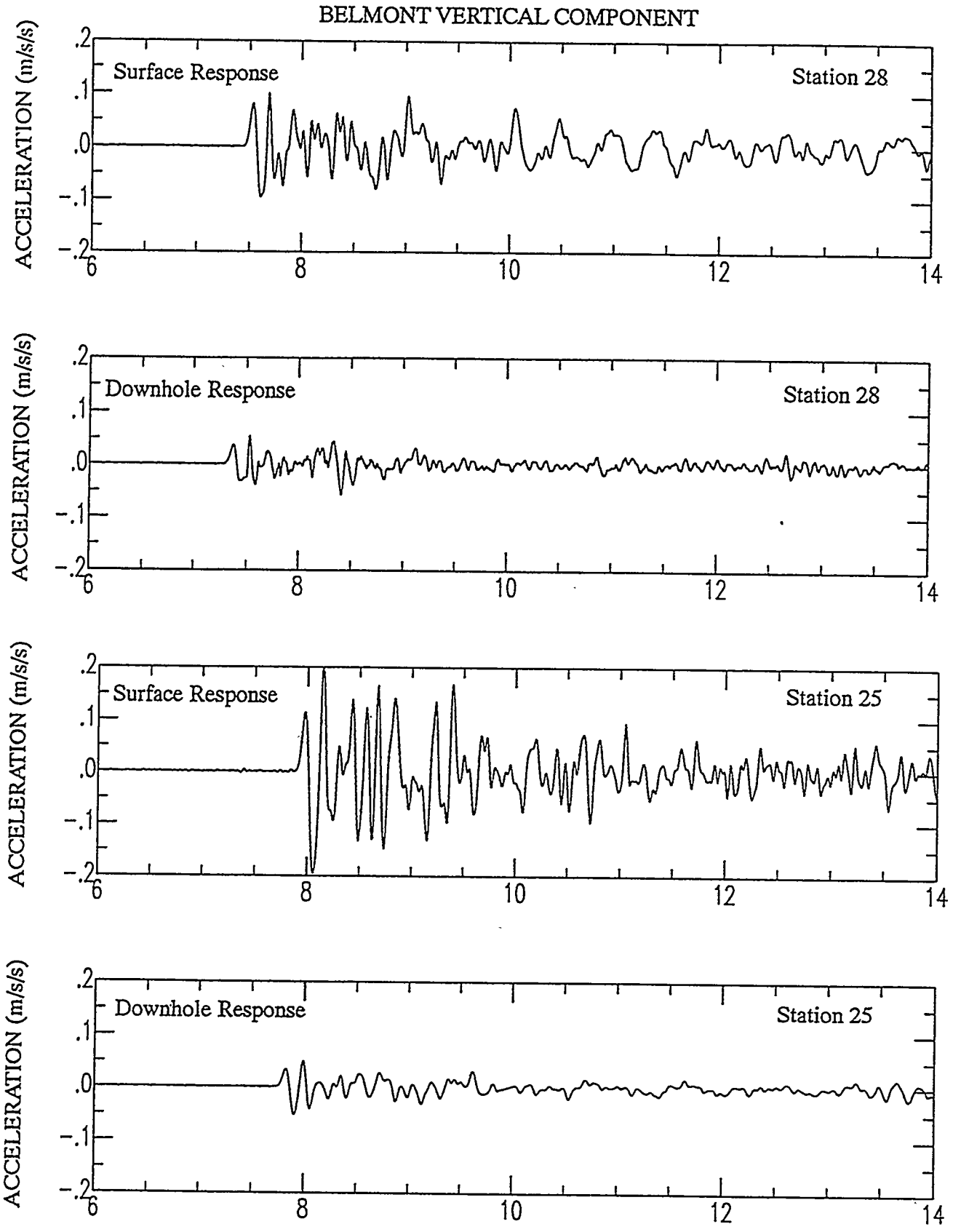

Figure 6: Comparison of vertical acceleration waveforms at the surface and downhole, stations 28 and 25, event Belmont (Pahute Mesa)

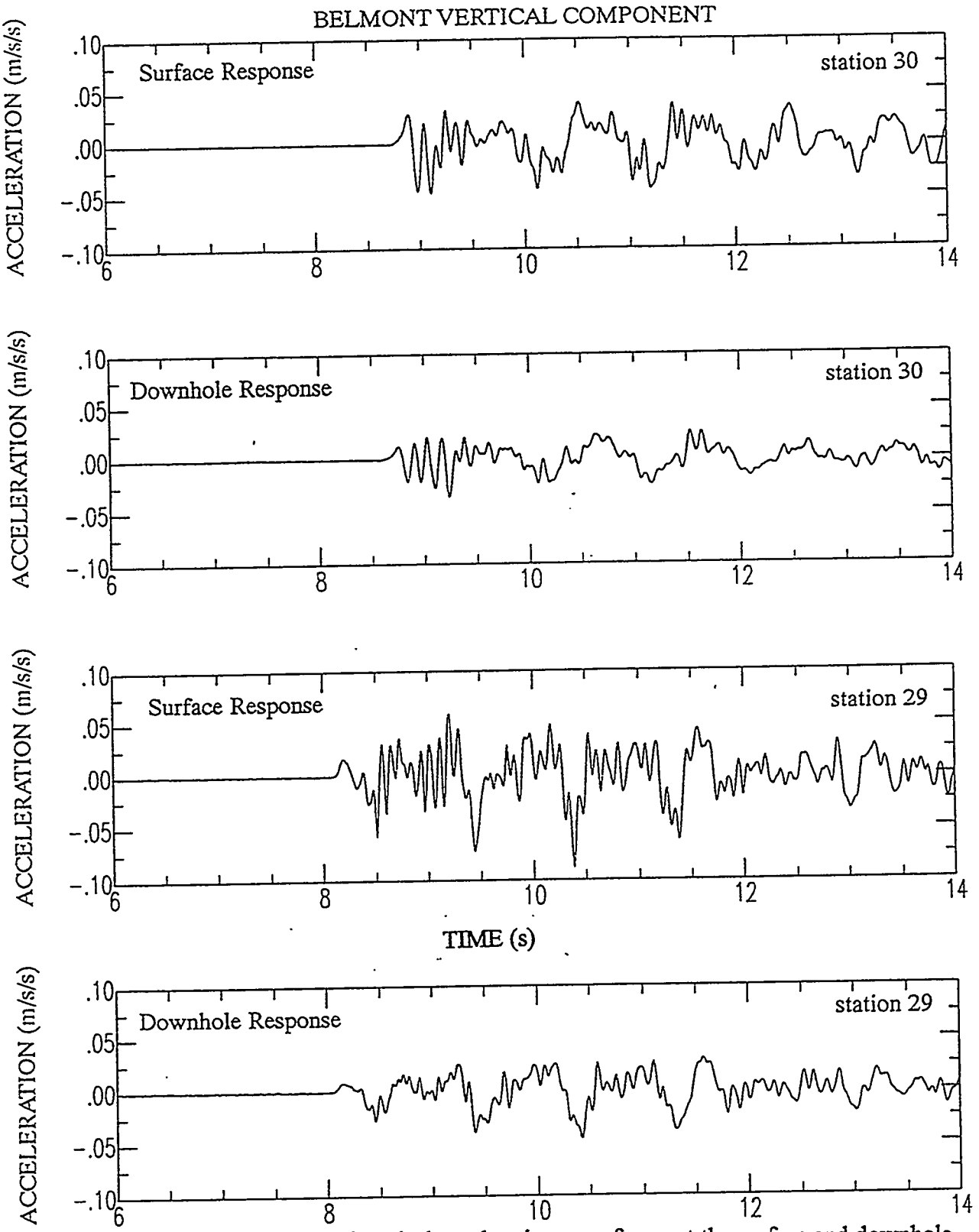

Figure 7: Comparison of vertical acceleration waveforms at the surface and downhole, stations 30 and 29, event Belmont (Pahute Mesa)

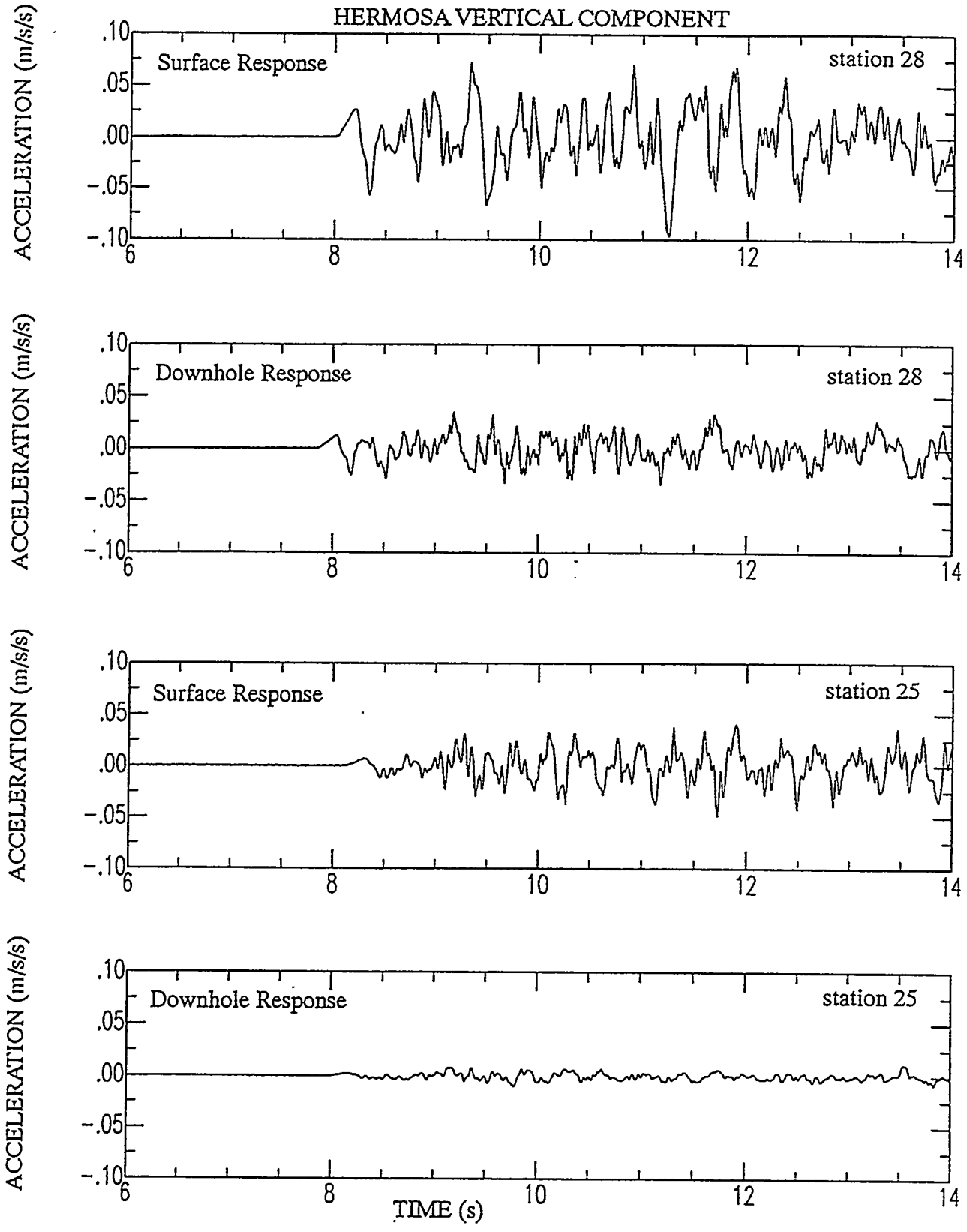

Figure 8: Comparison of vertical acceleration waveforms at the surface and downhole, stations 28 and 25, event Hermosa (Yucca Flat)

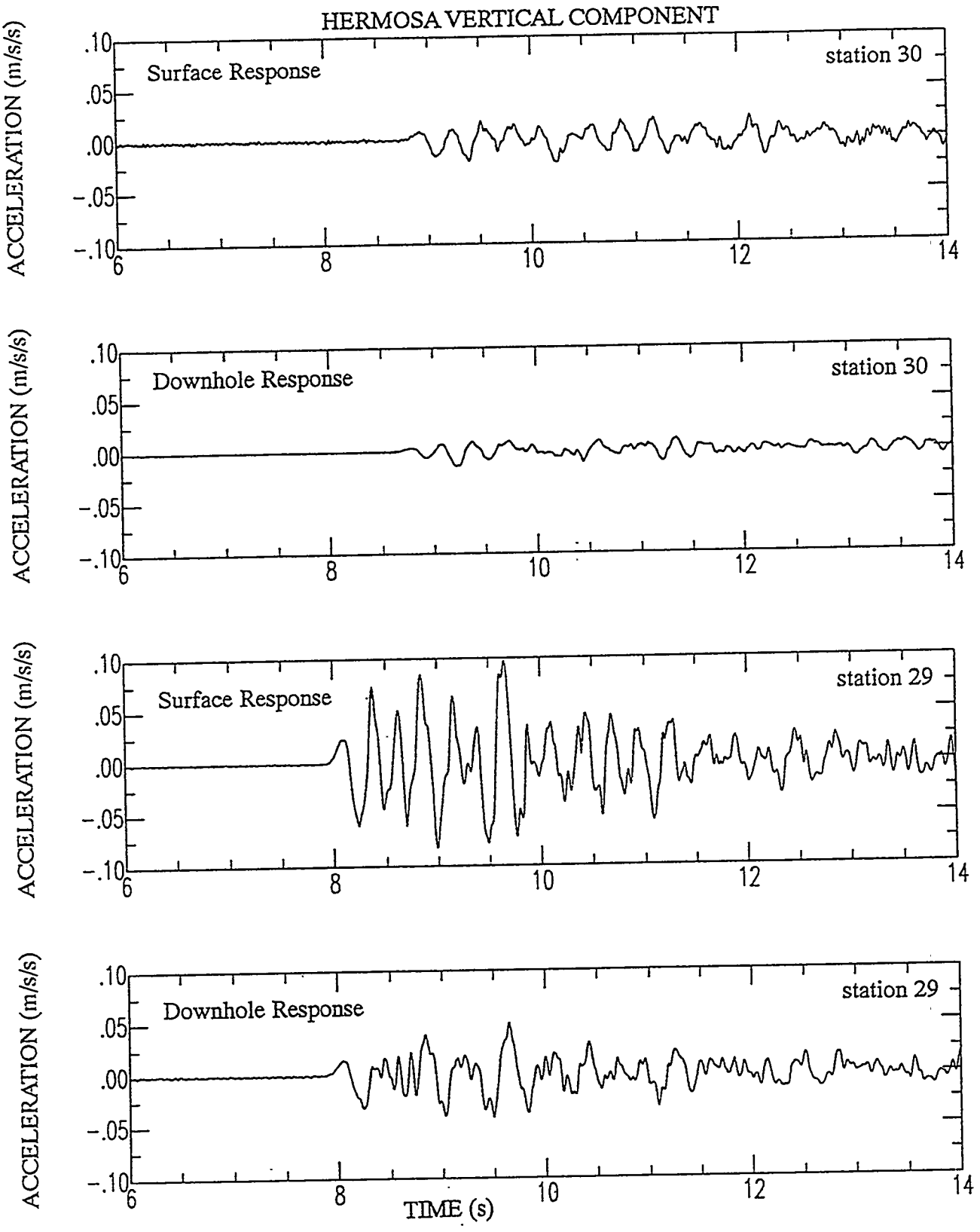

Figure 9: Comparison of vertical acceleration waveforms at the surface and downhole, stations 30 and 29, event Hermosa (Yucca Flat)

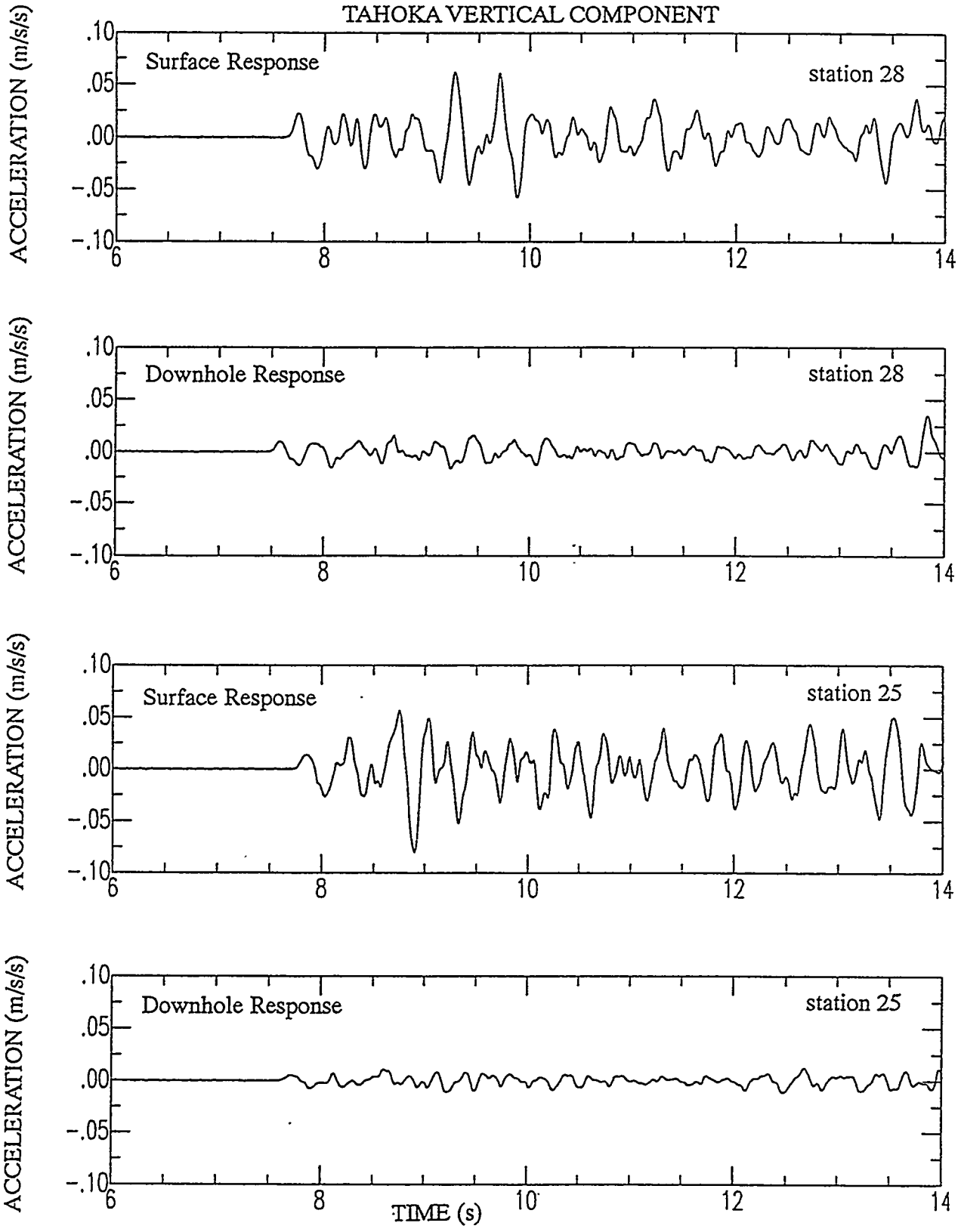

Figure 10: Comparison of vertical acceleration waveforms at the surface and downhole, stations 28 and 25, event Tahoka (Yucca Flat)

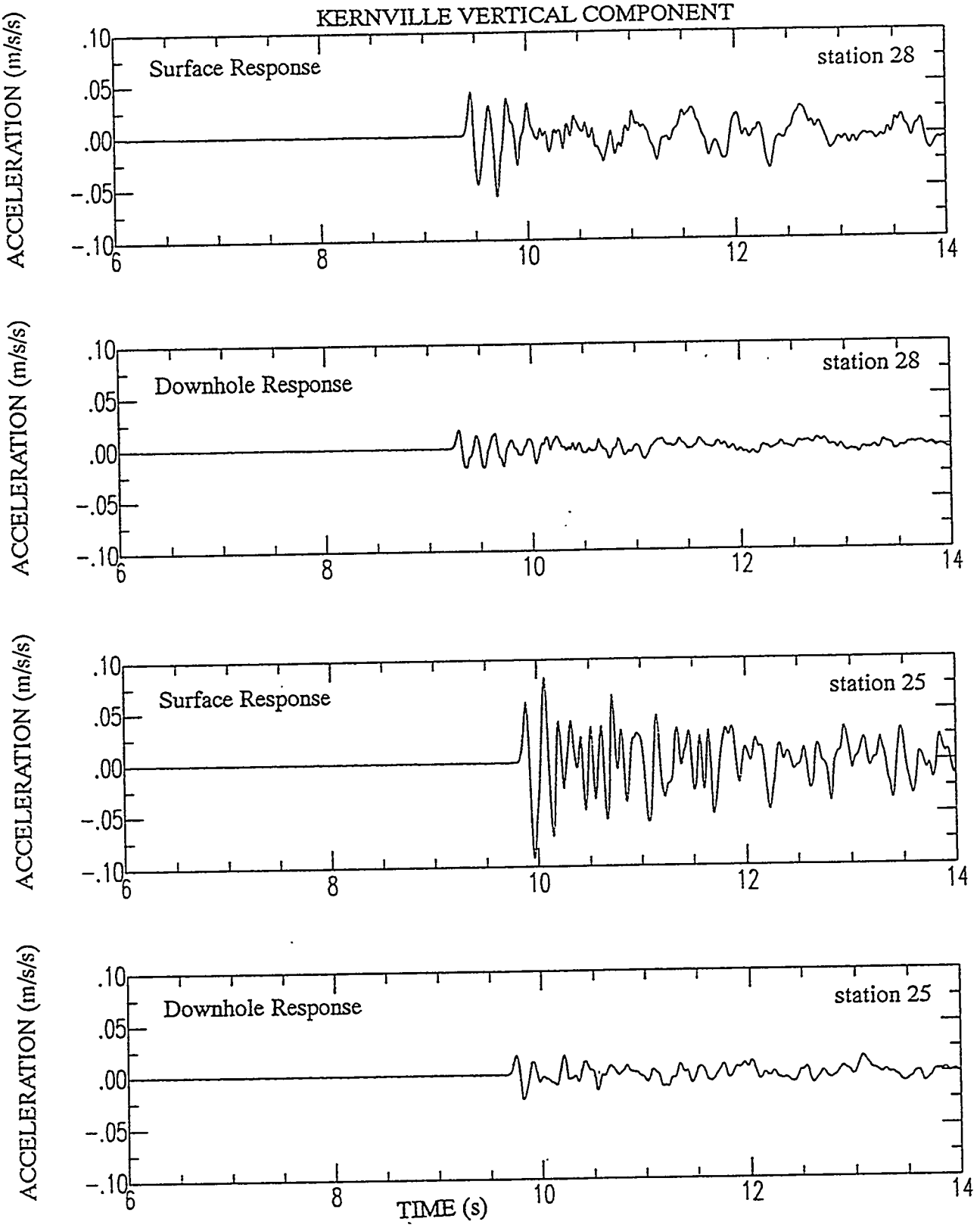

Figure 11: Comparison of vertical acceleration waveforms at the surface and downhole, stations 28 and 25, event Kernville (Pahute Mesa)

Modeling Technique

Our goal is to develop a means to predict subsurface ground motions at the repository location for a specified seismic source. The site's tectonic setting dictates that ground motions from a large, nearby earthquake would be larger than motions from any explosion sources. Because the natural seismicity at Yucca Mountain occurs at a very low rate, however, by far the largest motions that have been actually measured in boreholes are from underground nuclear explosions detonated at the nearby Nevada Test Site. Unfortunately, borehole accelerometer instrumentation that was installed to monitor UNE ground motions was operational only for the time immediately surrounding the planned explosion, thus no earthquake motions have been recorded downhole at the repository horizon. We therefore chose to use the explosion data to develop velocity models that can be used to predict subsurface ground motions at any depth for any specified surface source, earthquake or explosion.

Given the limitation of explosion data recorded downhole, our approach is to use multiple sets of single-source uphole/downhole data pairs to develop, in a forward modeling fashion, one-dimensional velocity models for each of the boreholes for which we have data. From these one-dimensional models we can calculate synthetic transfer functions, which are simply spectral ratios of the downhole model response to the surface model response. Convolution of a surface ground motion with the transfer function then results in a prediction of downhole ground motion, which can be accomplished for any depth within the model. Furthermore, the series of one-dimensional models can be generalized into a two-dimensional model along a north-south line through Yucca Mountain that intersects the proposed location of the repository and three of the four boreholes. This 2-D model is useful for predicting ground motions where we have no actual data. By taking a slice through the model at the desired location, we can calculate the subsurface body wave response for any specified input at the surface.

To develop the velocity models and transfer functions, we have used the explosion data coupled with detailed geologic information available for each borehole and nearby boreholes. Inspection of the surface/downhole record pairs (e.g., Figures 6-11) show that simple half-space velocity models will not explain the variations in amplitude, travel time, and waveform for the observed data, therefore geologic information was sought to constrain the starting models. Initial compressional velocity models were developed using geologic descriptions of the boreholes (e.g., Scott and Castellanos, 1984, Spengler et al., 1981, Maldonado and Koether, 1983), geophysical logs where available (Spengler et al., 1984, Muller and Kibler, 1983), available rock property information (Lappin et al., 1982), and the thermal-stratigraphic unit descriptions of Ortiz et al. (1985). Initial shear wave values were

specified using a Poisson's ratio of 0.25; in later experiments we also considered unpublished information on very shallow shear velocities from the recent vertical seismic profiling study by Daley and Majer (written communication, 1995). Vertical travel times through the trial models were compared to observed travel times differences between the uphole and downhole recordings of the same events to provide a control on the integrated velocity of the model above the depth of the downhole station.

We tested the velocity models using the data and the algorithm of Shearer and Orcutt (1987), which is based on the propagator matrix method first described by Haskell (1953, 1960, 1962). The code calculates the full plane wave response for incoming body waves through a layered stack. Surface waves are not calculated with this method. Complex spectra are computed at the surface and any specified depths. An example calculation is shown in Figure 12, where the vertical response of a model consisting of one layer over a halfspace, with receivers at depths of 0, 50, 100, 150, and 200m is illustrated. The surface layer's P velocity is 1.5 km/sec and the halfspace velocity is 4.0 km/sec; the P wave is incident at 42° from the vertical. On the left is shown the spectral amplitude as a function of frequency for each receiver depth. The time domain response is on the right. This formulation includes both upgoing and downgoing waves, and the source can be specified as either P waves only, S waves only, or both. In the modeling described below, P waves were used to simulate the explosion source. Either the vertical or horizontal (radial) component can be calculated. Attenuation is specified in the modeling but does not have a large effect on the calculations presented here (see Shearer and Orcutt, 1987). We specify the incidence angle of the incoming energy based on observed particle motions from the three component data. In general, the UNE data approach Yucca Mountain at a steep (< 30° from vertical) angle due to the large velocity gradient in the upper crust (Walck and Phillips, 1990).

The modeling process is shown in flow chart form in Figure 13. This procedure is followed separately for each borehole. Forward modeling of several surface/downhole data pairs, including data from both Pahute Mesa and Yucca Flat, determines the final model for each hole. The "goodness of fit" for each model was assessed visually. We attempted to match the downhole record both in amplitude and waveshape while maintaining simple velocity models. The vertical component data were modeled first. We then revised the models as necessary to provide the best possible fit to the combined radial and vertical data sets. Perhaps due to poor controls on shear velocities at the station sites, fits to our radial records using the models developed from the vertical data were not as good. We chose to maintain the good vertical data fits and match overall signal amplitude and frequency content for the radial records. For all of the modeling, the travel time between the uphole and downhole record was used as a check on the overall velocity structure determined for the borehole. Our one-dimensional models represent subjectively determined "best fits" to the data suite that is also consistent with the geological data, thermal stratigraphic units, and available geophysical data.

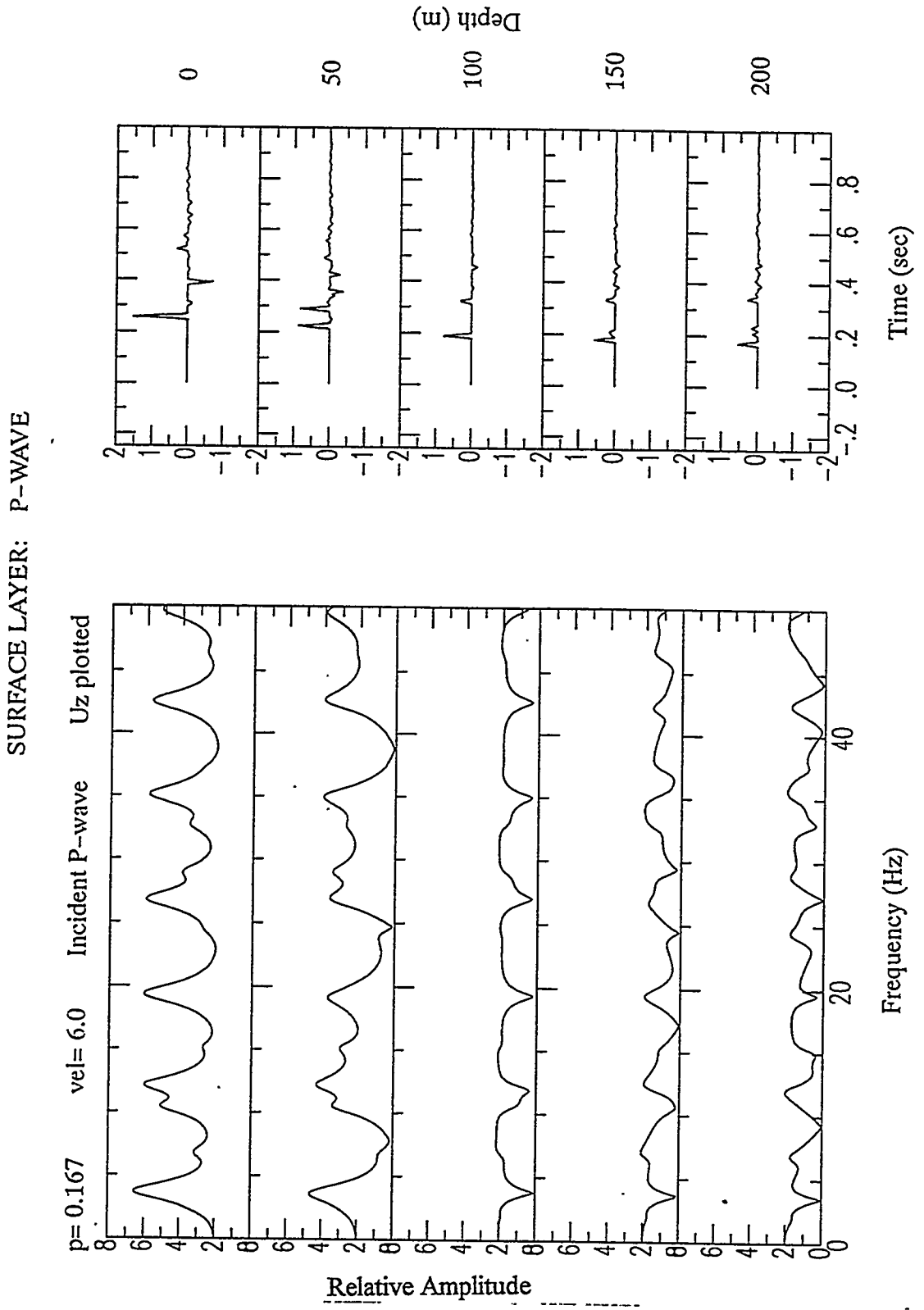

Figure 12: Theoretical spectral response for a delta function incident at 42° from vertical impinging on a layer over a halfspace velocity model (from Shearer and Orcutt, 1987). The vertical component is shown. On the left are the spectral amplitudes at each depth as a function of frequency, and on the right are the time domain responses.

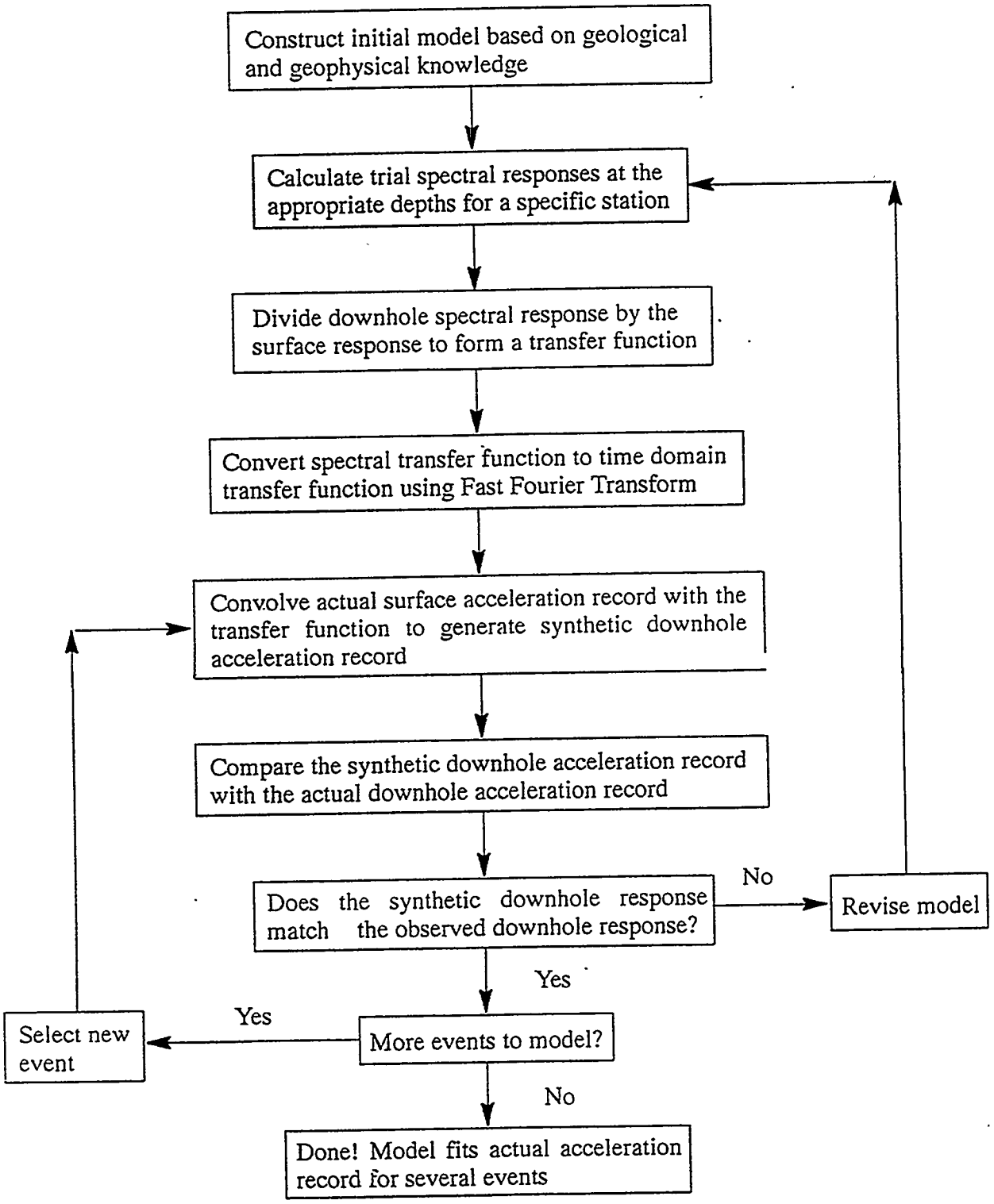

Figure 13: Flow chart showing modeling procedure.

Data Analysis

We have developed one-dimensional velocity models for four boreholes in the vicinity of Yucca Mountain. Station 29 (see Figure 2 for location), which has instrumentation at the surface and at 82m depth, is located east of the mountain itself near the proposed location of repository surface facilities. Stations 28, 25, and 30 (Figure 2) comprise a north-south profile through Yucca Mountain itself. None of the boreholes intersects the potential repository, but station 25 is just north of the repository boundary and station 30 is located just to the south. The stations were operational from the mid 1980s to 1990 and each station has approximately 20 uphole/downhole data recordings of underground nuclear explosions available for analysis. Data from both the Yucca Flat and Pahute Mesa source areas are available for all four stations. The downhole accelerometers for the three stations with deeper instrumentation were located in the Topopah Springs member of the Paintbrush Tuff , while the downhole accelerometer for station 29 was placed in the Tiva Canyon member (Phillips, 1991).

The detailed geology differs among the three stations due to local tilting and faulting. The Tiva Canyon member of the Paintbrush tuff tops the section for stations 30 and 28, but is absent at station 25, which has alluvium at the surface (Spengler et al., 1981). The Yucca Mountain and Pah Canyon members of the Paintbrush tuff are present at stations 25 and 28, but not at station 30 (Scott and Castellanos, 1984). All three boreholes penetrate significant thicknesses of the Topopah Springs member. This formation is also laterally heterogeneous, however, containing zones with significant proportions of lithophysal cavities that might be inferred to have a lower seismic velocity due to higher porosity (e.g., Muller and Kibler, 1983). The differences in geology translate into different seismic models for each station.

Four one-dimensional models representing the near-surface seismic velocities for the four Yucca Mountain borehole stations are presented in Figures 14 and 15 and summarized in Table 4. In the illustrations, TC denotes Tiva Canyon member, BT stands for bedded tuffs, which includes the Yucca Mountain and Pah Canyon members, and TS denotes the Topopah Springs member of the Paintbrush Tuff. In each case alluvium has been assigned a low velocity of less than 1.5 km/sec, and the Tiva Canyon member of the Paintbrush Tuff was assigned either 1.5 km/sec or 2.3 km/sec, depending on the degree of welding. Bedded tuffs were given velocities of 2.3 km/sec, the upper part of the Topopah Springs tuff was assigned 3.1 km/sec (the TSw1 thermal stratigraphic unit of Ortiz et al., 1985) and the lower part 3.9 km/sec (TSw2 unit of Ortiz et al., 1985).

For each station we present three examples of the uphole data, downhole data, and calculated downhole response based on the seismic model, for both vertical and radial

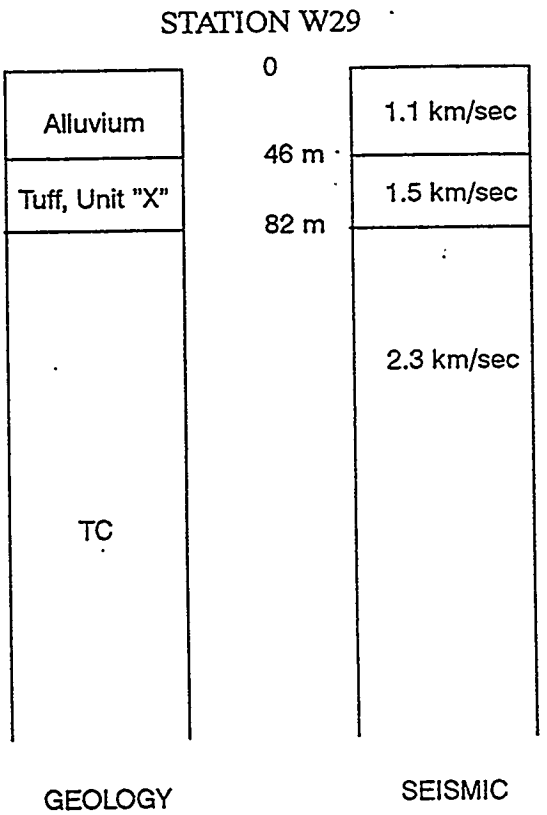

Figure 14: P-wave velocity model for station 29, located to the east of the Yucca Mountain block. Downhole station is located at 82 m depth. TC denotes Tiva Canyon Member of the Paintbrush Tuff.

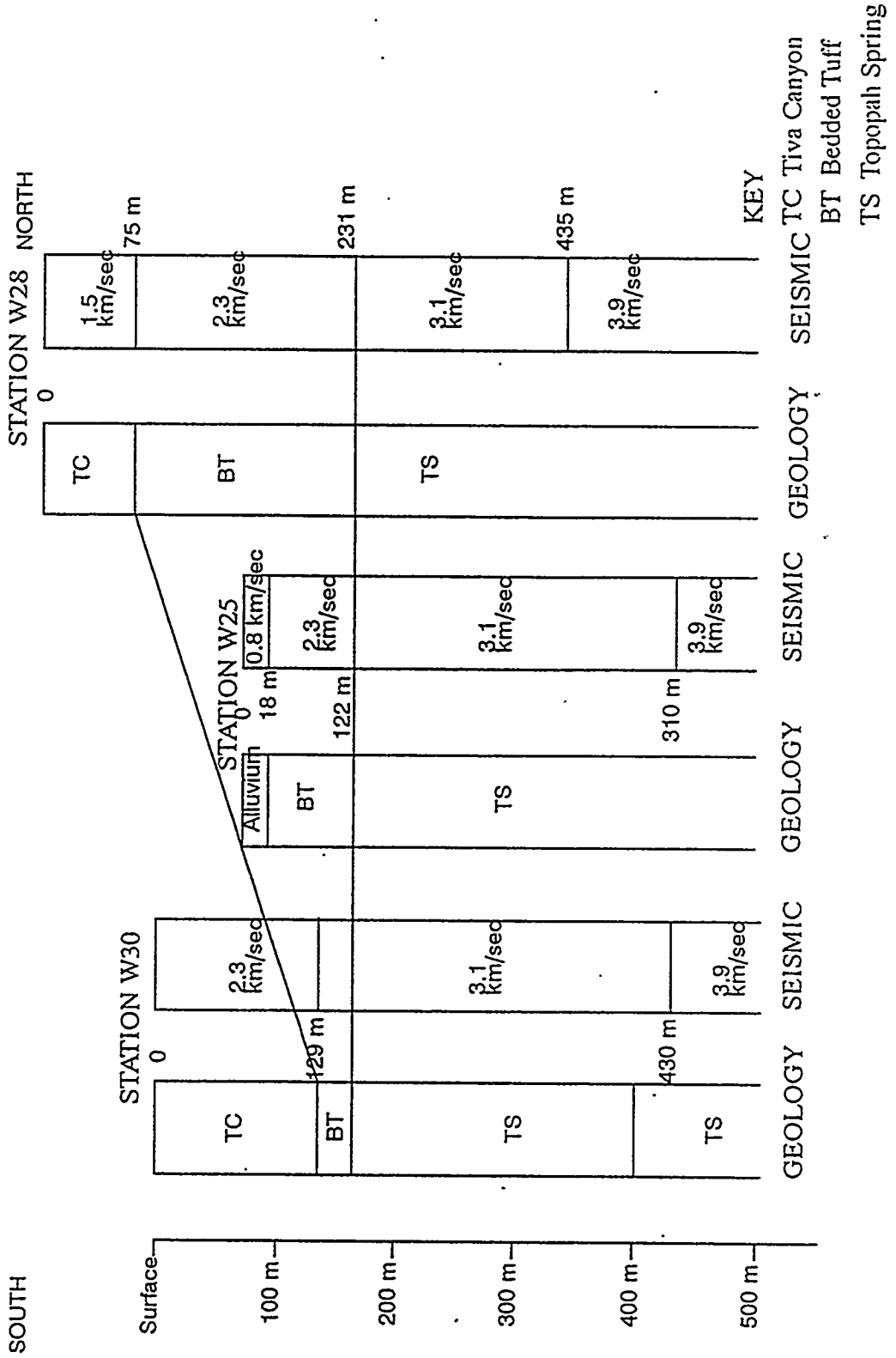

Figure 15: One-dimensional P-wave velocity models representing the near-surface seismic velocities for the three Yucca Mountain borehole stations (from south to north) 30, 25, and 28. Downhole station depths are 352m, 358m (305m after 4/87), and 375m (358m after 4/87), respectively. Depth scale is shown separately for each hole.

Station	Rock Type	Thickness km	Depth km	P-wave velocity km/s	S-wave velocity km/s
28	Alluvium	0.0	0.0	N/A	N/A
	Tiva Canyon	0.075	0.075	1.50	1.07
	Bedded Tuff	0.156	0.231	2.30	1.33
	Topopah Spg. (Tsw1)	0.204	0.435	3.10	1.79
	Topopah Spg. (Tsw2)	1.000	1.435	3.90	2.25
25	Alluvium	.018	0.018	0.7	0.4
	Tiva Canyon	0.0	0.0	N/A	N/A
	Bedded Tuff	0.122	0.140	2.30	1.64
	Topopah Spg. (Tsw1)	0.170	0.310	3.10	1.79
	Topopah Spg. (Tsw2)	0.101	0.411	3.90	2.25
30	Alluvium	0.0	0.0	N/A	N/A
	Tiva Canyon/ Bedded Tuff	0.129	0.129	2.30	1.33
	Topopah Spg. (Tsw1)	0.301	0.430	3.10	1.79
	Topopah Spg. (Tsw2)	1.000	1.430	3.90	2.25
29	Alluvium	0.046	0.046	1.10	0.64
	Unit "X"	0.036	0.082	1.50	0.87
	Tiva Canyon	1.000	1.082	2.30	1.33

Table 4: One-dimensional velocity models: stations 28, 25, 30, and 29.

components of motion. The transfer functions were computed based on incoming compressional energy alone. The data fits for the vertical component data are quite good; the radial component data fits, while generally not as good, are also acceptable in terms of overall ground motion amplitude and frequency content. These data examples demonstrate that simple one-dimensional models are sufficient for understanding of the general differences between the observed uphole and downhole data for each borehole.

Station 29

Yucca Mountain station 29 is located east of the mountain block near the proposed location for the repository surface facilities in hole UE-25 RF#4 (Figure 2). The site geology is relatively simple, with 46m of alluvium overlying 35m of nonwelded Unit "X" tuff over the Tiva Canyon member of the Paintbrush tuff (Gibson et al., 1992). The downhole accelerometer was located 82m below the surface, just below the boundary between Unit "X" and the Tiva Canyon. A schematic of the hole geology and the final model is shown in Figure 14. Table 4 contains the complete specification of the model. The alluvium was assigned a P-wave velocity of 1.1 km/sec, the Unit "X" tuff a velocity of 1.5 km/sec, and the Tiva Canyon unit a velocity of 2.3 km/sec. The S-wave velocities for this hole are set using a Poisson's ratio of 0.25. The simple two-layer over a halfspace model matches the observed data quite well, as shown in the Figures 16-21 for three sample events. The vertical simulated downhole records match the observed data nearly perfectly for the Pahute Mesa events Belmont and Kearsarg; the predicted downhole record for the Yucca Flat event Tahoka has the proper waveshape with an overall amplitude level that is slightly too large. The radial component simulated downhole data also match the actual records quite well in both amplitude and frequency content for both source areas. The excellent match between the synthetic downhole records and the actual accelerograms demonstrate the consistency of the recorded data and the validity of the modeling approach.

Station 28

Station 28 occupied drillhole USW G-2 (see Figure 2 for location). Maldonado and Koether (1983) describe the geological units encountered in the hole. This station is at the northern end of the north-south profile through the Yucca Mountain ridge defined by stations 28, 25, and 30 (see Figure 15). The downhole accelerometer was located at 375m depth until April, 1987; it was then moved to 358m depth until the instrumentation was removed in 1990. While detailed geological information is available for hole G-2, we found no reliable seismic velocity measurements to use in developing an initial model. The ultrasonic log for the nearby hole G-1 (station 25; Muller and Kibler, 1983) contained no resolvable velocity information for the uppermost 350m. We used the seismic velocity log for nearby hole G-4 (Spengler,

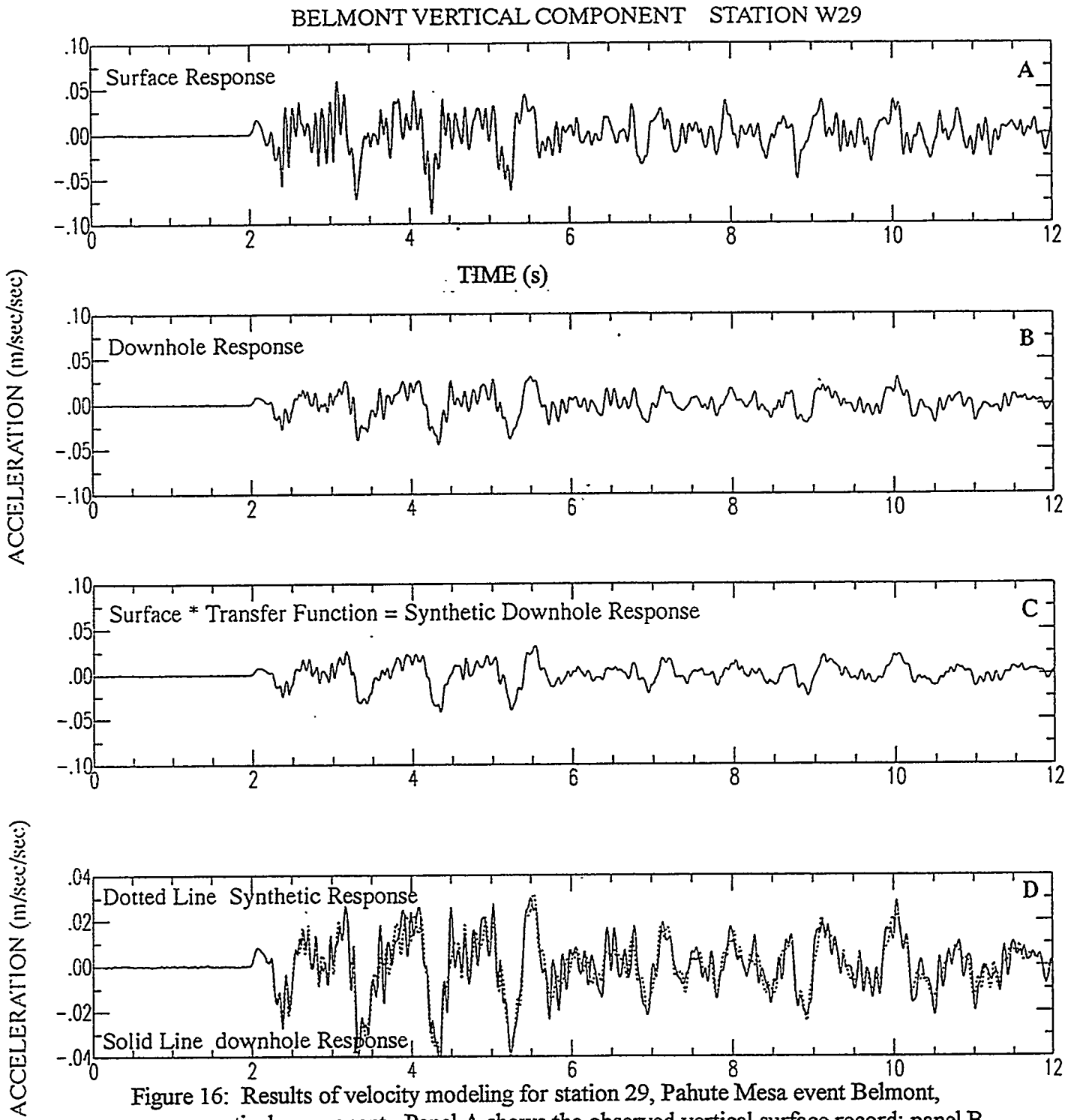

Figure 16: Results of velocity modeling for station 29, Pahute Mesa event Belmont, vertical component. Panel A shows the observed vertical surface record; panel B is the observed downhole record. Panel C displays the synthetic downhole response obtained by convolving the transfer function generated from the velocity model in Figure 14 with the observed surface record in panel A. Panel D is an overlay of the observed and synthetic downhole traces. The dotted line is the synthetic response and the solid line is the data.

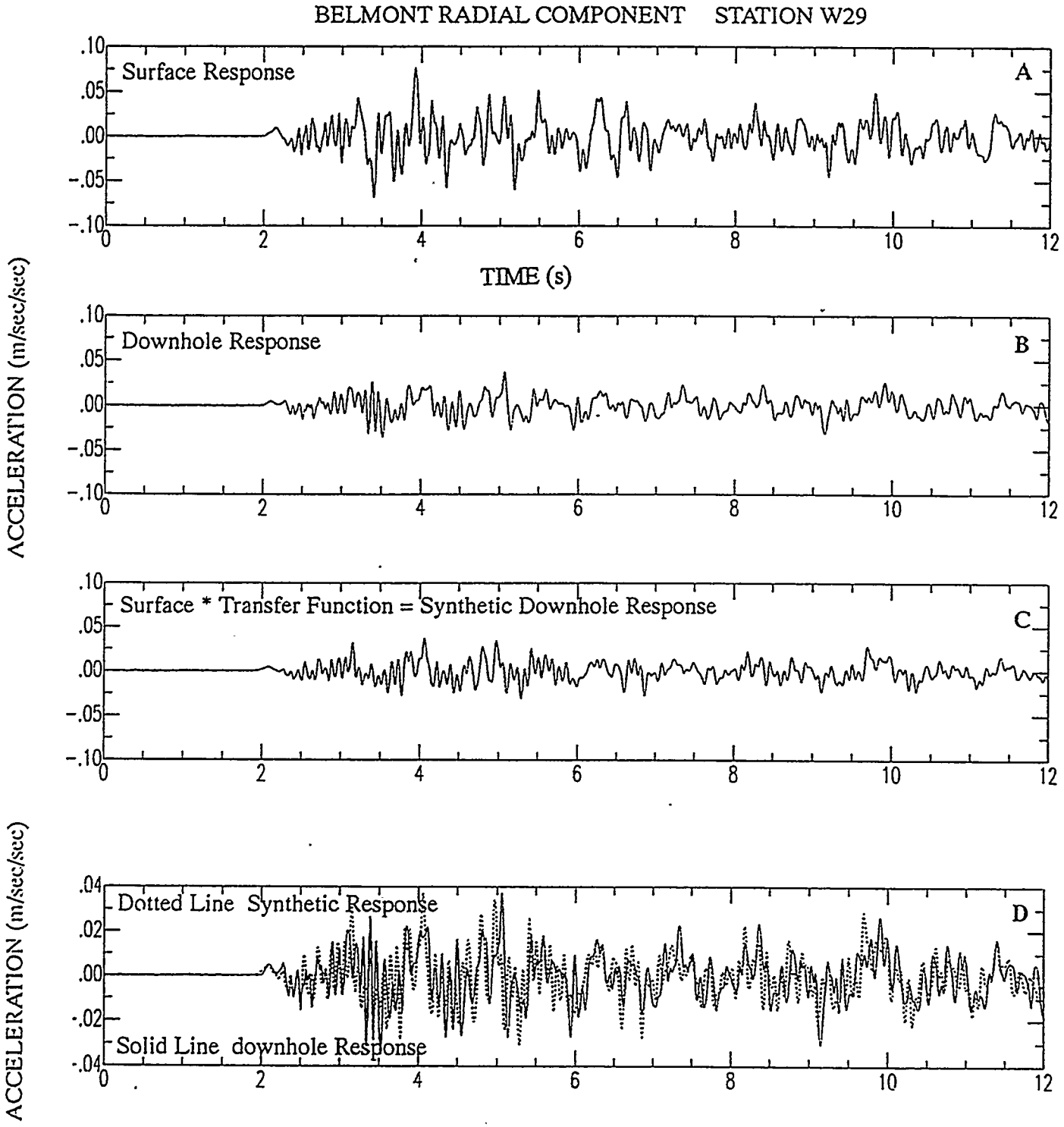

Figure 17: Results of velocity modeling for station 29, Pahute Mesa event Belmont, radial component. Figure layout is the same as figure 16.

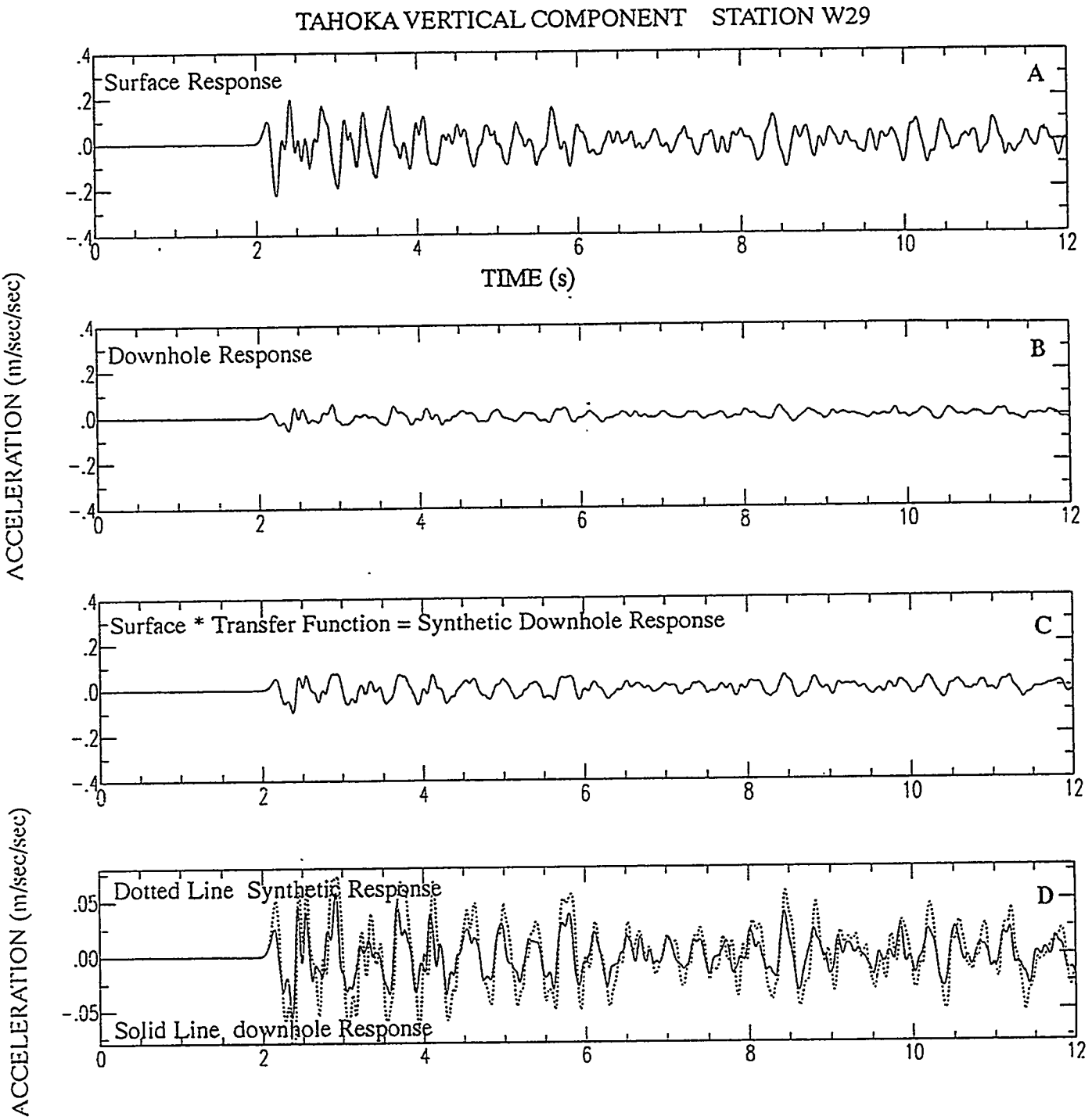

Figure 18: Results of velocity modeling for station 29, Yucca Flat event Tahoka, vertical component. Figure layout is the same as figure 16.

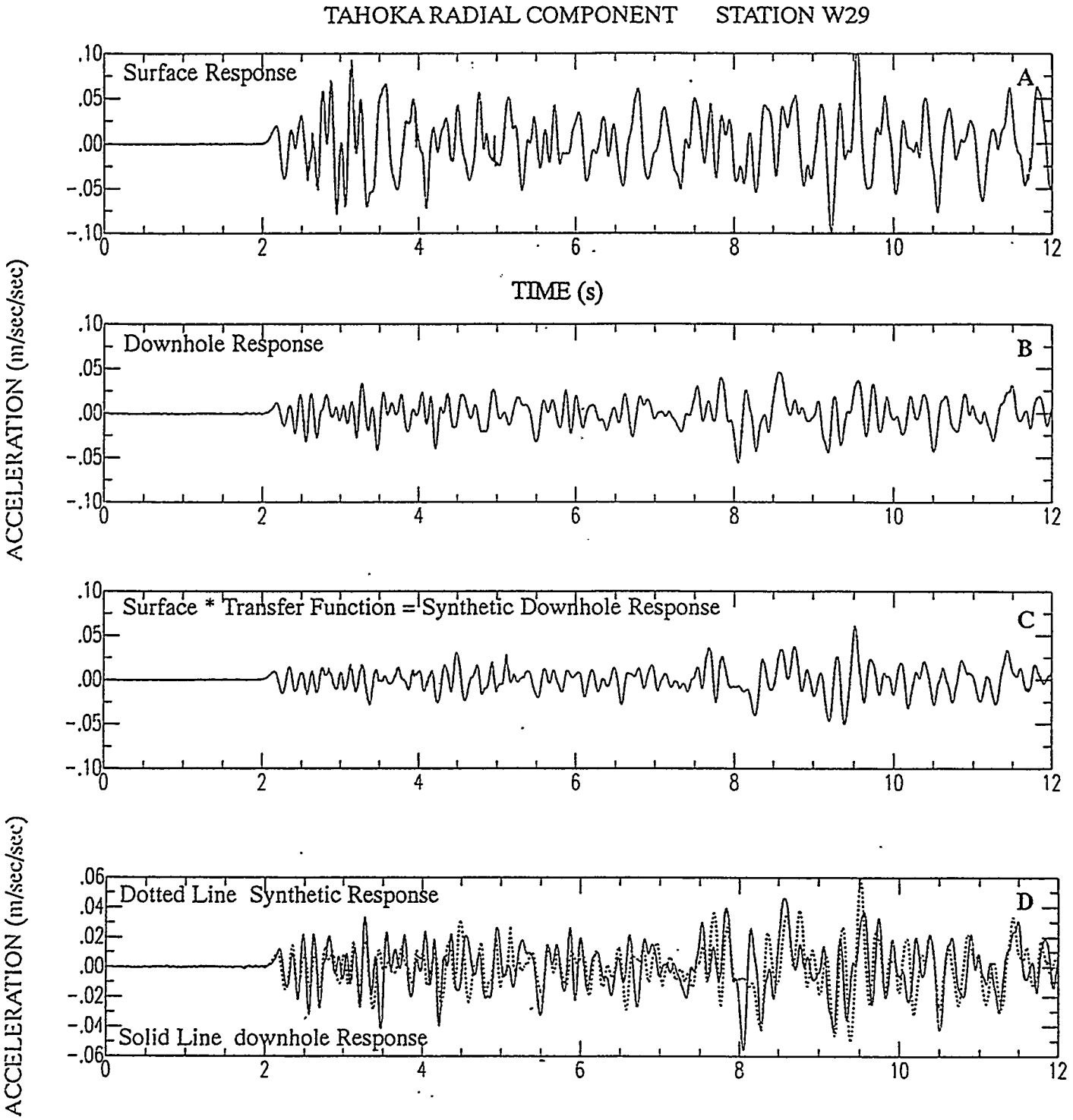

Figure 19: Results of velocity modeling for station 29, Yucca Flat event Tahoka, radial component. Figure layout is the same as figure 16.

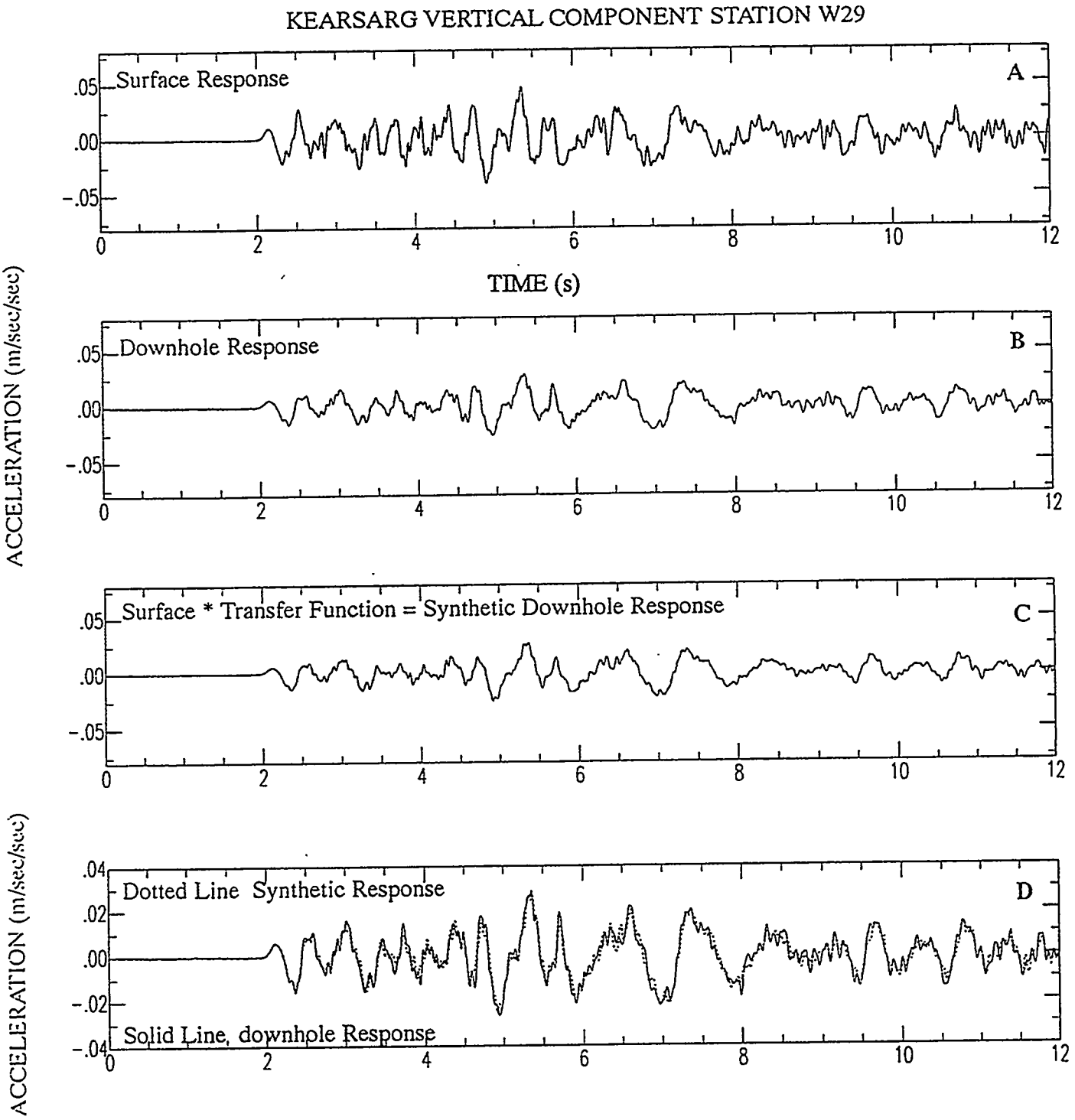

Figure 20: Results of velocity modeling for station 29, Pahute Mesa event Kearsarg, vertical component. Figure layout is the same as figure 16.

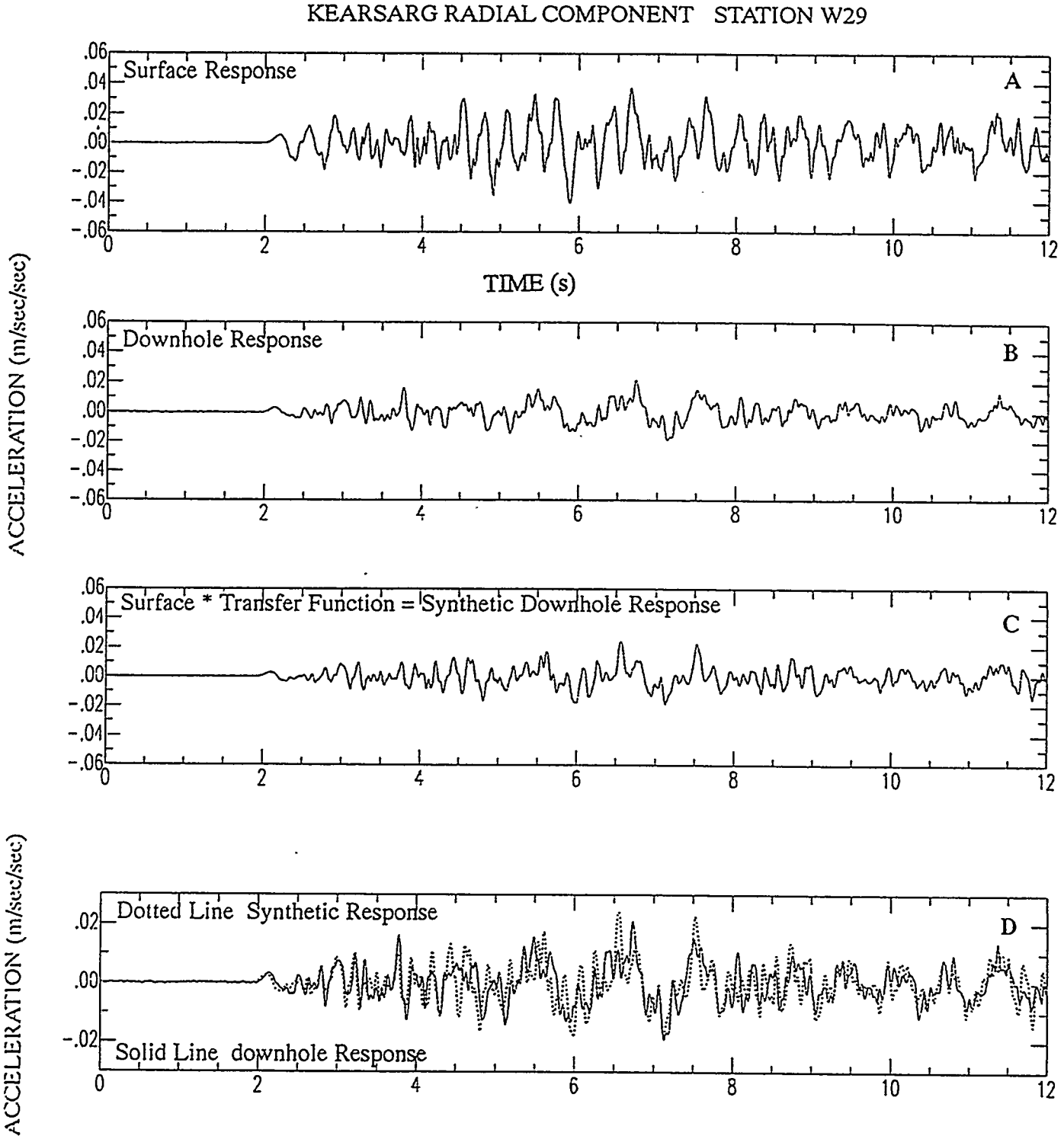

Figure 21: Results of velocity modeling for station 29, Pahute Mesa event Kearsarg, radial component. Figure layout is the same as figure 16.

Chornack, Muller and Kibler, 1984) coupled with the geological information for the hole to tentatively assign compressional velocities to specific geologic units. Tying the velocities to the thermal stratigraphic units of Ortiz et al. (1985) was also useful in assuring consistency among the three deeper boreholes.

The model for station 28 has several layers that correlate to the thermal stratigraphic units of Ortiz et al. (1985). The Tiva Canyon tuff (TCw thermal stratigraphic unit) is 1.5 km/sec; the Yucca Mountain and Pah Canyon members (PTn thermal stratigraphic unit) are assigned 2.3 km/sec, and the two thermal stratigraphic units corresponding to the Topopah Springs member, TSw1 and TSw2, are assigned velocities of 3.1 and 3.9 km/sec, respectively. The Tiva Canyon member of the Paintbrush Tuff, which tops the hole, is quite slow where measured in Midway Valley (see Gibson et al., 1992); this is consistent with the value of 1.5 km/sec found here. The velocity of the Topopah Springs member is variable, depending on the degree of welding and lithophysal content (Spengler, Chornack, Muller and Kibler, 1984), but the modeling process revealed it to be relatively homogeneous at the wavelengths sampled here, thus we differentiate only between the two major thermal stratigraphic units. The model for station 28 appears in Figure 15, and three examples of waveform modeling are seen in Figures 22-27. The vertical component downhole records are matched quite well by the synthetics, as seen in Figures 22, 24, and 26. The matches for the radial records are not quite as good (Figures 23, 25, 27), however the overall level of radial ground motion predicted by the transfer function is quite consistent with the observations. The data fits obtained for the Yucca Flat event Dalhart (Figures 26 and 27) are similar in quality to that obtained for the Pahute Mesa events, indicating that a one-dimensional transfer function is adequate for the very shallow structure at this location.

Station 25

Located in drillhole USW G-1, station 25's downhole instrumentation was located at 358m until April, 1987 and thereafter at 305m below the ground surface. According to Spengler et al., (1981), 18m of alluvium is present at the surface, underlain by the Yucca Mountain, Pah Canyon, and Topopah Springs members of the Paintbrush tuff down to a depth of 416m. The hole continues to a depth of 1810m. Some additional information is available from the geophysical logs for this hole (Muller and Kibler, 1983), although the seismic velocities in the upper 305m were deemed unreliable. The density values used in all of the models were determined largely from the work of Lappin et al. (1982); their density measurements were made on rocks from this hole.

Probably due to the presence of the alluvium layer, this station was the most difficult to model. Surface records at station 25 typically have very large amplitudes for Pahute

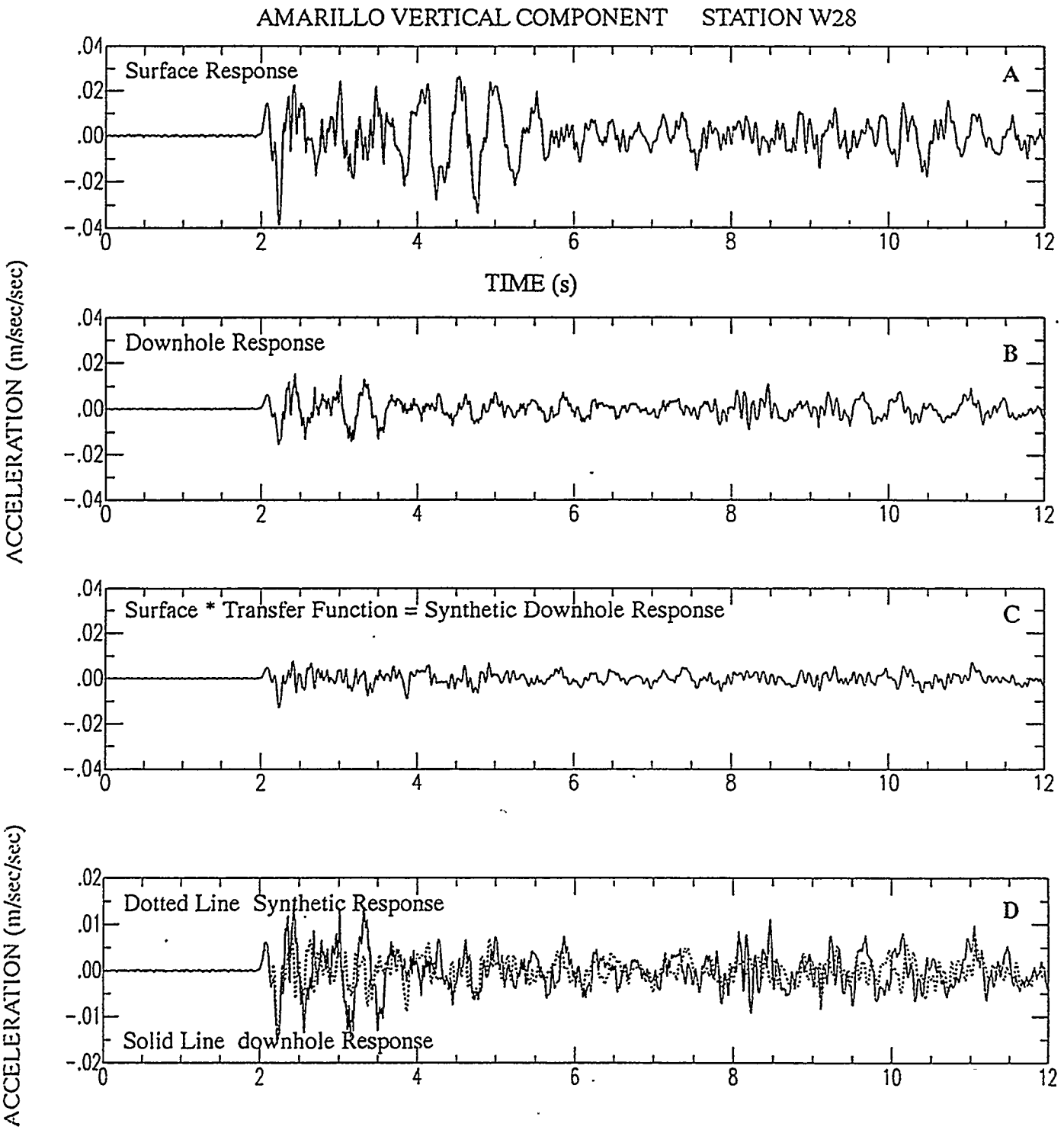

Figure 22: Results of velocity modeling for station 28, Pahute Mesa event Amarillo, vertical component. Figure layout is the same as figure 16.

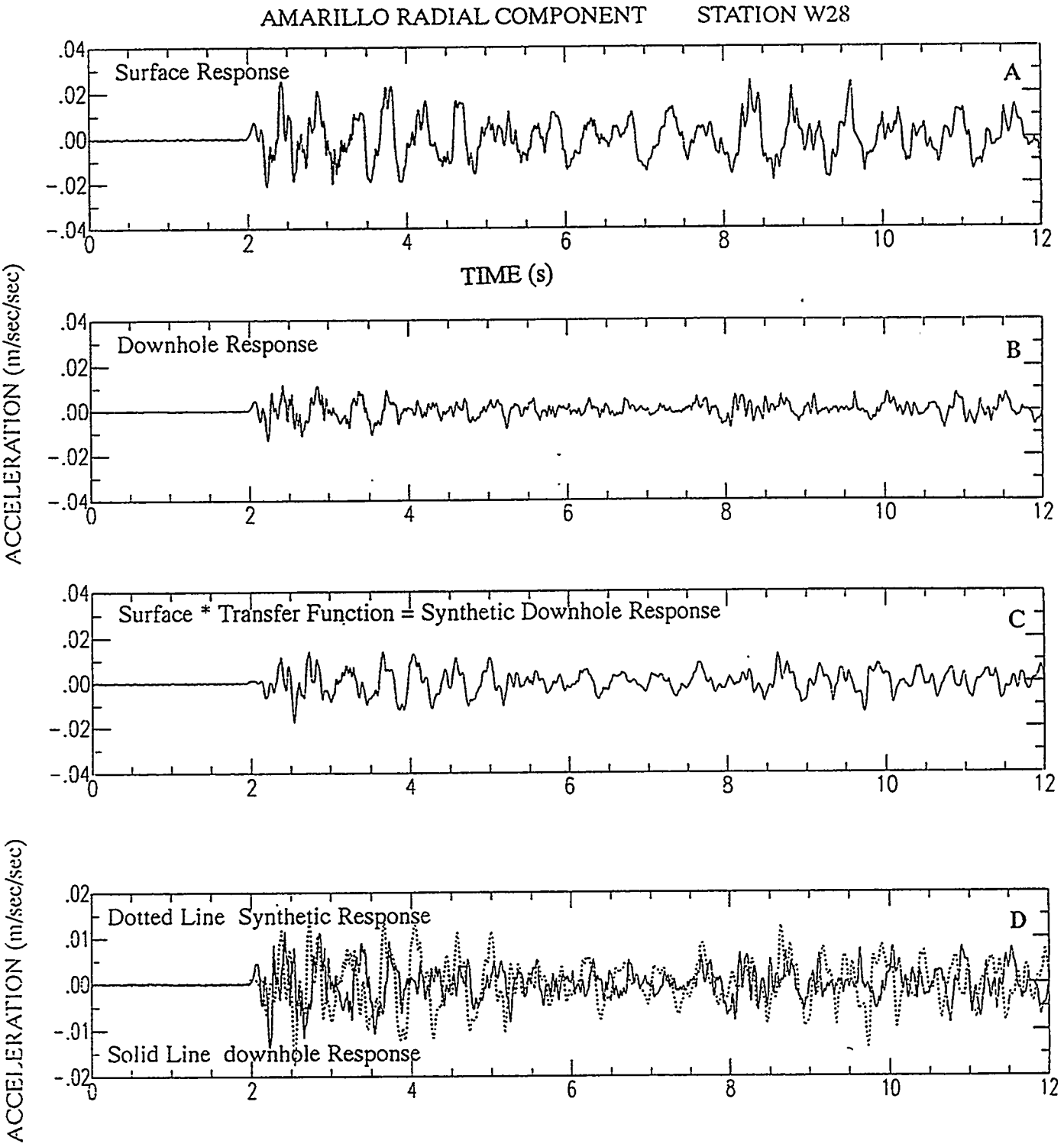

Figure 23: Results of velocity modeling for station 28, Pahute Mesa event Amarillo, radial component. Figure layout is the same as figure 16.

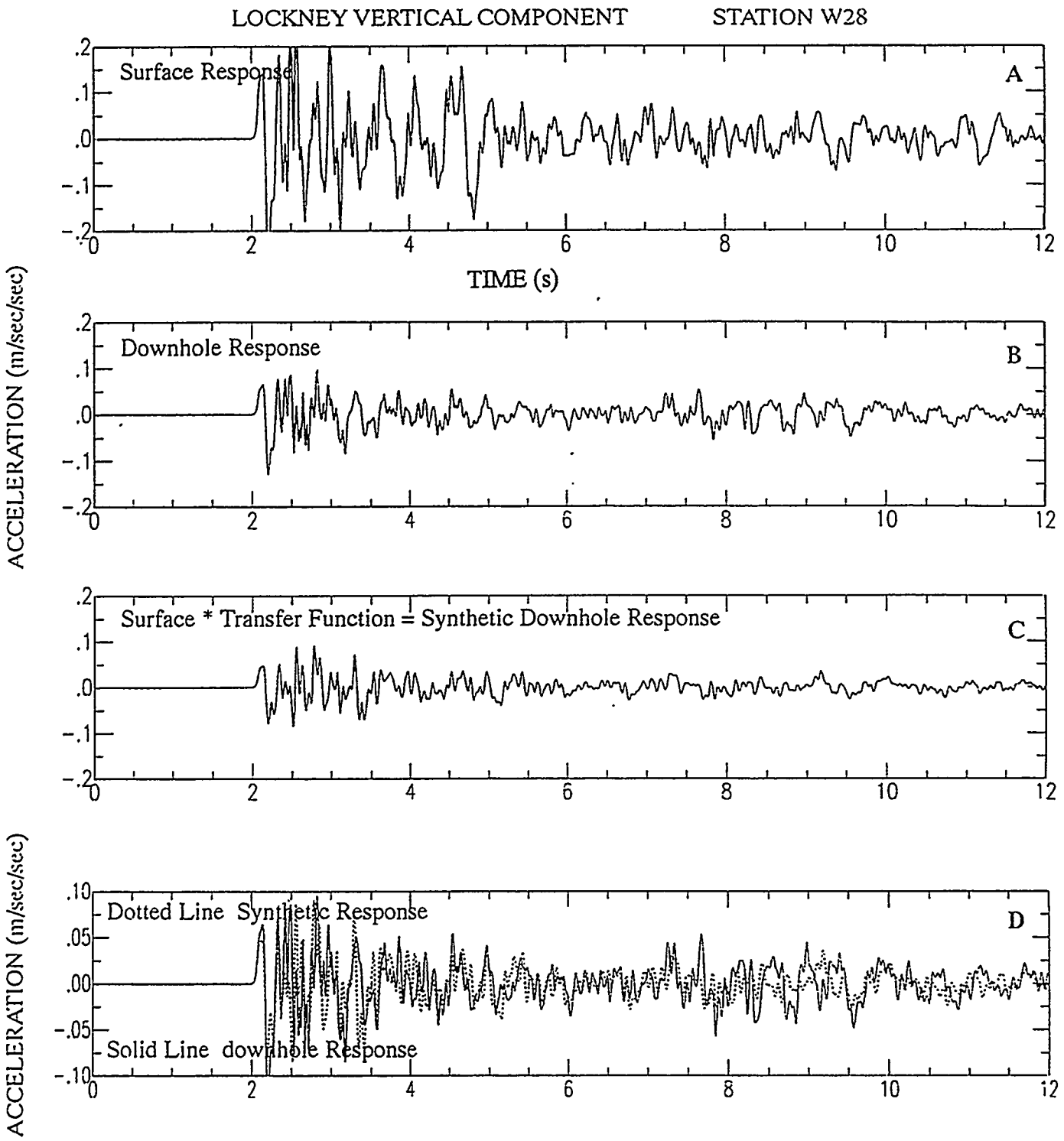

Figure 24: Results of velocity modeling for station 28, Pahute Mesa event Lockney, vertical component. Figure layout is the same as figure 16.

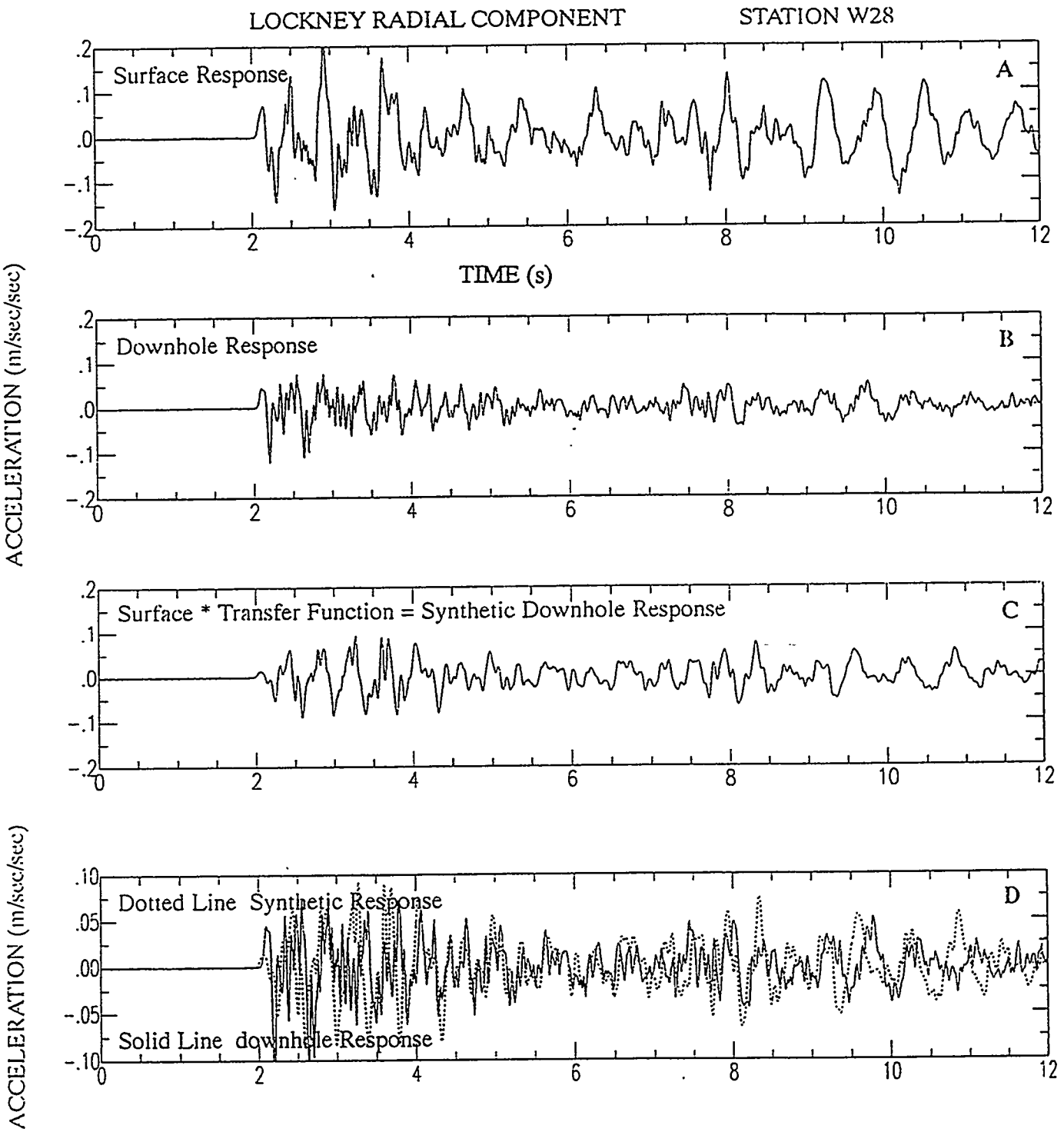

Figure 25: Results of velocity modeling for station 28, Pahute Mesa event Lockney, radial component. Figure layout is the same as figure 16.

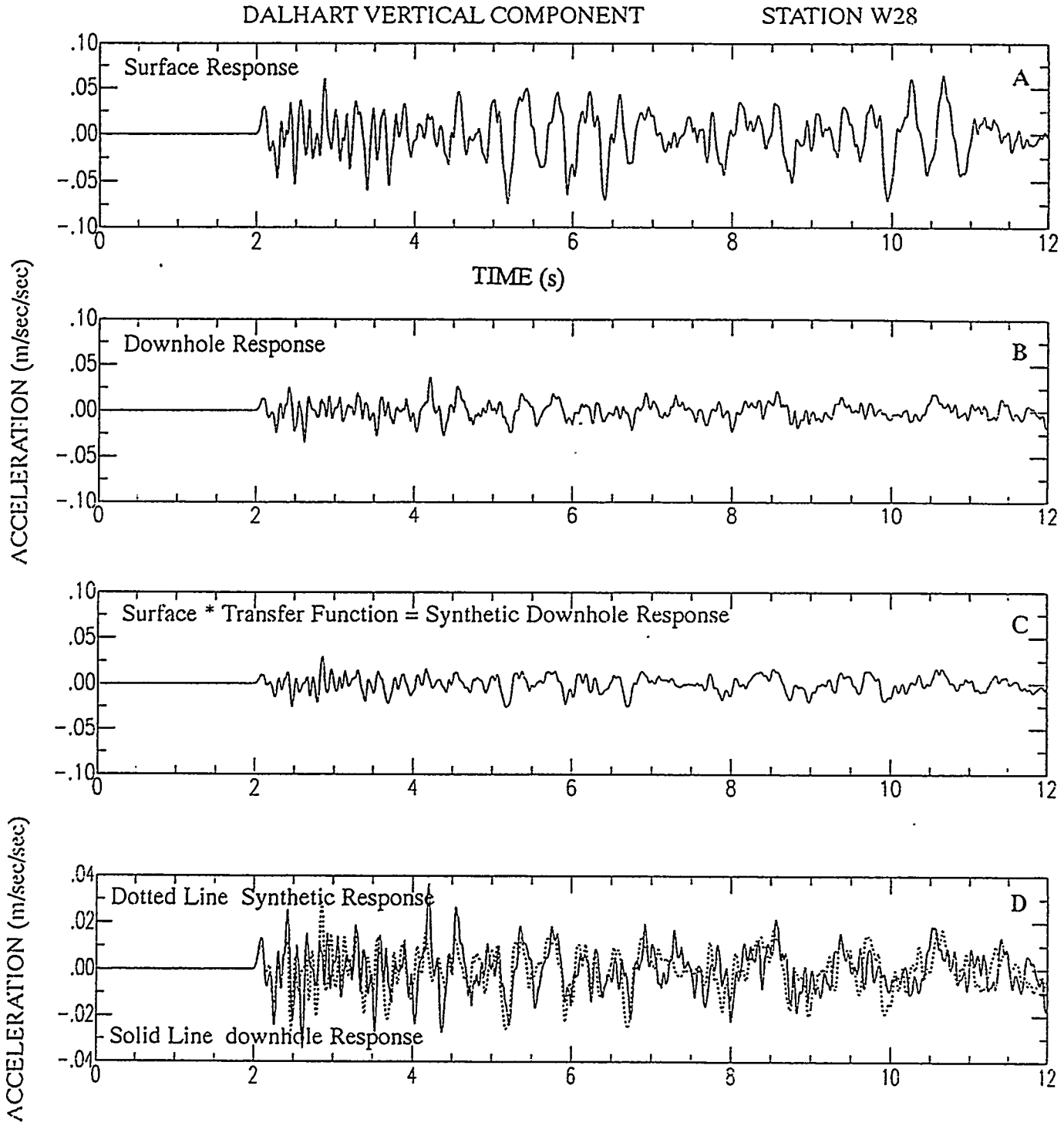

Figure 26: Results of velocity modeling for station 28, Yucca Flat event Dalhart, vertical component. Figure layout is the same as figure 16.

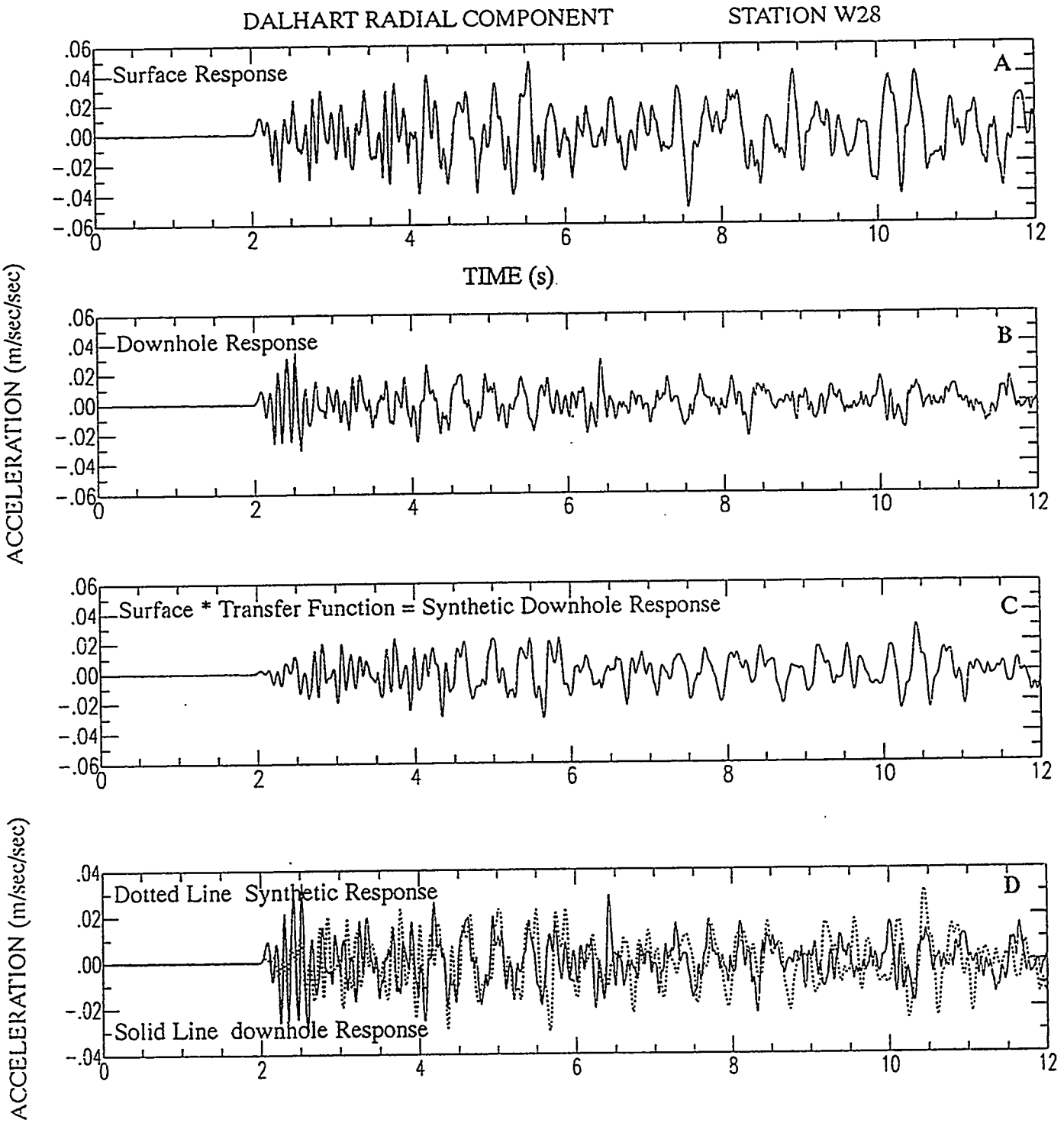

Figure 27: Results of velocity modeling for station 28, Yucca Flat event Dalhart, radial component. Figure layout is the same as figure 16.

Mesa tests, but not for Yucca Flat events. A compressional velocity of 0.7 km/sec was assigned to the alluvium, underlain by a 122m thick layer of 2.3 km/sec representing the Yucca Mountain and Pah Canyon members (PTn thermal stratigraphic unit). The TSw1 and TSw2 thermal stratigraphic units of the Topopah Springs unit were assigned 3.1 km/sec and 3.9 km/sec, respectively. This model (Figure 15; Table 4) works fairly well at predicting the downhole records from the surface data (Figures 28-32), however, the data fits are not as good for station 25 as they are for the other stations, particularly for the vertical component records. For the vertical component, the synthetic downhole first arrival amplitudes (about the first 0.5 second of waveform) are very well matched. The fit degrades farther into the record, with the synthetic waveform often somewhat larger than the data. The detailed waveshapes of the radial records are not particularly well-matched, although the overall amplitudes predicted by the transfer function are quite reasonable. We attempted to improve the fit of the radial records by trying different Poisson's ratios, consistent with the results of Daley and Majer (written communication, 1995), however the results are still not ideal. The final model has a Vp/Vs ratio of 1.35 for the alluvium layer and 1.40 for the bedded tuffs before returning to typical 1.73 for the deeper portion of the model.

Station 30

The geology for the shallow portion of hole USW G-3 (station 30, Figure 2) is relatively simple, with the Tiva Canyon member overlaying the Topopah Springs member of the Paintbrush Tuff (Scott and Castellanos, 1984). We found that a simple model with velocities of 2.3 km/sec for the Tiva Canyon and 3.1 km/sec and 3.9 km/sec for the Topopah Springs member does a good job predicting the downhole records at 352m depth (Figure 15). The Tiva Canyon was given a faster velocity at the station 30 location than for stations 28 and 29 based on faster travel times between the downhole and uphole instruments. Also, Scott and Castellanos (1984) observed that at USW G-3, the non-welded upper portion of the Tiva Canyon is missing and only the welded lower portion (with faster velocity) is present. The Topopah Springs members were assigned the same velocities as for the other stations, but not strictly in alignment with the Ortiz et al. (1985) depths for thermal stratigraphic units. Ortiz et al. (1985) define the TSw1/TSw2 boundary to be at 210m depth in this hole, but our modeling indicates that the faster velocity material must be located deeper, and we make the velocity transition at 430m depth (Figure 15; Table 4). The simple model for station 30 does an excellent job of predicting the vertical observed downhole vertical waveforms for events from both Pahute Mesa and Yucca Flat (Figures 34, 36, and 38). The radial component waveforms are not fit as well. In particular, for event Hermosa (Yucca Flat) the overall amplitude of the downhole radial record is overpredicted by this model. The overall amplitude response for the Pahute Mesa events is better, however the waveform fits are not particularly good. Attempts

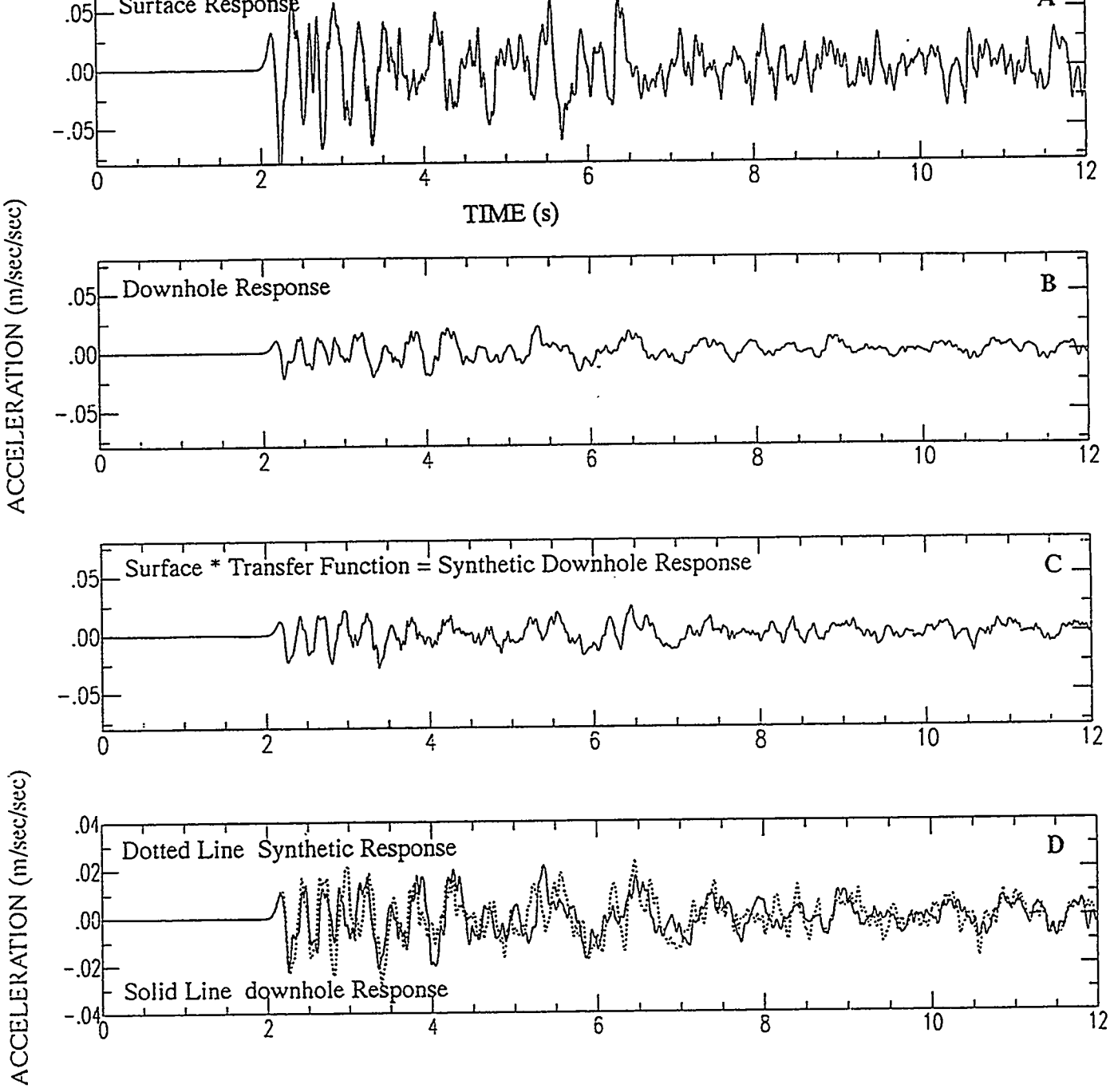

Figure 28: Results of velocity modeling for station 25, Pahute Mesa event Kearsarg, vertical component. Figure layout is the same as figure 16.

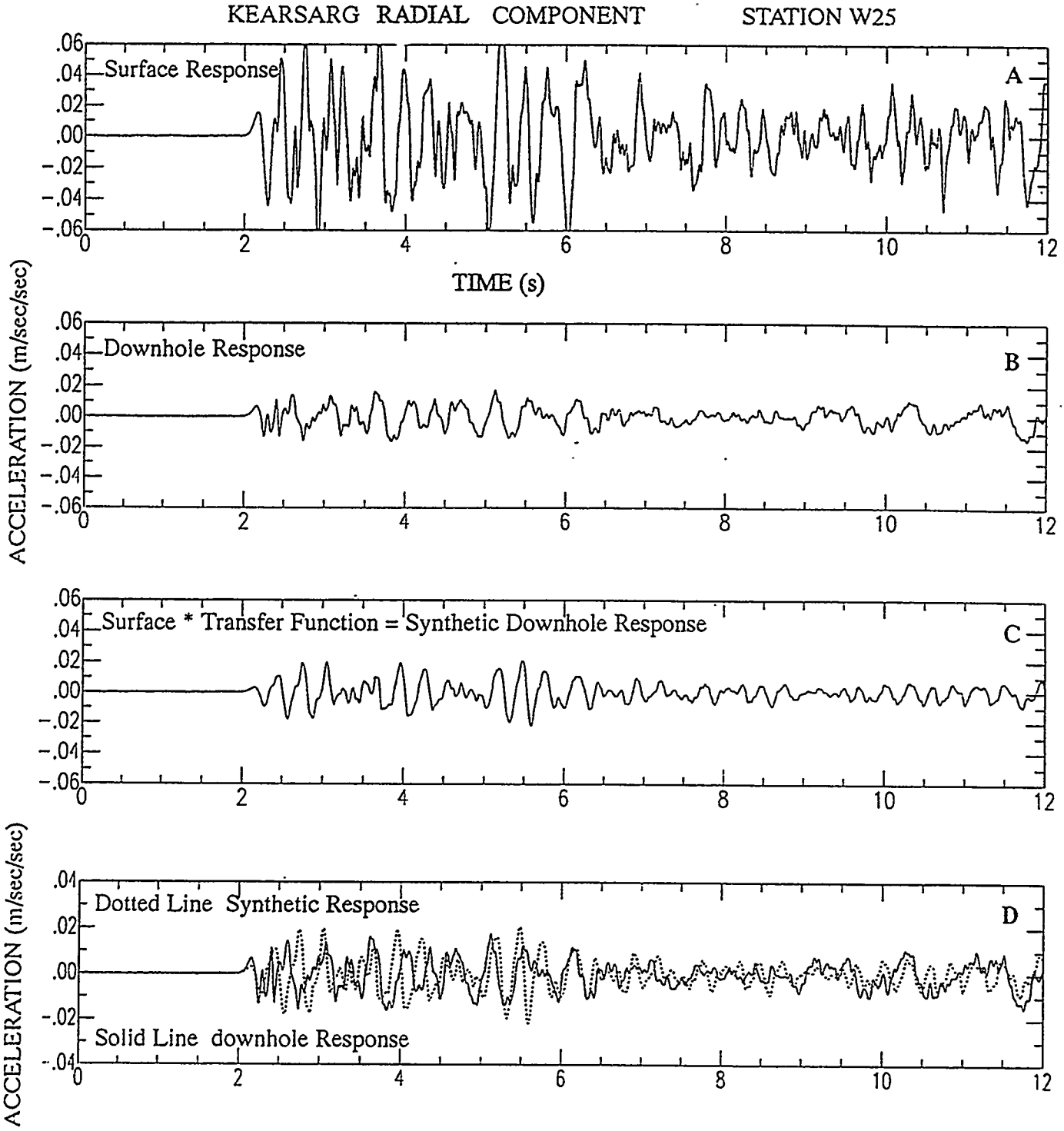

Figure 29: Results of velocity modeling for station 25, Pahute Mesa event Kearsarg, radial component. Figure layout is the same as figure 16.

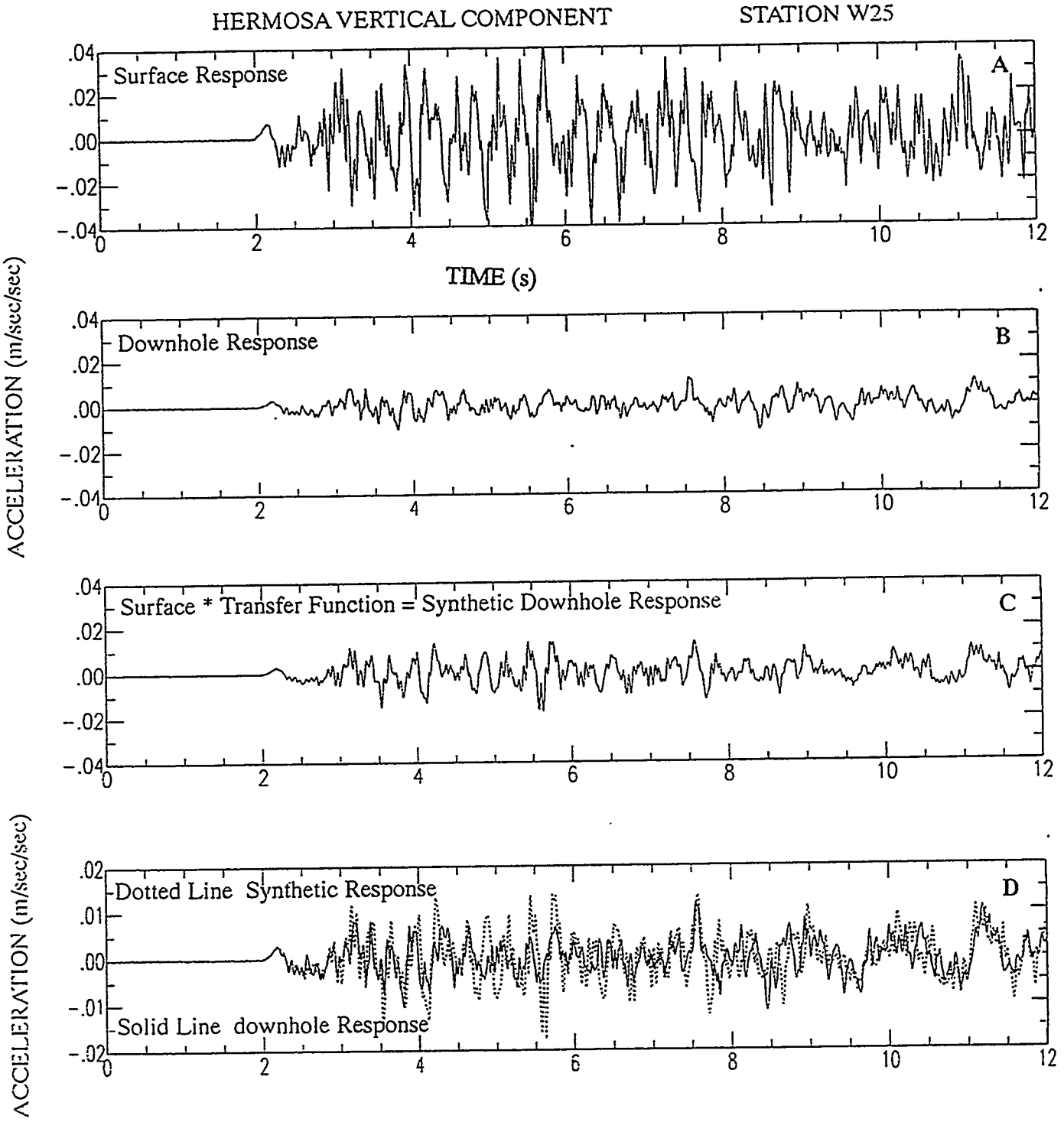

Figure 30: Results of velocity modeling for station 25, Yucca Flat event Hermosa, vertical component. Figure layout is the same as figure 16.

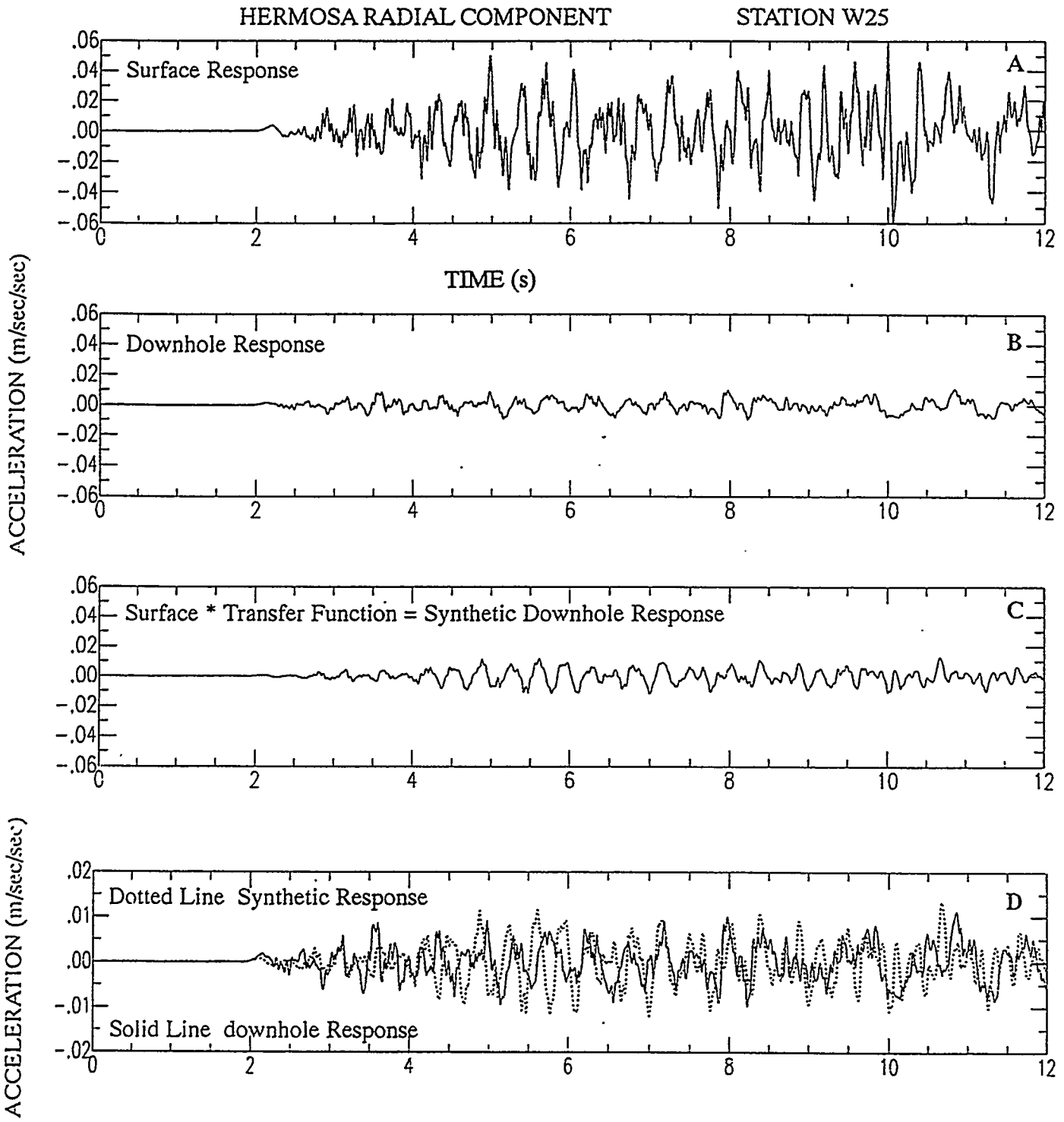

Figure 31: Results of velocity modeling for station 25, Yucca Flat event Hermosa, radial component. Figure layout is the same as figure 16.

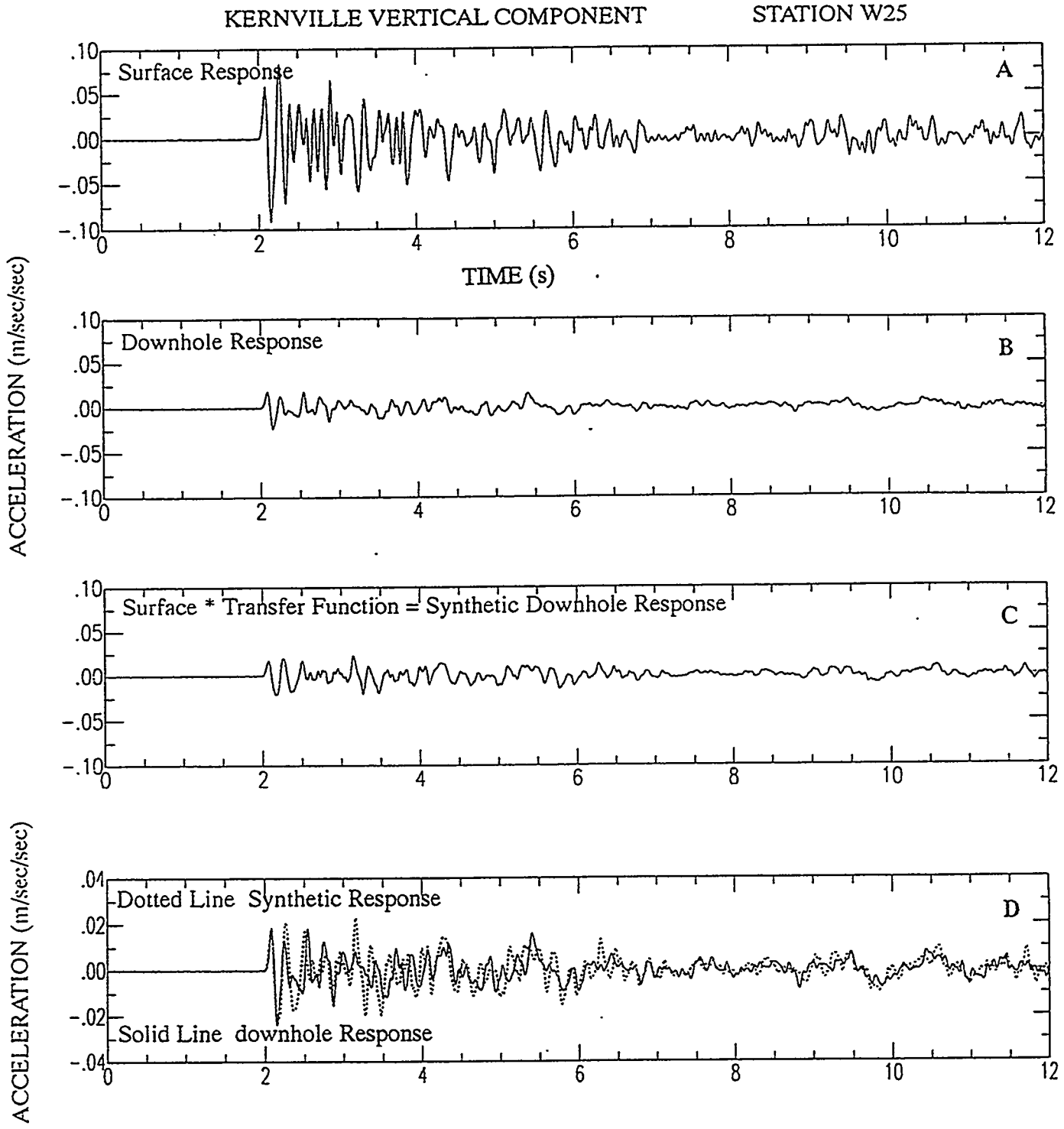

Figure 32: Results of velocity modeling for station 25, Pahute Mesa event Kernville, vertical component. Figure layout is the same as figure 16.

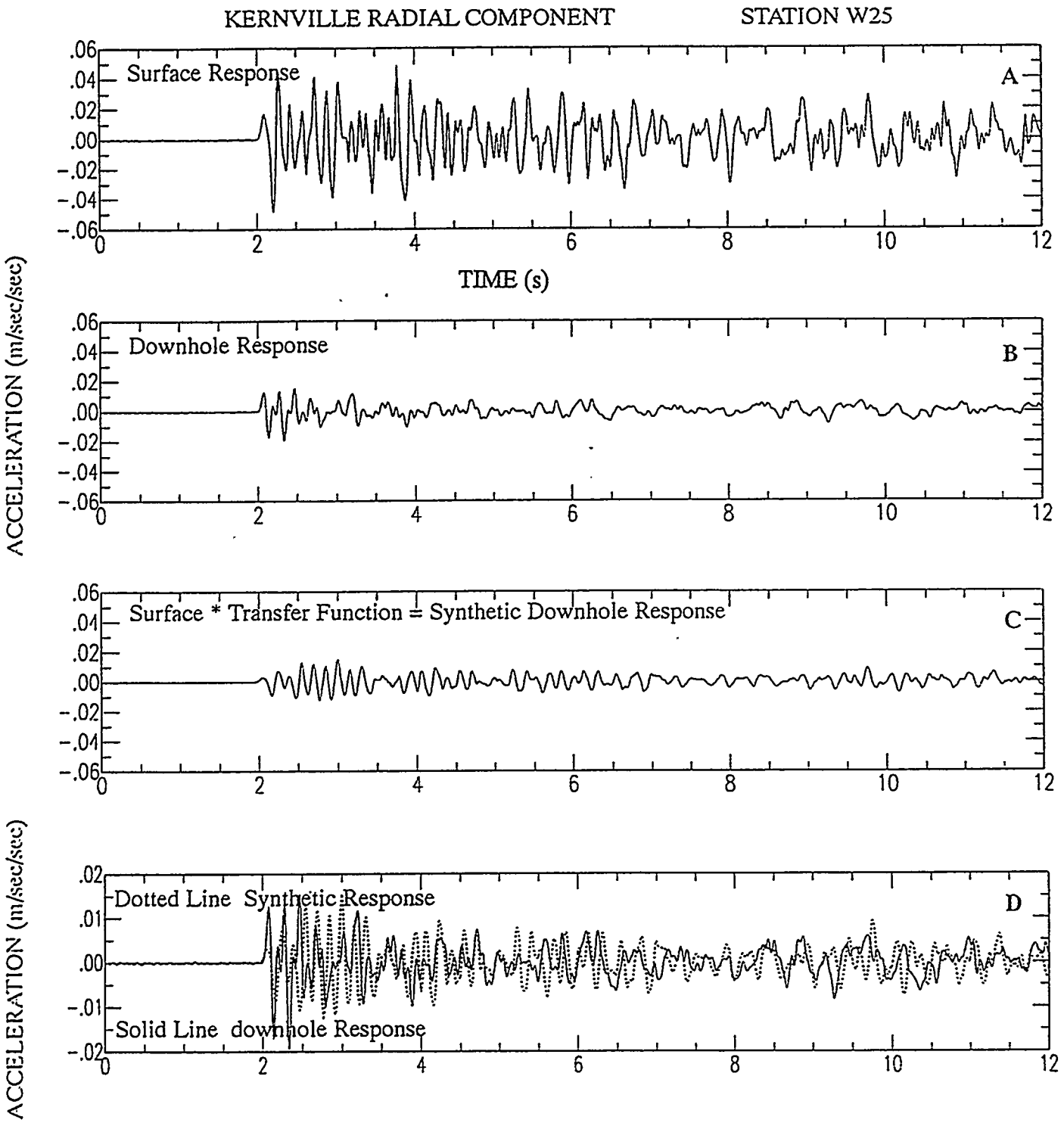

Figure 33: Results of velocity modeling for station 25, Pahute Mesa event Kernville, radial component. Figure layout is the same as figure 16.

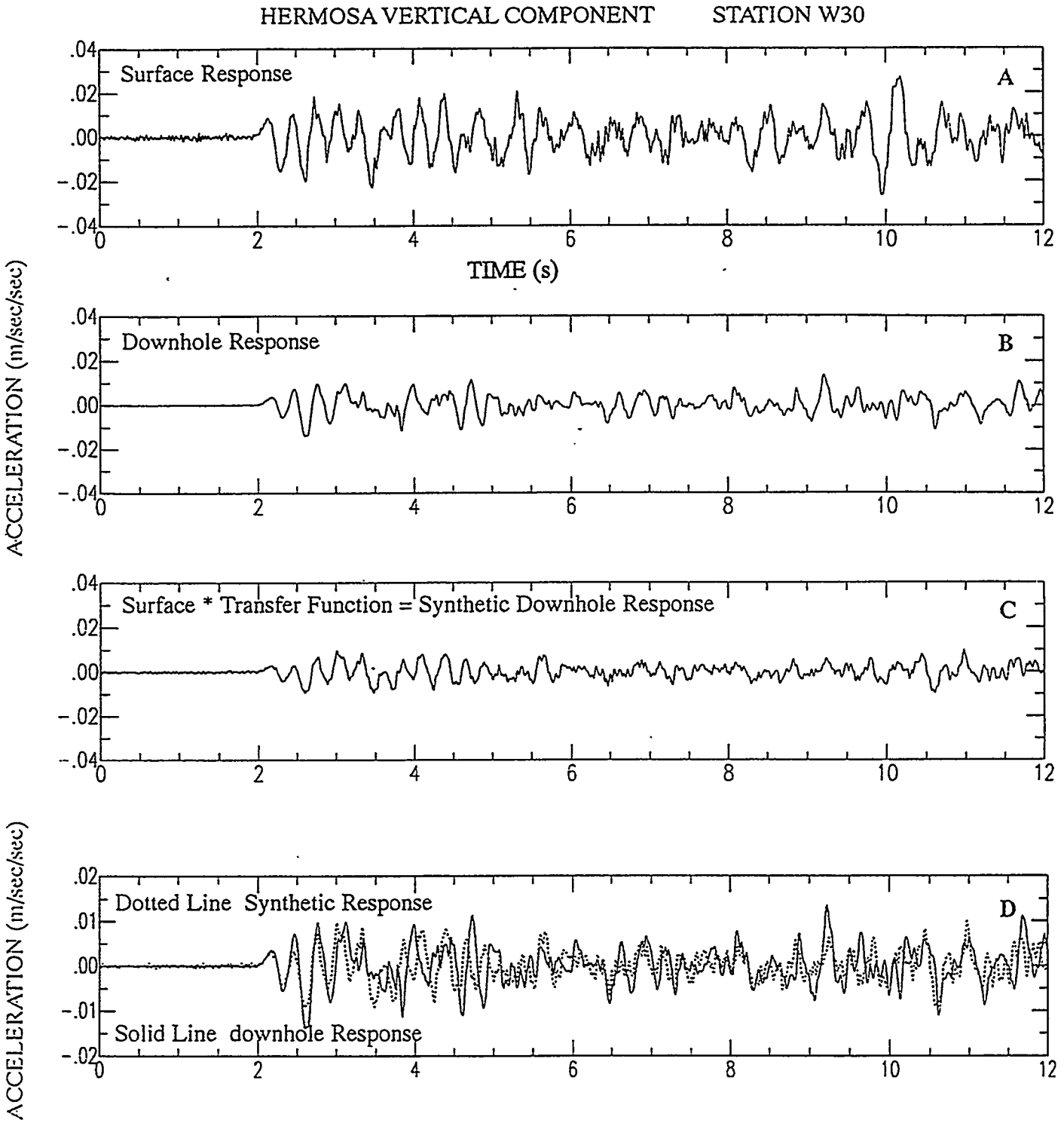

Figure 34: Results of velocity modeling for station 30, Yucca Flat event Hermosa, vertical component. Figure layout is the same as figure 16.

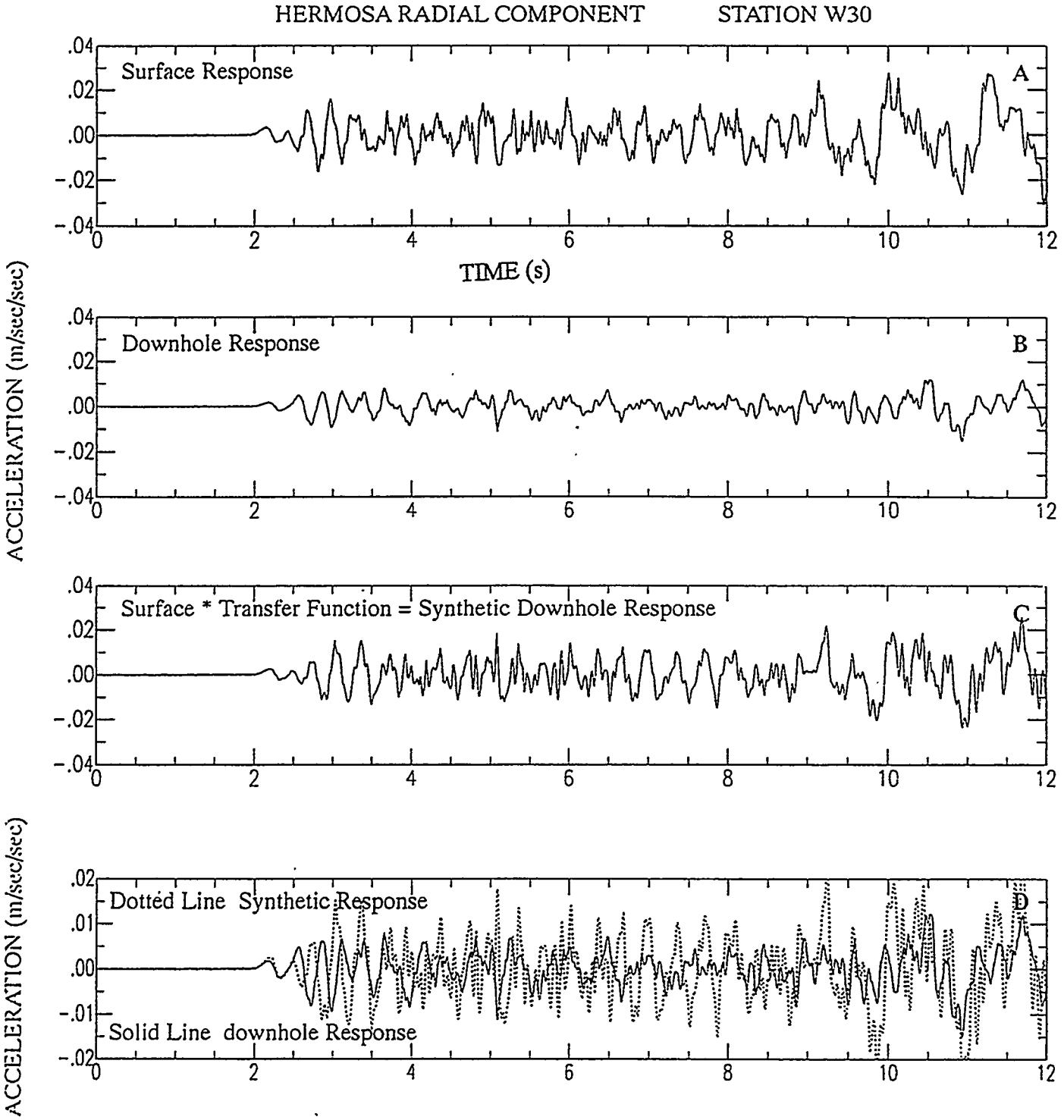

Figure 35: Results of velocity modeling for station 30, Yucca Flat event Hermosa, radial component. Figure layout is the same as figure 16.

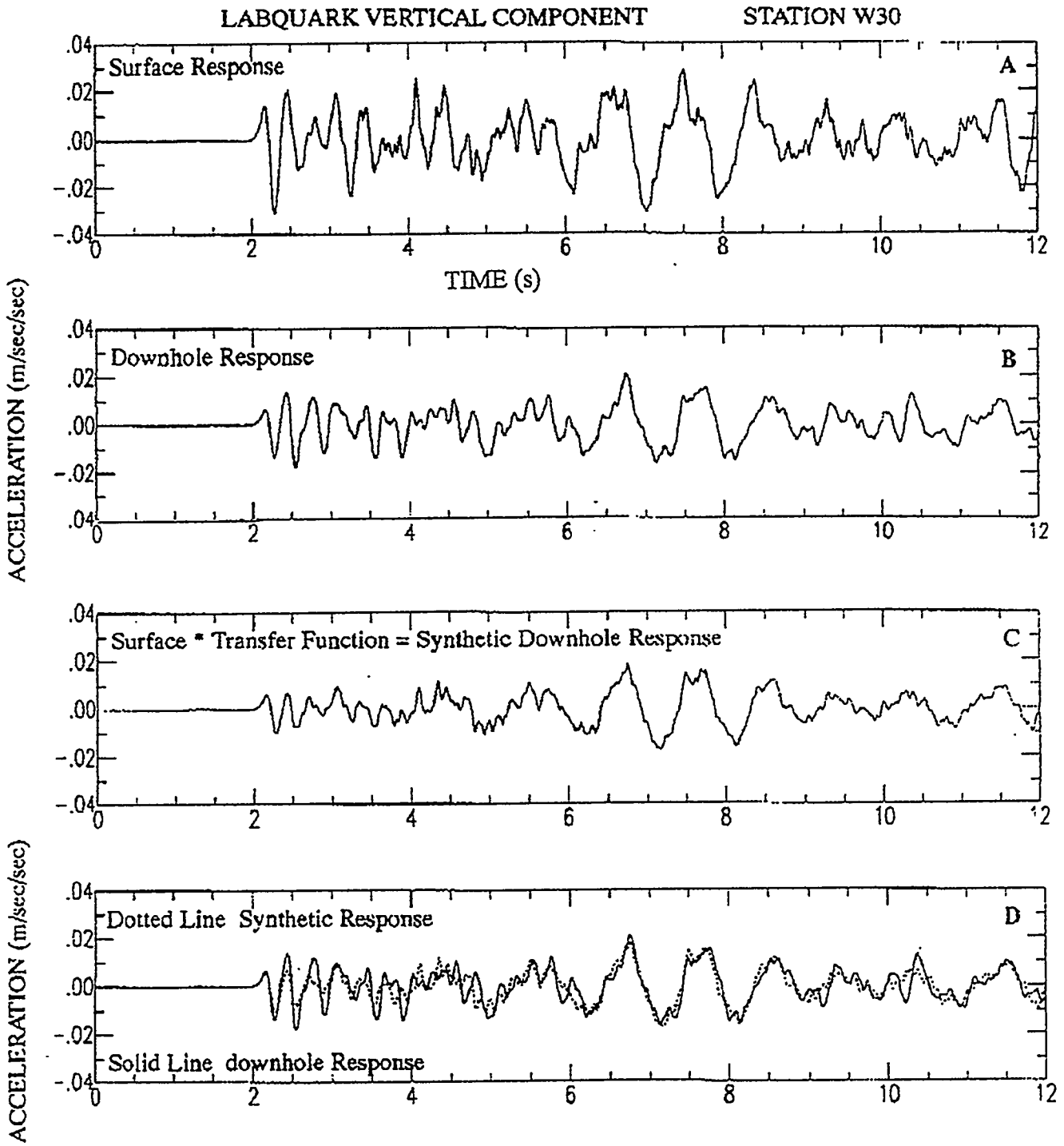

Figure 36: Results of velocity modeling for station 30, Pahute Mesa event Labquark, vertical component. Figure layout is the same as figure 16.

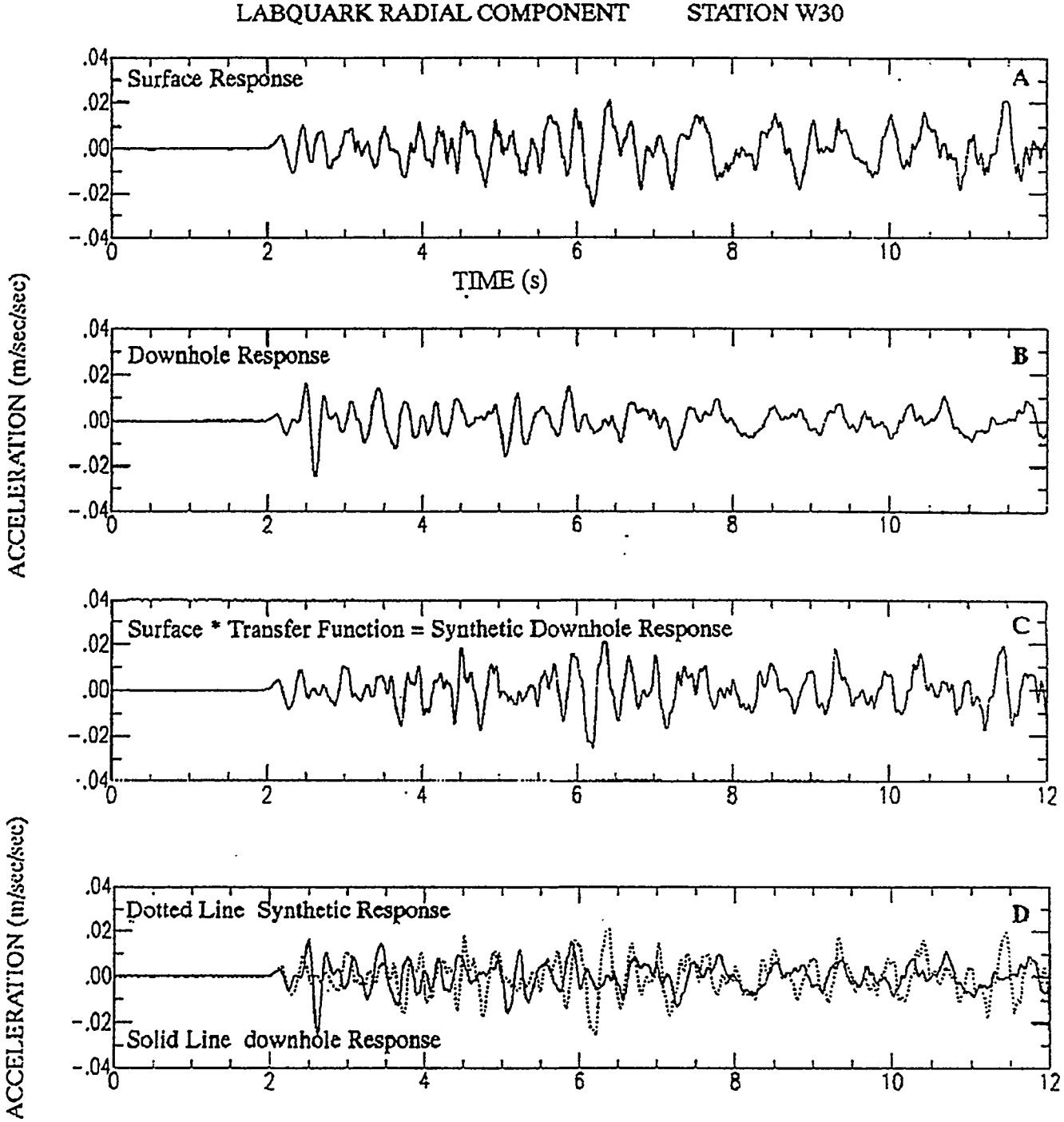

Figure 37: Results of velocity modeling for station 30, Pahute Mesa event Labquark, radial component. Figure layout is the same as figure 16.

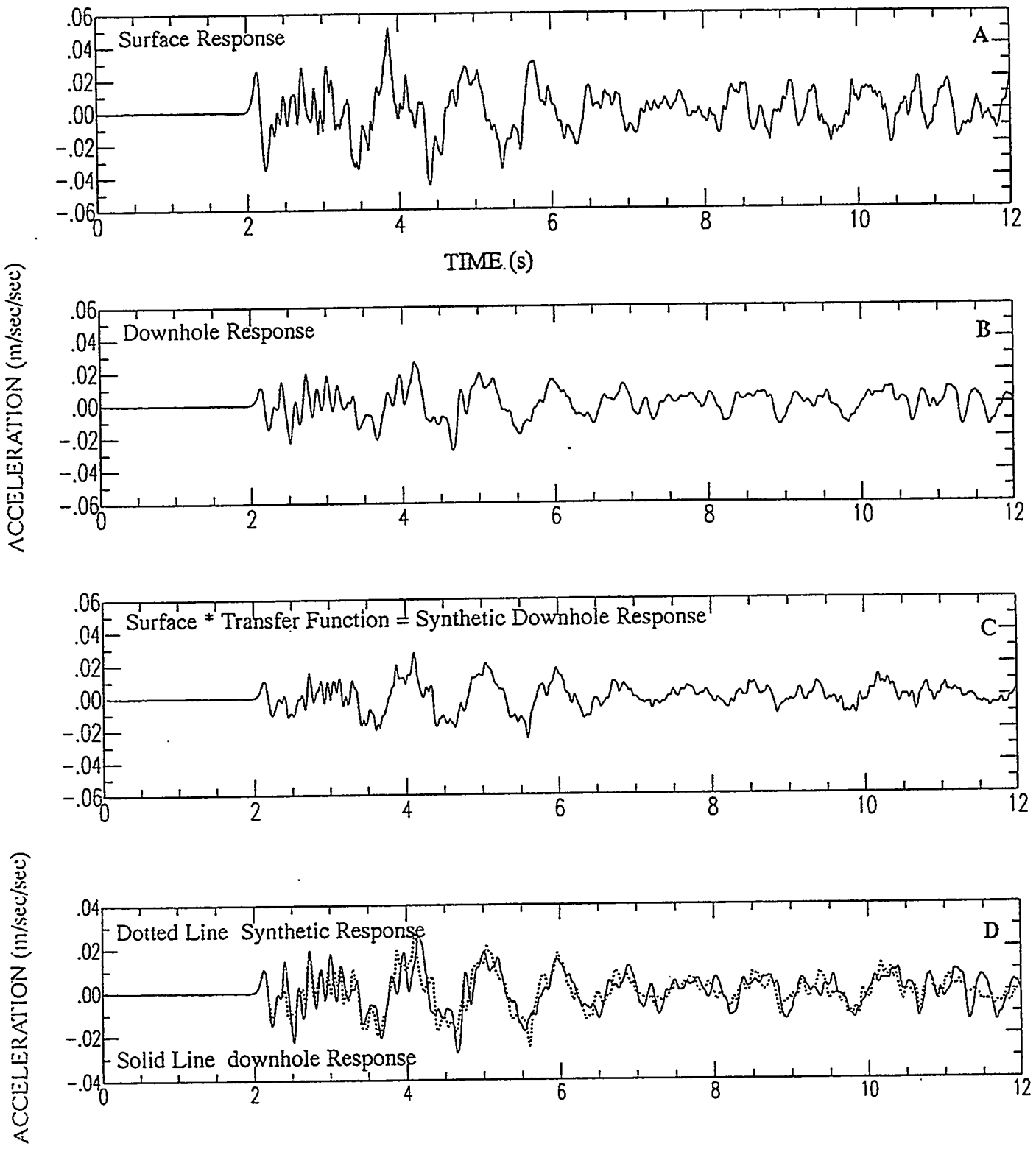

Figure 38: Results of velocity modeling for station 30, Pahute Mesa event Delamar, vertical component. Figure layout is the same as figure 16.

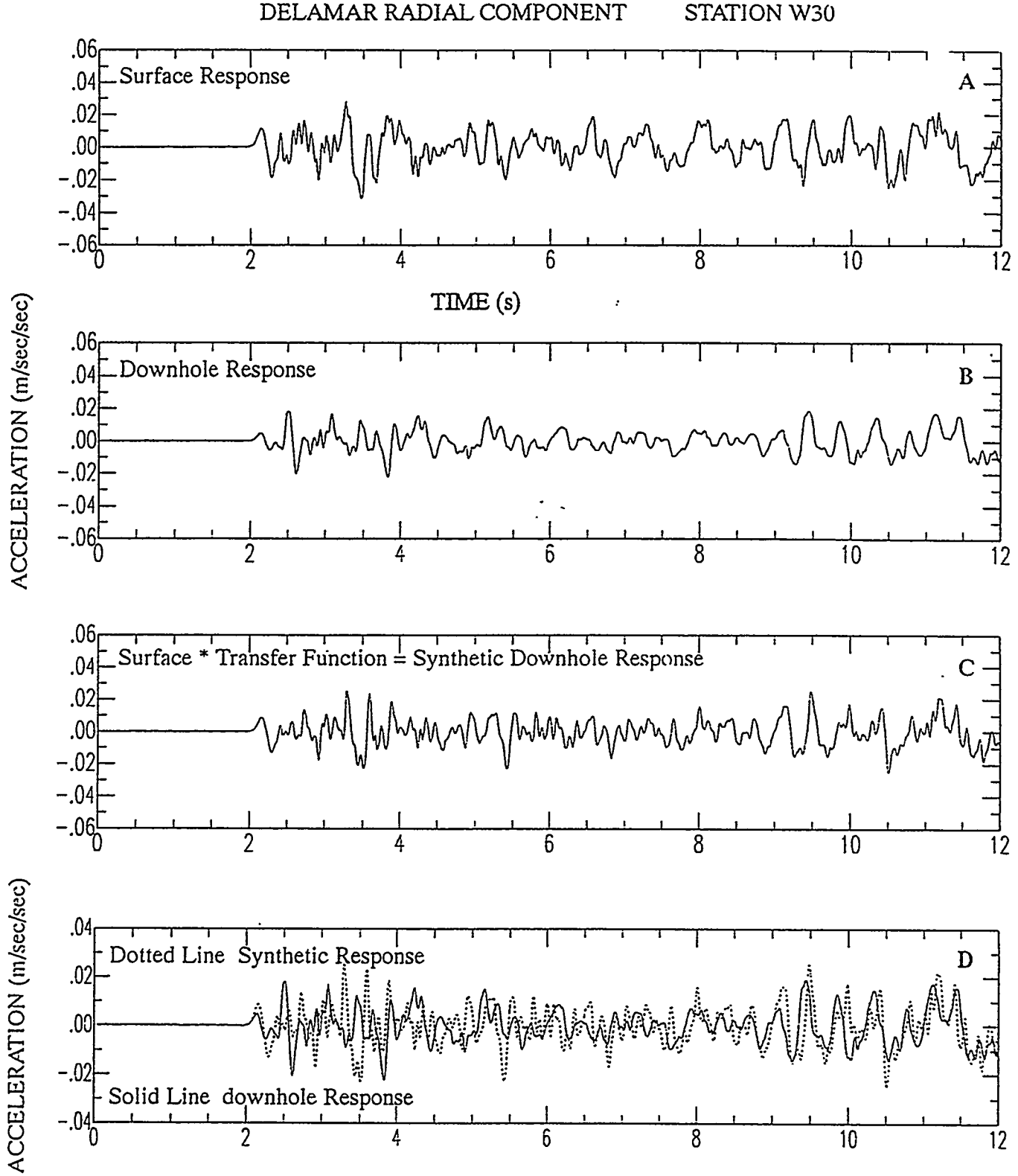

Figure 39: Results of velocity modeling for station 30, Pahute Mesa event Delamar, radial component. Figure layout is the same as figure 16.

to improve the match of the synthetics by altering the shallow shear velocities were not very successful; the final model contains Vp/Vs ratios of 1.73 at all depths.

Two-dimensional model

The four one-dimensional models developed in the previous sections allow us to predict downhole body-wave ground motions, both vertical and horizontal, for a specified surface input at the location of the borehole. None of the boreholes intersects the potential repository location, however, so in order to predict ground motions that might occur in the repository from a seismic event, it is necessary to develop a two-dimensional model that includes the repository location. Because stations 30, 25, and 28 define a north-south line that crosses the proposed location for waste storage (Figure 2), we have used the one-dimensional models developed above to define a simplified seismic velocity model for this cross section (Figure 40). The locations of the various drillholes in the vicinity are marked at the top of the figure, as is the location of the seismic station 21, which overlies the repository location. While the actual geologic structure along this profile is obviously much more complex than shown here, these seismic velocities represent the level of sensitivity of seismic waves of frequencies up to about 10 Hz to the velocity structure.

The southern part of Yucca Mountain itself is quite flat, as seen from the topography in the figure, while station 25 lies in a topographic depression, and the elevation begins to rise to the north by station 28. While the 2.3 km/s material is described as 'bedded tuff' in the illustration, it should be noted that for much of this area, the Tiva Canyon member is present and included in that 2.3 km/s layer. The Topopah Springs member is assigned velocities of 3.1 km/s and 3.9 km/s, corresponding to the TSw1 and TSw2 thermal stratigraphic units of Ortiz et al. (1985). The depth of the potential repository would lie near the bottom of the illustration, in the TSw2 thermal stratigraphic unit. In the section below, we use this model to define a one-dimensional model for the station 21 site to use in prediction of UNE-like ground motion at the proposed repository location (see Table 5 for the model).

Repository-level ground motion predictions

The velocity model for material immediately overlying the repository is quite similar to the model for station 30 (Table 4). Using this model and actual surface accelerations from underground nuclear explosions recorded at station 21, we have predicted downhole responses at 350m depth for the vertical and radial components for three sample nuclear events (Figures 41-46). These UNEs had body wave magnitudes ranging from 5.2 to 5.9 and were located at distances of 44 to 50 km from station 21. The predicted time series generally have

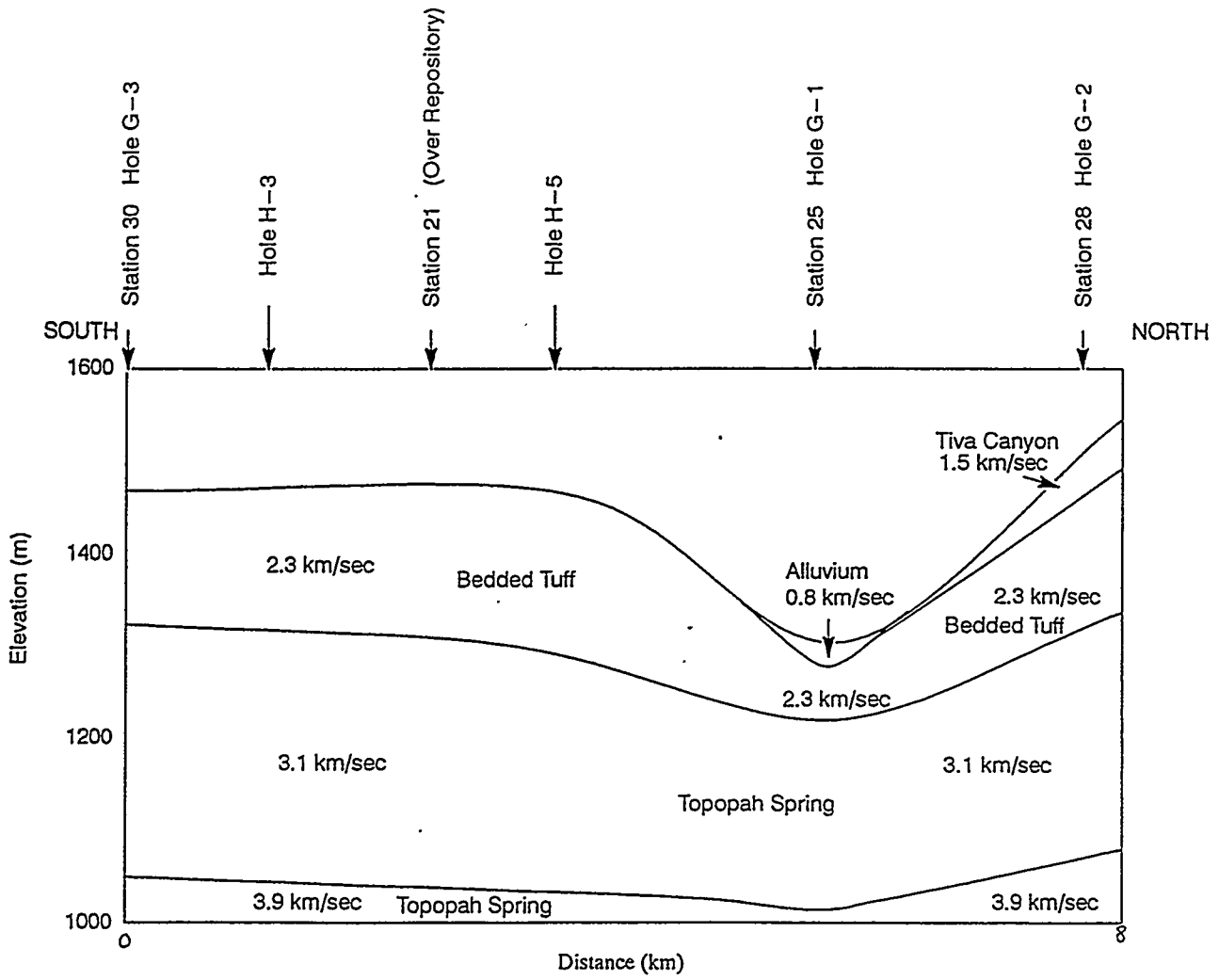

Figure 40: A simple two-dimensional compressional velocity model running approximately north-south through Yucca Mountain from station 30 at the south to station 28 at the north.

Station	Rock Type	Thickness km	Depth km	P-wave velocity km/s	S-wave velocity km/s
21	Alluvium	0.0	0.0	N/A	N/A
	Tiva Canyon/ Bedded Tuff	0.140	0.140	2.30	1.33
	Topopah Spg. (Tsw1)	0.290	0.430	3.10	1.79
	Topopah Spg. (Tsw2)	1.000	1.430	3.90	2.25

Table 5: Velocity model at location of station 21.

frequency content similar to that of the observed surface trace, and maximum amplitudes that are at most 50% of the observed data. The accelerations recorded from these explosions, while easily recordable, are not large enough to cause damage at either the surface or at the repository depth. Earthquakes of concern at the site would be larger (in the magnitude 6.0 to 7.0 range) and closer (perhaps as close as a few km) than these sample events. The seismic radiation pattern of earthquakes is also significantly different from explosions. So while these examples are illustrative, they do not define expected ranges of accelerations for the seismic events of interest at Yucca Mountain.

While the UNE-based predictions have definite limitations, it is still interesting to examine the characteristics of the 12 events for which we calculated simulated downhole accelerograms at station 21. Four of these events were detonated at Yucca Flat and eight on Pahute Mesa. Perhaps surprisingly, the larger events (m_b = 5.6-5.9) in this data set occurred at Yucca Flat, while the Pahute Mesa explosions were in the body wave magnitude range of 5.2-5.7. Plots of peak amplitude as a function of distance and also as a function of event magnitude showed no obvious correlations. Figure 47 shows the range of peak-to-peak vertical acceleration amplitude for these events, separated by source area. The average peak-to-peak acceleration for Pahute Mesa events is .138 $\pm$.04 m/s^2 and for Yucca Flat events is .105$\pm$.03 m/s^2. These values correspond to .014 and .011g, respectively. While these acceleration ranges overlap, there appears to be a tendency for Pahute Mesa explosions to have somewhat larger peak accelerations than Yucca Flat explosions for the same distance range and with somewhat smaller magnitude events. This amplitude difference may be due to a propagation effect; as noted by Walck and Phillips (1990), first-arrival amplitude variations for the two source areas exist and can be explained by laterally varying crustal structure along the propagation path.

Although it is beyond the scope of this study, in order to predict ground motions at the repository depth from earthquakes instead of UNEs, it would be quite possible to use the transfer function from the station 21 model in Table 5 to predict repository-level earthquake ground motions using microearthquakes recorded at the surface of Yucca Mountain. While these simulations would not be of the proper amplitude for design calculations, they would contain more earthquake-appropriate spectral content and radiation partitioning. A simulated time history or spectrum for a close, large earthquake could also be used with the transfer function from this model to predict the associated downhole motions.

The one-dimensional transfer functions do not include surface wave propagation, which can cause very significant ground motions in large earthquakes. Surface waves can be included in future calculations by using the model with a different calculational method, such as a finite difference scheme. The validity of the extrapolated two-dimensional model presented

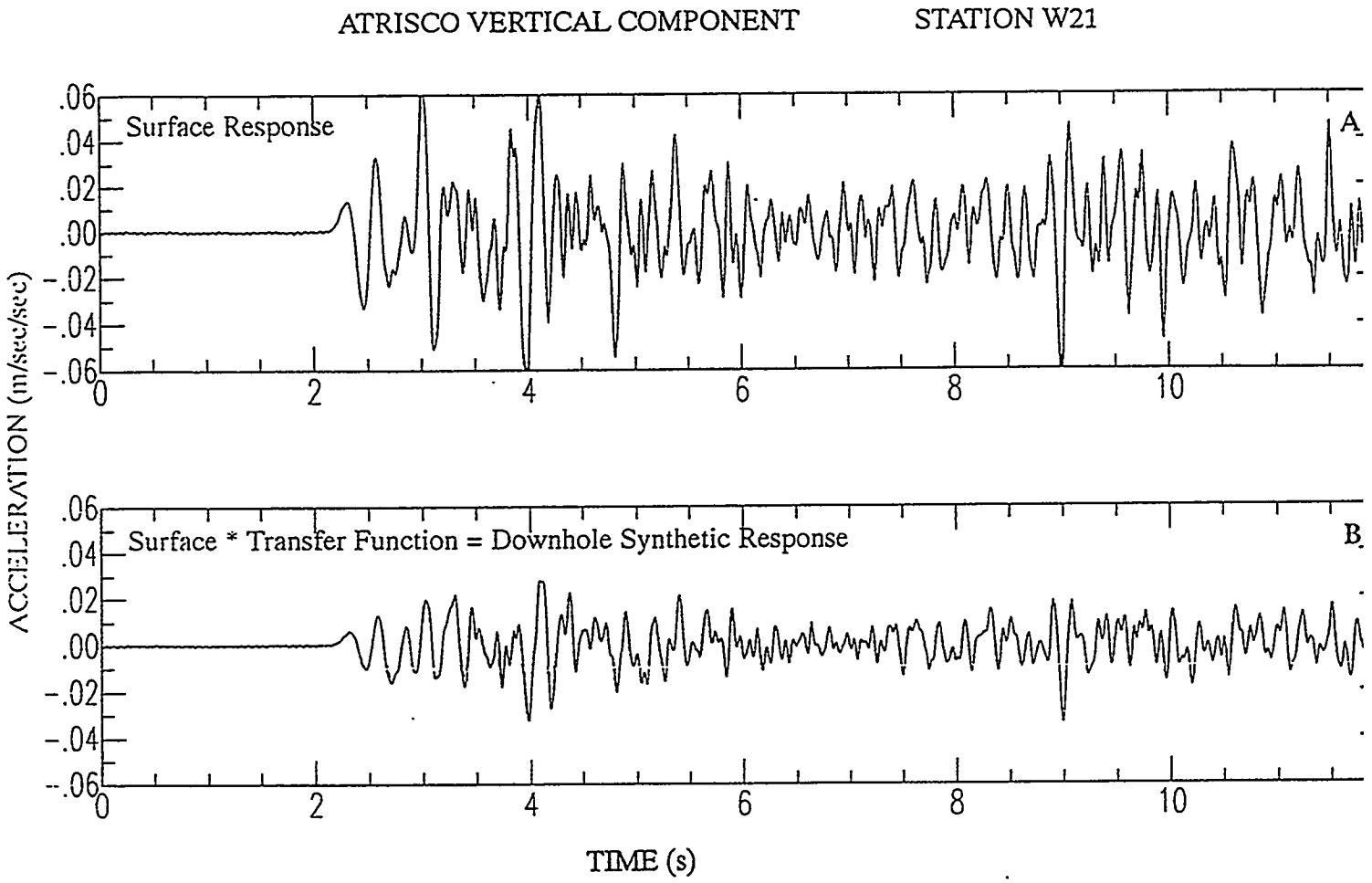

Figure 41: Vertical component observed (A) and "downhole" (depth=350m) simulated (B) records for station 21 (located directly over the potential repository) for event Atrisco.

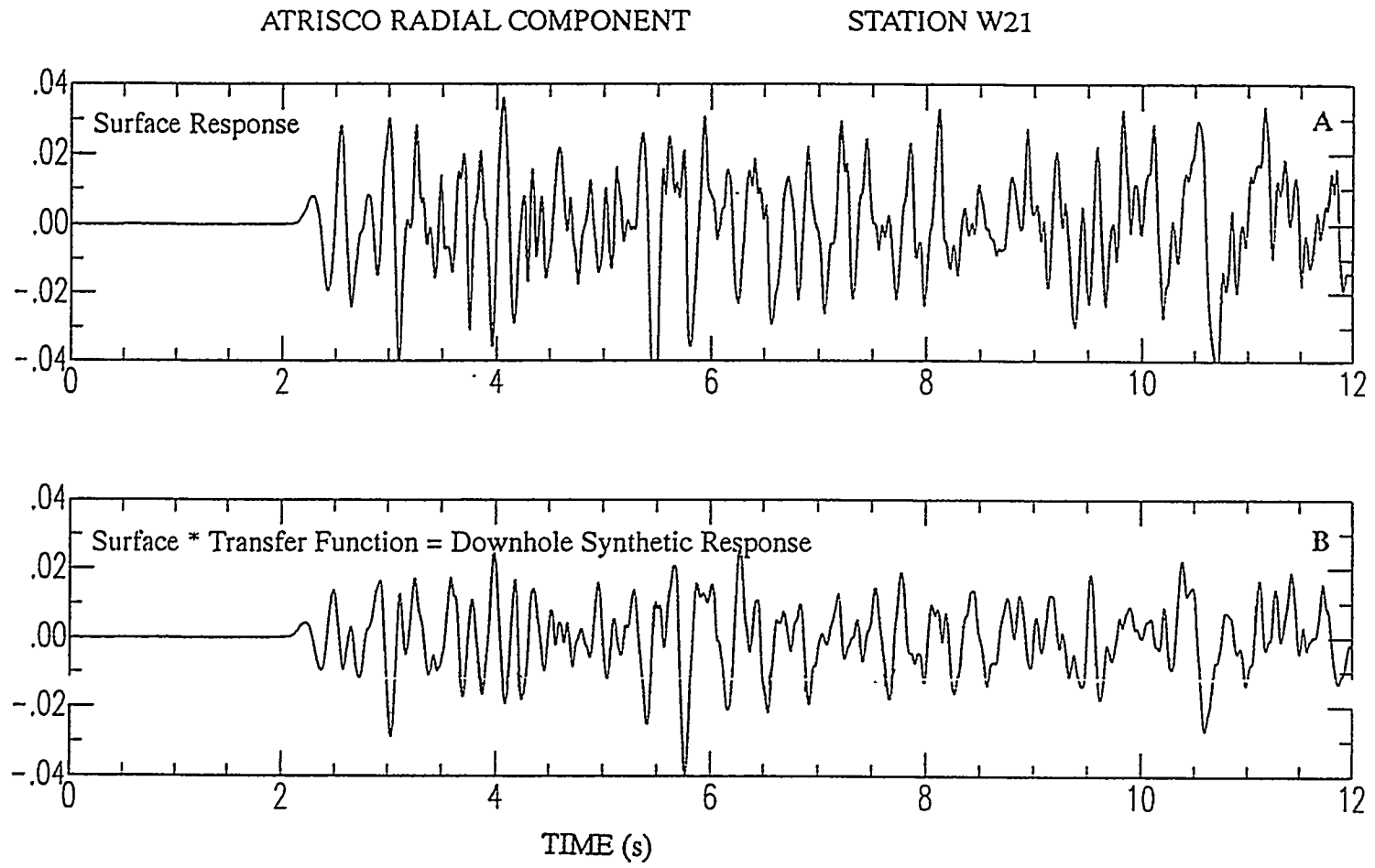

Figure 42: Same as figure 41 for the radial component of the Yucca Flat event Atrisco.

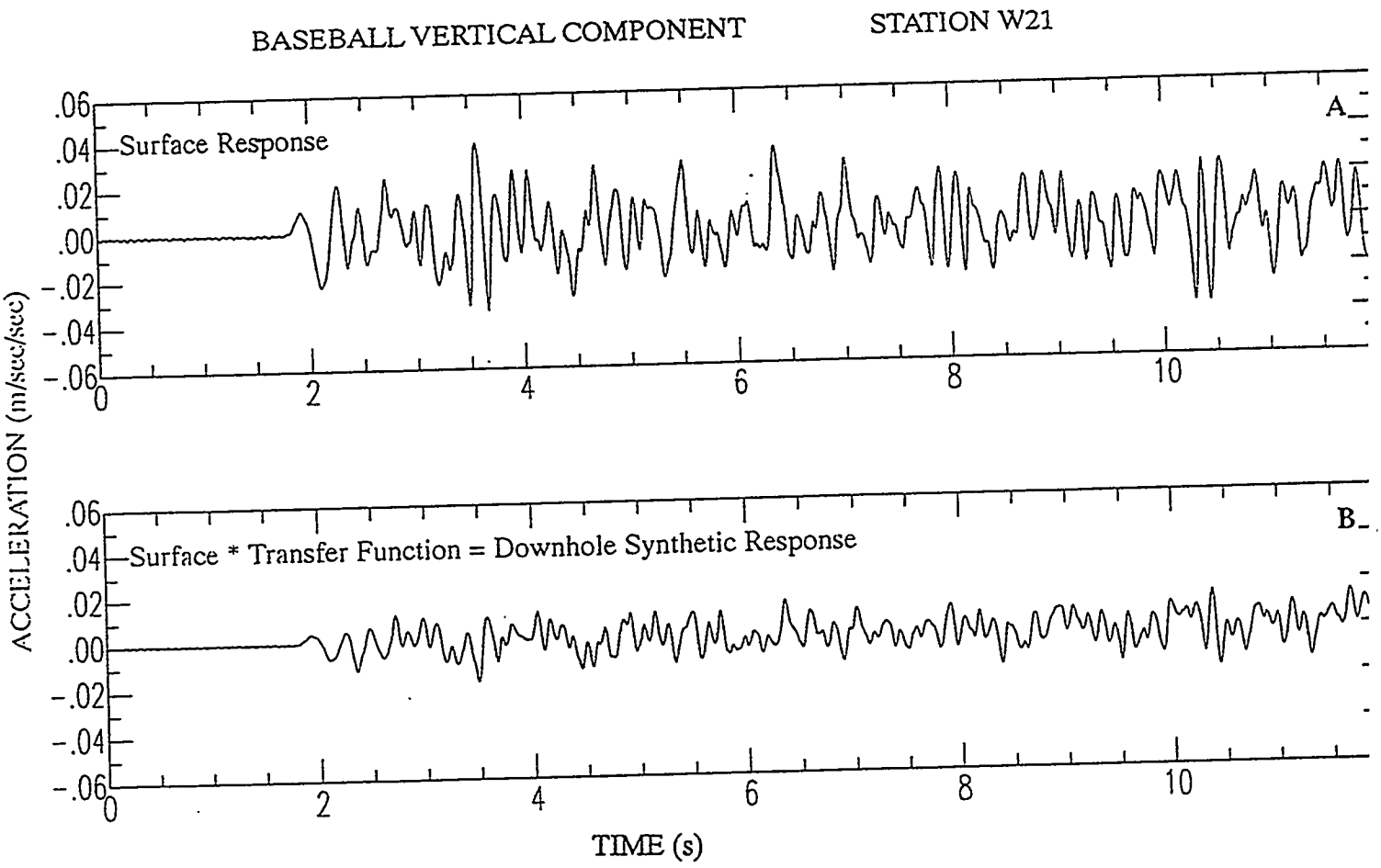

Figure 43: Same as figure 41 for the vertical component of the Yucca Flat event Baseball.

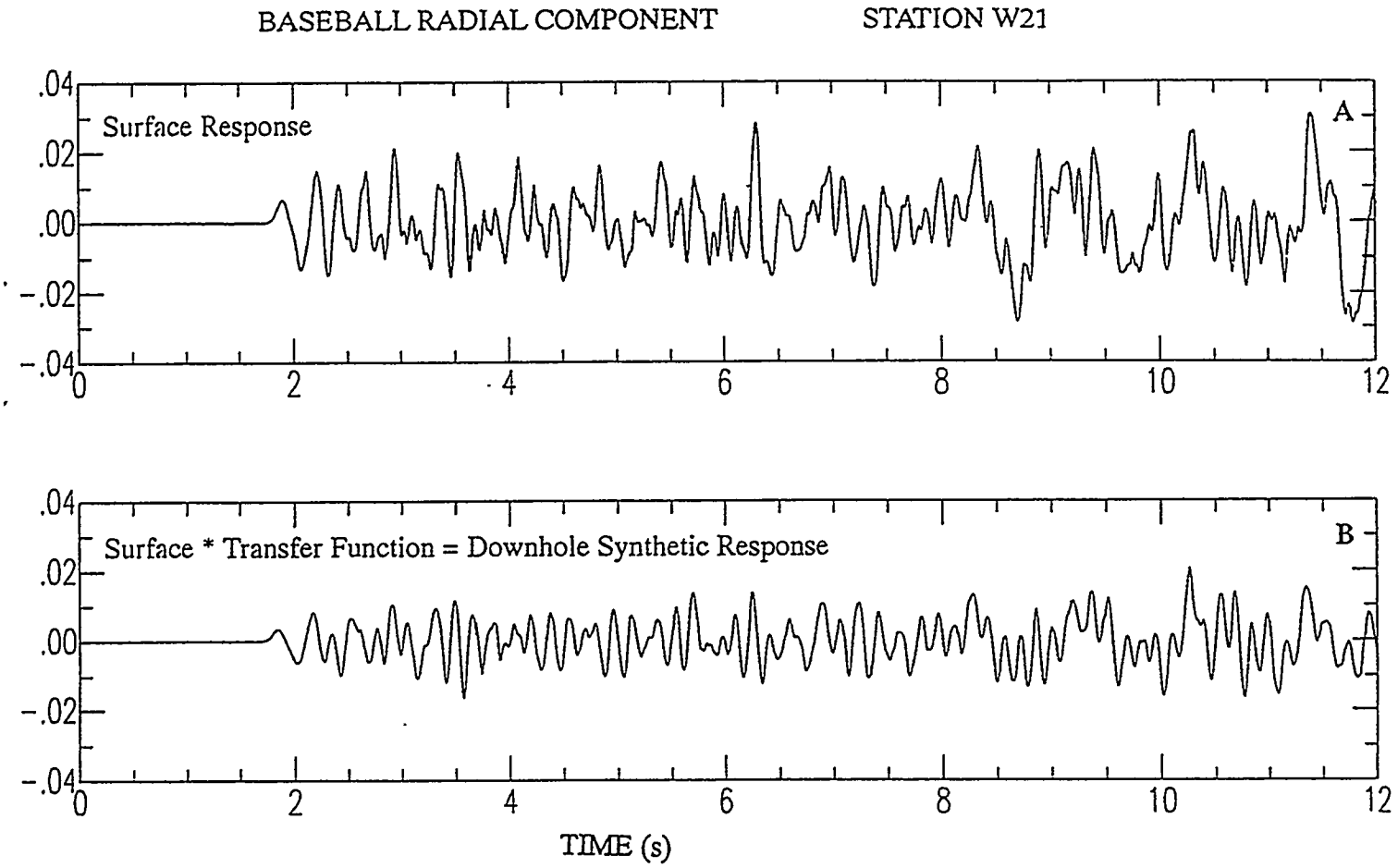

Figure 44: Same as figure 41 for the radial component of the Yucca Flat event Baseball.

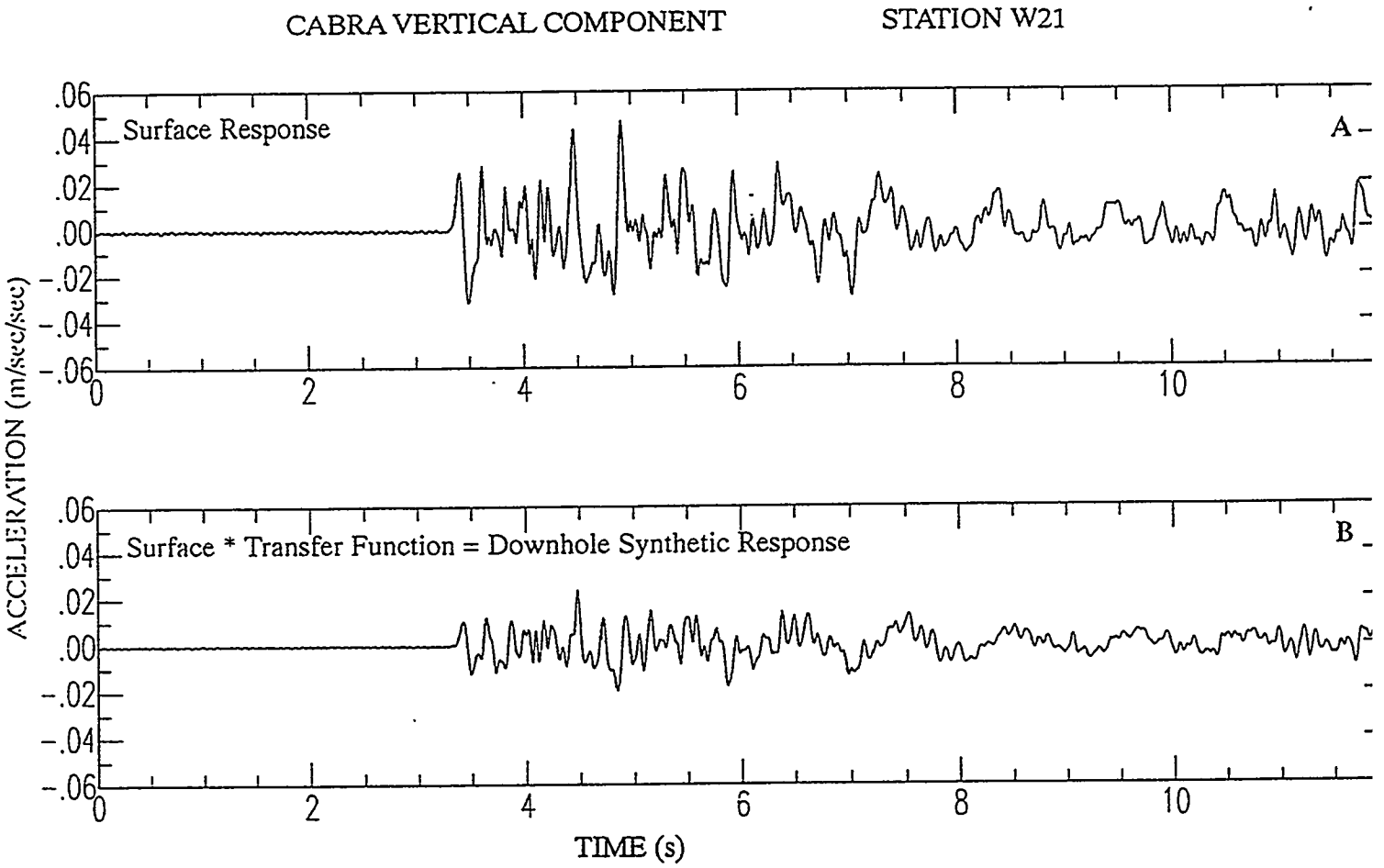

Figure 45: Same as figure 41 for the vertical component of Pahute Mesa event Cabra.

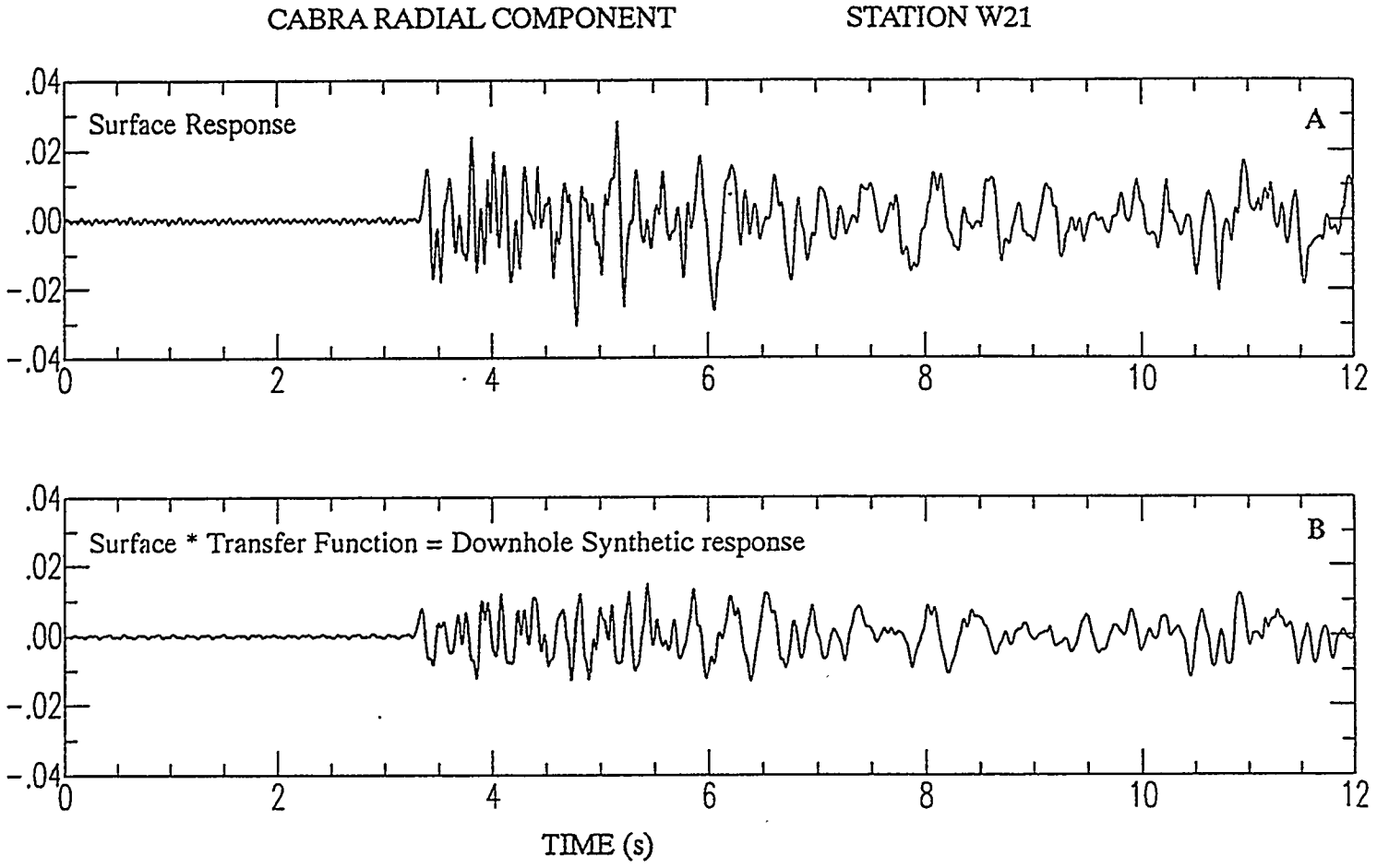

Figure 46: Same as figure 41 for the radial component of Pahute Mesa event Cabra.

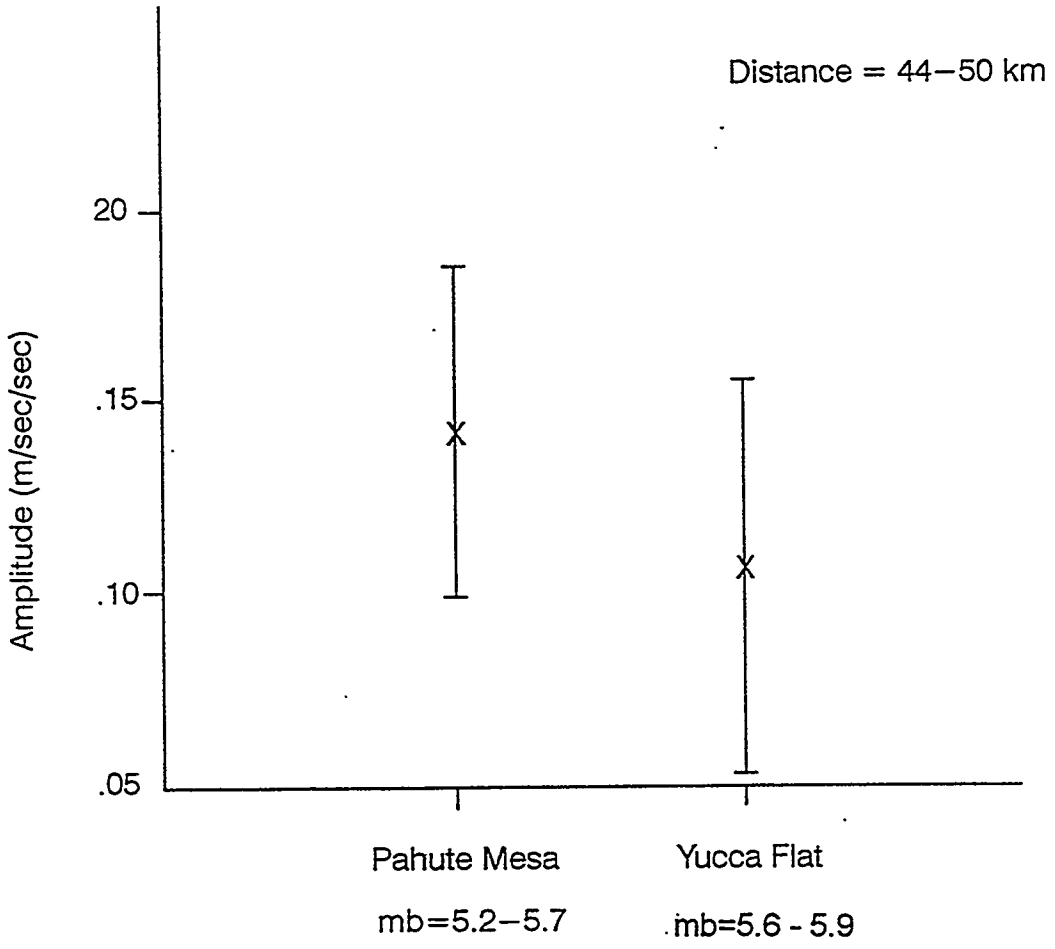

Figure 47: Comparison of predicted peak-to-peak ground motion amplitudes at 350 m depth, station 21 site, for 12 events observed at the surface, as a function of source area.

here could be checked using a true two-dimensional method, and more sophisticated calculations carried out in order to include the effects of surface waves.

Conclusions

We have developed four one-dimensional velocity models for boreholes located at and near Yucca Mountain using a propagator matrix technique and a suite of uphole/downhole triaxial recordings of underground nuclear explosions. These models, while relatively simple layered structures, are consistent with the available geologic and well-log information and produce synthetic downhole seismograms that match the data very well in overall amplitude and frequency content. Individual waveforms were also very well fit for several of the stations, particularly for the vertical component. The radial component ground motion predictions do not fit the detailed waveforms as well as the verticals, but still provide a reasonable estimate of overall ground motion levels. The poorer fit of the radials probably reflects a lack of constraints on the shear wave velocities in the very uppermost part of Yucca Mountain.

This series of one-dimensional models was used to develop a two-dimensional model for a north-south cross section through Yucca Mountain. A vertical slice through the two-dimensional model provides a one-dimensional velocity model at the location of a former surface-only station that was located directly over the repository site. Nuclear events recorded at this station (21) have been used to simulate expected vertical and radial body-wave ground motions for events similar in size and distance to the observed nuclear events (45-50 km, body wave magnitude between 5.2-5.9). These predicted ground motions are relatively small.

References

Gibson, J. D., F. Swan, J. Wesling, T. Bullard, R. Perman, M. Angell, L. DiSilvestro, Summary and evaluation of existing geological and geophysical data near prospective surface facilities in Midway Valley, Yucca Mountain Project, Nye County, Nevada, SAND90-2491, Sandia National Laboratories, Albuquerque, NM, 1992.

Haskell, N. A., The dispersion of surface waves in multilayered media, *Bull. Seism. Soc. Am.*, 43, 17-34, 1953.

Haskell, N. A., Crustal reflection of plane SH waves, *J. Geophys. Res.*, 65, 4147-4150, 1960.

Haskell, N. A., Crustal reflection of plane P and SV waves, *J. Geophys. Res.*, 67, 4751-4767, 1962.

Lappin, A. R, R. VanBuskirk, D. Enniss, S. Butters, F. Prater, C. Muller, J. Bergosh, Thermal conductivity, bulk properties, and thermal stratigraphy of silicic tuffs from the upper portion of hole USW-G1, Yucca Mountain, Nye County, Nevada, SAND81-1873, Sandia National Laboratories, Albuquerque, NM, 1982.

Maldonado, F., and S. Koether, Stratigraphy, structure and some petrographic features of tertiary volcanic rocks at the USW G-2 drill hole, Yucca Mountain, Nye County, Nevada, U. S. Geological Survey Open File Report 83-732, 1983.

Muller, D. C. and J. E. Kibler, Commercial geophysical well logs from the USW G-1 drill hole, Nevada Test Site, Nevada, U. S. Geological Survey Open File Report, 83-321, 1983.

Ortiz, T., R. Williams, F. Nimick, B. Whittet, D. South, A three-dimensional model of reference thermal/mechanical and hydrological stratigraphy at Yucca Mountain, southern Nevada, SAND84-1076, Sandia National Laboratories, Albuquerque, NM, 1985. (NNA.890315.0013; HQS.880517.1691)

Phillips, J. S., Analysis of component surface/downhole ground motions at Yucca Mountain for underground nuclear explosions in Pahute Mesa, SAND87-2381, Sandia National Laboratories, Albuquerque, NM, 1991. (NNA.901127.0287)

Scott, R. B., and M. Castellanos, Stratigraphic and structural relations of volcanic rocks in drill holes USW GU-3 and USW G-3, Yucca Mountain, Nye County, Nevada, U. S. Geological Survey Open File Report 84-491, 1984.

Shearer, P. M. and J. A. Orcutt, Surface and near-surface effects on seismic waves -- theory and borehole seismometer results, *Bull. Seism. Soc. Am.*, 77, 1168-1196, 1987.

Spengler, R., F. Byers Jr., J. Warner, Stratigraphy and structure of volcanic rocks in drill hole USW G-1, Yucca Mountain, Nye County, Nevada, U. S. Geological Survey Open File Report, 81-1349, 1981.

Spengler, R. W. and M. P. Chornack, with D. C. Muller and J. E. Kibler, Stratigraphic and structural characteristics of volcanic rocks in core hole USW G-4, Yucca Mountain, Nye County, Nevada, with a section on geophysical logs, U. S. Geological Survey Open File Report, 84-789, 1984.

Walck, M. C. and J. S. Phillips, Two-dimensional velocity models for paths from Pahute Mesa and Yucca Flat to Yucca Mountain, SAND88-3033, Sandia National Laboratories, Albuquerque, NM, 1990. (NNA.901005.0051)

YUCCA MOUNTAIN SITE CHARACTERIZATION PROJECT
SAND95-1606 - DISTRIBUTION LIST

1 D. A. Dreyfus (RW-1)
Director
OCRWM
US Department of Energy
1000 Independence Avenue SW
Washington, DC 20585

1 L. H. Barrett (RW-2)
Acting Deputy Director
OCRWM
US Department of Energy
1000 Independence Avenue SW
Washington, DC 20585

1 S. Rousso (RW-40)
Office of Storage and Transportation
OCRWM
US Department of Energy
1000 Independence Avenue SW
Washington, DC 20585

1 R. A. Milner (RW-30)
Office of Program Management
and Integration
OCRWM
US Department of Energy
1000 Independence Avenue SW
Washington, DC 20585

1 D. R. Elle, Director
Environmental Protection Division
DOE Nevada Field Office
US Department of Energy
P.O. Box 98518
Las Vegas, NV 89193-8518

1 T. Wood (RW-14)
Contract Management Division
OCRWM
US Department of Energy
1000 Independence Avenue SW
Washington, DC 20585

4 Victoria F. Reich, Librarian
Nuclear Waste Technical Review Board
1100 Wilson Blvd., Suite 910
Arlington, VA 22209

1 Wesley Barnes, Project Manager
Yucca Mountain Site Characterization
Office
US Department of Energy
P.O. Box 98608--MS 523
Las Vegas, NV 89193-8608

1 Director, Public Affairs Office
c/o Technical Information Resource Center
DOE Nevada Operations Office
US Department of Energy
P.O. Box 98518
Las Vegas, NV 89193-8518

8 Technical Information Officer
DOE Nevada Operations Office
US Department of Energy
P.O. Box 98518
Las Vegas, NV 89193-8518

1 J. R. Dyer, Deputy Project Manager
Yucca Mountain Site Characterization Office
US Department of Energy
P.O. Box 98608 -- MS 523
Las Vegas, NV 89193-88608

1 M. C. Brady
Laboratory Lead for YMP
M&O/Sandia National Laboratories
1261 Town Center Drive
Bldg. 4, Room 421A
Las Vegas, NV 89134

1 J. A. Canepa
Laboratory Lead for YMP
EES-13, Mail Stop J521
M&O/Los Alamos National Laboratory
P.O. Box 1663
Los Alamos, NM 87545

1 Repository Licensing & Quality
Assurance
Project Directorate
Division of Waste Management, MS T7J-9
US NRC
Washington, DC 20555

1 Senior Project Manager for Yucca
Mountain
Repository Project Branch
Division of Waste Management, MS T7J-9
US NRC
Washington, DC 20555

1 NRC Document Control Desk
Division of Waste Management, MS T7J-9
US NRC
Washington, DC 20555

1 Chad Glenn
NRC Site Representative
301 E Stewart Avenue, Room 203
Las Vegas, NV 89101

1 Center for Nuclear Waste
Regulatory Analyses
Southwest Research Institute
6220 Culebra Road
Drawer 28510
San Antonio, TX 78284

2 W. L. Clarke
Laboratory Lead for YMP
M&O/ Lawrence Livermore Nat'l Lab
P.O. Box 808 (L-51)
Livermore, CA 94550

1 Robert W. Craig
Acting Technical Project Officer/YMP
US Geological Survey
101 Convention Center Drive, Suite P-110
Las Vegas, NV 89109

1 J. S. Stuckless, Chief
Geologic Studies Program
MS 425
Yucca Mountain Project Branch
US Geological Survey
P.O. Box 25046
Denver, CO 80225

1 L. D. Foust
Technical Project Officer for YMP
TRW Environmental Safety Systems
101 Convention Center Drive
Suite P-110
Las Vegas, NV 89109

1 A. L. Flint
U. S. Geological Survey
MS 721
P.O. Box 327
Mercury, NV 89023

1 Robert L. Strickler
Vice President & General Manager
TRW Environmental Safety Systems, Inc.
2650 Park Tower Dr.
Vienna, VA 22180

1 Jim Krulik, Geology Manager
US Bureau of Reclamation
Code D-8322
P.O. Box 25007
Denver, CO 80225-0007

1 B. T. Brady
Records Specialist
US Geological Survey
MS 421
P.O. Box 25046
Denver, CO 80225

1 M. D. Voegele
Deputy of Technical Operations
M&O/SAIC
101 Convention Center Drive
Suite P-110
Las Vegas, NV 89109

2 A. T. Tamura
Science and Technology Division
OSTI
US Department of Energy
P.O. Box 62
Oak Ridge, TN 37831

1 P. J. Weeden, Acting Director
Nuclear Radiation Assessment Div.
US EPA
Environmental Monitoring Sys. Lab
P.O. Box 93478
Las Vegas, NV 89193-3478

1 John Fordham, Deputy Director
Water Resources Center
Desert Research Institute
P.O. Box 60220
Reno, NV 89506

1 The Honorable Jim Regan
Chairman
Churchill County Board of
Commissioners
10 W. Williams Avenue
Fallon, NV 89406

1 R. R. Loux
Executive Director
Agency for Nuclear Projects
State of Nevada
Evergreen Center, Suite 252
1802 N. Carson Street
Carson City, NV 89710

1 Brad R. Mettam
County Yucca Mountain
Repository Assessment Office
P. O. Drawer L
Independence, CA 93526

1 Vernon E. Poe
Office of Nuclear Projects
Mineral County
P.O. Box 1600
Hawthorne, NV 89415

1 Les W. Bradshaw
Program Manager
Nye County Nuclear Waste Repository
Project Office
P.O. Box 1767
Tonopah, NV 89049

1 Florindo Mariani
White Pine County Coordinator
P. O. Box 135
Ely, NV 89301

1 Tammy Manzini
Lander County Yucca Mountain
Information Officer
P.O. Box 10
Austin, NV 89310

1 Jason Pitts
Lincoln County Nuclear Waste
Program Manager
P. O. Box 158
Pioche, NV 89043

1 Dennis Bechtel, Coordinator
Nuclear Waste Division
Clark County Dept. of Comprehensive
Planning
P.O. Box 55171
Las Vegas, NV 89155-1751

1 Juanita D. Hoffman
Nuclear Waste Repository
Oversight Program
Esmeralda County
P.O. Box 490
Goldfield, NV 89013

1 Sandy Green
Yucca Mountain Information Office
Eureka County
P.O. Box 714
Eureka, NV 89316

1 Economic Development Dept.
City of Las Vegas
400 E. Stewart Avenue
Las Vegas, NV 89101

1 Community Planning & Development
City of North Las Vegas
P.O. Box 4086
North Las Vegas, NV 89030

2 Librarian
YMP Research & Study Center
101 Convention Center Drive, Suite P-110
Las Vegas, NV 89109

1 Library Acquisitions
Argonne National Laboratory
Building 203, Room CE-111
9700 S. Cass Avenue
Argonne, IL 60439

1 Glenn Van Roekel
Manager, City of Caliente
P.O. Box 158
Caliente, NV 89008

1 Gudmundur S. Bodvarsson
Head, Nuclear Waste Department
Lawrence Berkeley National Laboratory
1 Cyclotron Road, MS 50E
Berkeley, CA 94720

1 Steve Hanauer (RW-2)
OCRWM
U. S. Department of Energy
1000 Independence Ave.
Washington, DC 20585

Robert W. Clayton
M&O/WCFS
101 Convention Center Drive/MS423
Las Vegas, NV 89109

1 Richard C. Quitmeyer
M&O/WCFS
101 Convention Center Drive/MS423
Las Vegas, NV 89109

1 Mark C. Tynan
DOE/YMPSCO
101 Convention Center Drive/MS523/HL
Las Vegas, NV 89109

1 John Whitney
U.S. Geological Survey
P.O. Box 25046, MS 425
Denver, CO 80225

1 Ivan Wang
Woodward-Clyde Federal Services
500 12th Street, Suite 100
Oakland, CA 94607

1 Tim Sullivan
U.S. Department of Energy
Yucca Mountain Site Characterization
Office
101 Convention Center Drive, Suite P200
Las Vegas, NV 89109

2	1330	B. Pierson, 6811
	100/1.2.3.2.8.3.3/SAND95-1606/QA	
20	1330	WMT Library, 6752
1	9018	Central Technical Files, 8523-2
5	0899	Technical Library, 4414
2	0619	Review and Approval Desk, 12630, For DOE/OSTI
15	0750	M. C. Walck, 6116
1	0750	G. J. Elbring, 6116
1	0750	C. J. Young, 6115
1	0750	D. J. Borns, 6116
1	1160	H. D. Garbin, 9312